

β -amyloid in Alzheimer's disease initiation and phenotypic diversity

Dissertation

zur Erlangung des Grades
eines Doktors der Naturwissenschaften

der Mathematisch-Naturwissenschaftlichen Fakultät
und
der Medizinischen Fakultät
der Eberhard-Karls-Universität Tübingen

vorgelegt

von

Jay Rasmussen
aus Orion, Kanada

Juni 2018

Tag der mündlichen Prüfung:

Dekan der Math.-Nat. Fakultät: Prof. Dr. W. Rosenstiel
Dekan der Medizinischen Fakultät: Prof. Dr. I. B. Autenrieth

1. Berichterstatter: Prof. Dr. M. Jucker
2. Berichterstatter: Prof. Dr. P. Heutink

Prüfungskommission:
Prof. Dr. M. Jucker
Prof. Dr. P. Heutink
Prof. Dr. M. Neumann
Prof. Dr. R. Feil

Erklärung

Ich erkläre, dass ich die zur Promotion eingereichte Arbeit mit dem Titel:

“ β -amyloid in Alzheimer’s disease initiation and phenotypic diversity”

selbständig verfasst, nur die angegebenen Quellen und Hilfsmittel benutzt und wörtlich oder inhaltlich übernommene Stellen als solche gekennzeichnet habe. Ich versichere an Eides statt, dass diese Angaben wahr sind und dass ich nichts verschwiegen habe. Mir ist bekannt, dass die falsche Angabe einer Versicherung des Eides statt mit Freiheitsstrafe bis zu drei Jahren oder mit Geldstrafe bestraft wird.

Tübingen,

.....

Acknowledgements

First, I would like to thank Prof. Mathias Jucker for giving me the opportunity to conduct research within his lab, giving guidance when necessary and giving me the freedom to develop as a scientist. Additionally, I would like to thank all members of my advisory board, namely, Profs. Jucker, Heutink and Neumann for providing constructive criticism about my research. Any accomplishments during my PhD have been made possible by a number of people including Dr. Lan Ye, Dr. Jasmin Mahler, Natalie Beschorner, Anika Bühler, Dr. Jörg Odenthal, Carina Leibssle, Ulrike Obermüller, Dr. Frank Baumann, Prof. Lary Walker and all other members of the Jucker lab, animal caretakers and collaborators around the world. Finally, I would like to thank Sarah, my family and my friends for their support.

Table of Contents

1. Summary	1
2. Synopsis	3
2.1 Overview of Alzheimer's disease	3
2.1.1 <i>Demographics and pathophysiology</i>	3
2.1.2 <i>The amyloid precursor protein and β-amyloid</i>	5
2.1.3 <i>The protein-only hypothesis: a unifying concept of disease</i>	14
2.2 Heterogeneity of β -amyloid aggregates in Alzheimer's disease	17
2.2.1 <i>Fibrillar β-amyloid structures and deposits</i>	17
2.2.2 <i>Prion-like strains and clouds of conformation</i>	21
2.3 β -amyloid seeds	27
2.3.1 <i>The seeding paradigm</i>	27
2.3.2 <i>The age-dependency of β-amyloid seeding potency</i>	31
2.4 Isolating bioactive <i>in vivo</i> A β seeds	34
2.4.1 <i>The varied forms of aggregated β-amyloid</i>	34
2.4.2 <i>Finding a suitable target for Alzheimer's disease therapies</i>	36
2.5 Conclusions and outlook	39
2.6 References	44
3. Publications	59
3.1 Description of personal contribution	59
3.2 Amyloid polymorphisms constitute distinct clouds of conformational variants in different etiological subtypes of Alzheimer's disease	61
3.3 A β seeding potency peaks in the early stages of cerebral β -amyloidosis	74
3.4 An agarose gel fractionation method for enriching brain-derived proteopathic seeds	85
4. Appendix	98
4.1 Abbreviations	98
4.2 Curriculum vitae	100

1. Summary

Alzheimer's disease (AD) is a progressive neurodegenerative condition characterized by behavioral changes and memory impairments, predominantly observed in the elderly population. As the most common form of dementia worldwide, AD has a large socioeconomic burden that is expected to grow in the next decades, given that no potent therapeutic strategy exists to treat the increasing population of aged individuals. The deposition of misfolded β -amyloid ($A\beta$) within extracellular senile plaques is a pathological hallmark of disease. The appearance of $A\beta$ plaques has been identified as one of the earliest events in AD, and the prevailing amyloid cascade hypothesis suggests that the abnormal cleavage and misfolding of $A\beta$ is the trigger of disease. The focus on misfolded $A\beta$ as a central agent in AD has drawn parallels to the infectious prion protein and the protein-only hypothesis of disease transmission for prion disease. A number of studies have demonstrated that $A\beta$ assembles into amyloid fibrils and that misfolded species can seed the aggregation of monomeric $A\beta$ both *in vitro* and *in vivo*. Although the seeding properties of aggregated $A\beta$ are robust, a more recent line of investigation aimed to characterize how variations in $A\beta$ aggregate assembly influence the potency of seeding and also the progression of disease.

In this doctoral dissertation, the structural features of amyloid plaque cores within a diverse cohort of 40 patients, with either sporadic or familial AD, were assessed using a unique class of conformation sensitive amyloid binding dyes referred to as luminescent conjugated oligothiophenes or LCOs. The fluorescence spectral signature of LCO stained plaque cores was strikingly different between familial AD and sporadic AD, and subtle differences were also identified between the typical and posterior cortical atrophy variants of sporadic AD. This demonstrates that the amyloid structure is distinct between AD subtypes, an observation not explained by $A\beta$ biochemical features or clinical data. Surprisingly, within a single AD brain, multiple spectral signatures for amyloid were present and are referred to as clouds of conformational $A\beta$ variants. The structural features of human AD-derived $A\beta$ aggregates were also preserved upon transmission to human APP transgenic mice. The direct analysis of $A\beta$ conformations within post-mortem human tissue provided insight into the spectrum of species present within a brain, but the presence of such $A\beta$ variation at earlier stages of disease is unknown.

In a second study, the change in conformational and biological A β features with aging was studied in APP transgenic mouse models with either slow or rapid cerebral β -amyloidosis. Both histological and biochemical levels of A β increased with aging, but the ratio of specific A β species, namely A β 42/40, surprisingly peaked at the early stage of plaque appearance in the two models. An *in vivo* bioassay was then used to show that different aged brain extracts had increasing seeding activities, or seeding dosages (SD_{50}), that plateaued with advanced age when injected into a transgenic host. Interestingly, when seeding activity was normalized to the amount of A β within the extracts, a peak in specific activity became apparent at the age when A β deposition first appears and A β 42/40 was highest. This study provides further evidence that treatment of AD should be initiated early, i.e. at the time point when these potent seeds are present and before a cascade of neurodegeneration can occur.

Finally, in a third study, a novel methodology capable of investigating various native A β assemblies in the brain was described. Here, the use of agarose electrophoresis facilitated the separation of A β aggregation states by size, and demonstrated that transgenic mouse brain extracts harbor A β aggregates with a different size distribution than *in vitro* A β fibrils. Agarose fractions were collected and enzymatically digested to produce a liquid sample, which could be used for further analysis. Immunoprecipitation with an amyloid-conformation-specific antibody confirmed that A β migrating with a high molecular weight had a preserved quaternary structure after the enrichment protocol. Further evidence that the structure was preserved was demonstrated when a high molecular weight fraction induced A β deposition when injected into transgenic mice. This novel tool provides the opportunity to screen potential therapeutic antibodies or compounds against native *in vivo* aggregates, while generating samples that can be further analyzed to determine the relationship between aggregate size and structure with biological features such as seeding activity.

The original research within this dissertation has provided a significant contribution to the knowledge of A β structural features within AD, and the seeding properties over the course of disease. Additionally, the establishment of a new method for isolating *in vivo* seeds using agarose fractionation will allow for further basic investigations of these findings and aid in the development of novel therapeutics. Specifically targeting the earliest generated seeds within an AD subtype using immunotherapies could enhance the removal of pathogenic A β and provide a viable strategy to prevent AD.

2. Synopsis

2.1 Overview of Alzheimer's disease

2.1.1 Demographics and pathophysiology

The first characterization of AD occurred over 100 years ago by a physician for whom the disease was later named, Alois Alzheimer (Alzheimer 1907). This seminal description of the subject Auguste D. outlined the typical clinical presentation, which current AD patients share, namely, pronounced cognitive impairment and behavioral changes. The presentation by Alois Alzheimer of his work at a conference received little attention and was rather thought of as an unexceptional case of general age-related dementia. It was not until later that the importance of this description was fully appreciated. With further investigation, it was realized that AD was an affliction that classified the largest portion of patients with dementia. In the decades since, significant advancements have been made to better understand AD and more specifically, the molecular players and the subtleties that lead to divergent clinical presentation.

At the moment, AD is the most common form of dementia and thus has a large socioeconomic burden. It is estimated that by 2030, more than 70 million people will be living with AD with a healthcare burden of over \$2 trillion (USD) annually worldwide (World Alzheimer Report 2015). Although there are some recent studies to suggest that the incidence of dementia may be decreasing in developed nations, it is important to consider that as lesser-developed countries advance, the number of AD cases worldwide will increase in parallel with the number of aged individuals (Rocca *et al.* 2011; Satizabal *et al.* 2016). Such increases in global AD numbers underline that a persistent research effort is imperative to halting the progression of this disease.

AD predominantly affects the elderly population, with advanced age being the strongest predictor of symptomology (Alzheimer's Association 2014). Gross structural changes in the brain are visible in patients due to neurodegeneration in the neocortex and hippocampus which progresses to other brain areas at advanced stages of disease (Alzheimer's Association 2014). The cortical neuron tissue is also populated by deposits of proteins, which are now recognized as the pathological hallmarks of disease and part of the diagnostic criteria of AD (Serrano-Pozo *et al.* 2011; Dubois *et al.* 2016). Extracellular senile plaques consist

predominantly of the β -amyloid peptide ($A\beta$) (Alzheimer 1907; Alzheimer 1911; Divry *et al.* 1927; Masters *et al.* 1985; Wong *et al.* 1985). The origin of the $A\beta$ peptide was later tracked to the amyloid precursor protein (APP), as a natural cleavage product of this larger transmembrane protein (Haass *et al.* 1992). The second protein pathology that is also part of the diagnostic criteria are intracellular tangles or neurofibrillary tangles (NFTs) which are composed of the microtubule-binding protein, tau (Goedert *et al.* 1988; Kondo *et al.* 1988; Wischik *et al.* 1988). It is worth noting that the AD brain is also characterized by an inflammatory reaction mediated by activated astrocytes and microglia (Heneka *et al.* 2015).

The relationship between the hallmark $A\beta$ and tau pathologies and the progression of disease has been strengthened using biomarkers and diagnostic imaging strategies. Progressive deposition of $A\beta$ in the brain has been investigated using the radioactive amyloid β -binding molecule, Pittsburgh compound B (PiB) paired with positron emission tomography (PET) (Klunk *et al.* 2004). Similar radioactive amyloid binding dyes with a longer half-life have also been used in recent years (Clark *et al.* 2012; Wolk *et al.* 2012). Through PET imaging the longitudinal accumulation of $A\beta$ deposits in brain tissue has been elucidated and confirms the cross-sectional histology stages in post-mortem brain tissue, however, the sensitivity of PET is not optimized for the detection of the earliest $A\beta$ deposits (Thal *et al.* 2002; Thal *et al.* 2015). Additionally, using sensitive immunoassays against $A\beta$, it has been determined that a low concentration of the 42 amino acid long variant of $A\beta$ in the cerebrospinal fluid (CSF) is a strong predictor of cognitive decline (Shaw *et al.* 2009; van Harten *et al.* 2013; Dubois *et al.* 2016). Astonishingly, the changes in CSF $A\beta$ content occur decades before the presence of cognitive symptoms within a patient (Bateman *et al.* 2012; Buchhave *et al.* 2012; Dubois *et al.* 2016). This emphasizes that AD is not only a geriatric disease but also starts early and progresses slowly when considering brain physiology. Similar perturbations in tau physiology can be tracked in the CSF during the progression of AD and, although not as early, CSF-tau levels increase prior to the onset of cognitive decline (Fagan *et al.* 2007; Bateman *et al.* 2012; Buchhave *et al.* 2012; Dubois *et al.* 2016). There are a number of promising imaging molecules being developed for detecting tau pathology, such as flortaucipir and T807, similar to the $A\beta$ radioligands mentioned above, however, their specificity is not yet satisfactory (Brier *et al.* 2016; Pontecorvo *et al.* 2017; Saint-Aubert *et al.* 2017). Together, these analytical methods not only strengthen the link of these proteins to the progression of AD but also give a context for the temporal occurrence of brain

disturbances. This is important for determining whether a patient with cognitive impairment has AD prior to confirmation at autopsy and it also provides a way to track the efficacy of therapeutic agents in clinical trials (Jack *et al.* 2013; Dubois *et al.* 2016; McDade and Bateman 2017).

2.1.2 The amyloid precursor protein and β -amyloid

APP is a single pass type I membrane protein and, although it is better known for its presence in the brain, it is expressed throughout the body (Goldgaber *et al.* 1987; Kang *et al.* 1987; Tanzi *et al.* 1987; Muller *et al.* 2017). In the brain, the 695 amino acid long splice variant is predominantly expressed, while longer variants (751 and 770 mostly) are found in non-neuronal tissue (Muller *et al.* 2017). Research into the function of APP as a membrane protein has yielded a number of diverse roles (Muller *et al.* 2017). Specifically, there has been evidence to show that APP is involved in cell adhesion and neurite outgrowth through interactions between the extracellular portion and extracellular matrix proteins (Soba *et al.* 2005; Olsen *et al.* 2014; Muller *et al.* 2017). However, when the APP protein is deleted in mice, there are no severe phenotypes, suggesting that redundant functions by the APP family of proteins are compensated for by APP loss (Zheng *et al.* 1995; Muller *et al.* 2017).

Cleavage Pathways

The APP protein is not only present as a full-length membrane protein but is also cleaved by secretases generating multiple peptide fragments. The most common pathway is referred to as the non-amyloidogenic pathway where the initial cleavage is made by α -secretase (α -secretase disintegrin and metalloproteinase domain-containing protein 10, ADAM10) yielding a soluble extracellular fragment of APP (sAPP- α) and the membrane bound C-terminal C83 fragment (**Figure 1**; Kuhn *et al.* 2010). This fragment is then further processed by the γ -secretase complex, producing the APP intracellular domain (AICD) and p3 peptides (Takami *et al.* 2009). The sAPP- α fragment is important for long-term potentiation (LTP) and even rescues some of the subtle deficits seen in APP knock-out mice (Ring *et al.* 2007; Taylor *et al.* 2008). AICD has been linked to transcriptional regulation, while the function of p3 has not been clearly identified (Cao and Sudhof 2001; Gao and Pimplikar 2001; Muller *et al.* 2017). Thus, it seems that not only full-length APP, but also the fragments generated by cleavage have a role in brain physiology.

APP can alternatively be processed through the amyloidogenic pathway, which is associated with the disease state in AD (**Figure 1**). In contrast to the above pathways, the initial cleavage of APP is carried out by the β -secretase, β -site APP cleavage enzyme 1 (BACE1) which is the BACE isoform expressed in the brain (Vassar *et al.* 2014). Cleavage of APP by BACE1 generates a shorter soluble fragment (sAPP- β) than the non-amyloidogenic pathway (Vassar *et al.* 2014). The remaining C-terminal fragment, C99, is then cleaved by the γ -secretase complex and, similar to the non-amyloidogenic pathway, generates the AICD peptide but releases the disease-associated A β peptide as well (De Strooper *et al.* 1998; Wolfe *et al.* 1999). The A β peptide has been extensively studied to determine its amyloidogenic properties and their contribution to disease.

More recently, another cleavage pathway has been identified that generates a peptide with neurotoxic features and is referred to as the η -secretase pathway (**Figure 1**; Willem *et al.* 2015). In this pathway, η -secretase, suggested to be the matrix metalloprotease MT5-MMP, cleaves the APP protein releasing a soluble fragment (sAPP- η) while subsequent cleavage by either α - or β -secretase generates the A η peptide (A η - α or A η - β , respectively) (Willem *et al.* 2015). This small, extracellularly shed fragment, A η - α , has synapse impairing properties both in cell culture and *in vivo* (Willem *et al.* 2015). Surprisingly, it was also found that inhibition of β -secretase causes an increase in A η - α , suggesting that such therapeutic interventions can have unintended and potentially detrimental effects on patient health through the generation of neurotoxic peptides (Willem *et al.* 2015). The elucidation of the η -secretase pathway has added another dimension to APP cleavage and the fragments generated by physiological processing.

Mechanism of γ -secretase cleavage

The generation of multiple different amino acid length species of A β is largely controlled by the γ -secretase complex mentioned above, which is a membrane bound secretase capable of intramembranous cleavage of proteins (Voytyuk *et al.* 2017). This phenomenon was first discovered with the γ -secretase complex but similar intramembranous cleavage has since been identified for other proteins (De Strooper *et al.* 1998; Wolfe *et al.* 1999; Voytyuk *et al.* 2017). The γ -secretase multi-protein complex comprises nicastrin, anterior pharynx-defective-1, presenilin enhancer 2 and presenilin-1 or 2 (PSEN1 or 2). Either PSEN1 or 2 is

the catalytic subunit of γ -secretase responsible for cleaving the APP protein, and, as mentioned above, liberates A β at the carboxy-terminus from the membrane associated C99 fragment (De Strooper *et al.* 1998; Wolfe *et al.* 1999). Recently, a study demonstrated that PSEN1 and PSEN2 have distinct subcellular locations, with PSEN1 being found throughout the cell and PSEN2 localizing to the endosomes (Sannerud *et al.* 2016). This leads to an intracellular pool of longer A β peptides when APP is processed by PSEN2, demonstrating that while both active subunits cleave the C-terminal fragment, the subcellular location determines their effect on APP physiology (Sannerud *et al.* 2016). In general, it is known that A β exists as multiple different length variants at both termini of the peptide, including N-terminal pyroglutamation at position 3 or 11 within the brain (Mori *et al.* 1992; Naslund *et al.* 1994; Saido *et al.* 1996; Portelius *et al.* 2010). Recently, the precise mechanism for the generation of different C-terminal variants of A β was described (Takami *et al.* 2009; Bolduc *et al.* 2016). It was shown that γ -secretase cleaves the peptide in a sequential tripeptide fashion (Bolduc *et al.* 2016). In other words, C99 is cut by PSEN1 and subsequent cleavage occurs three amino acids closer to the N-terminus with this process occurring multiple times (Bolduc *et al.* 2016). This process also validated previous work showing that there are two pathways of A β generation, one generating A β ending in amino acid 40 (A β 40) (A β 49-->46-->43-->40) and another generating A β ending in amino acid 42 (A β 42) (A β 48-->45-->42-->38) (**Figure 1**; Takami *et al.* 2009; Bolduc *et al.* 2016). A β 40 and A β 42 are the two peptide-variants most abundant in the AD brain and have been recently suggested to prefer different sites of deposition, with A β 40 in the vasculature as cerebral amyloid angiopathy and A β 42 in parenchymal plaques (Kakuda *et al.* 2017). A β 42 is the more aggregation prone variant and, consequently, has been a focus of studies on the pathogenicity of A β and the progression of disease through its use as a biomarker (Jarrett *et al.* 1993; Haass and Selkoe 2007; Shaw *et al.* 2009; Bateman *et al.* 2012).

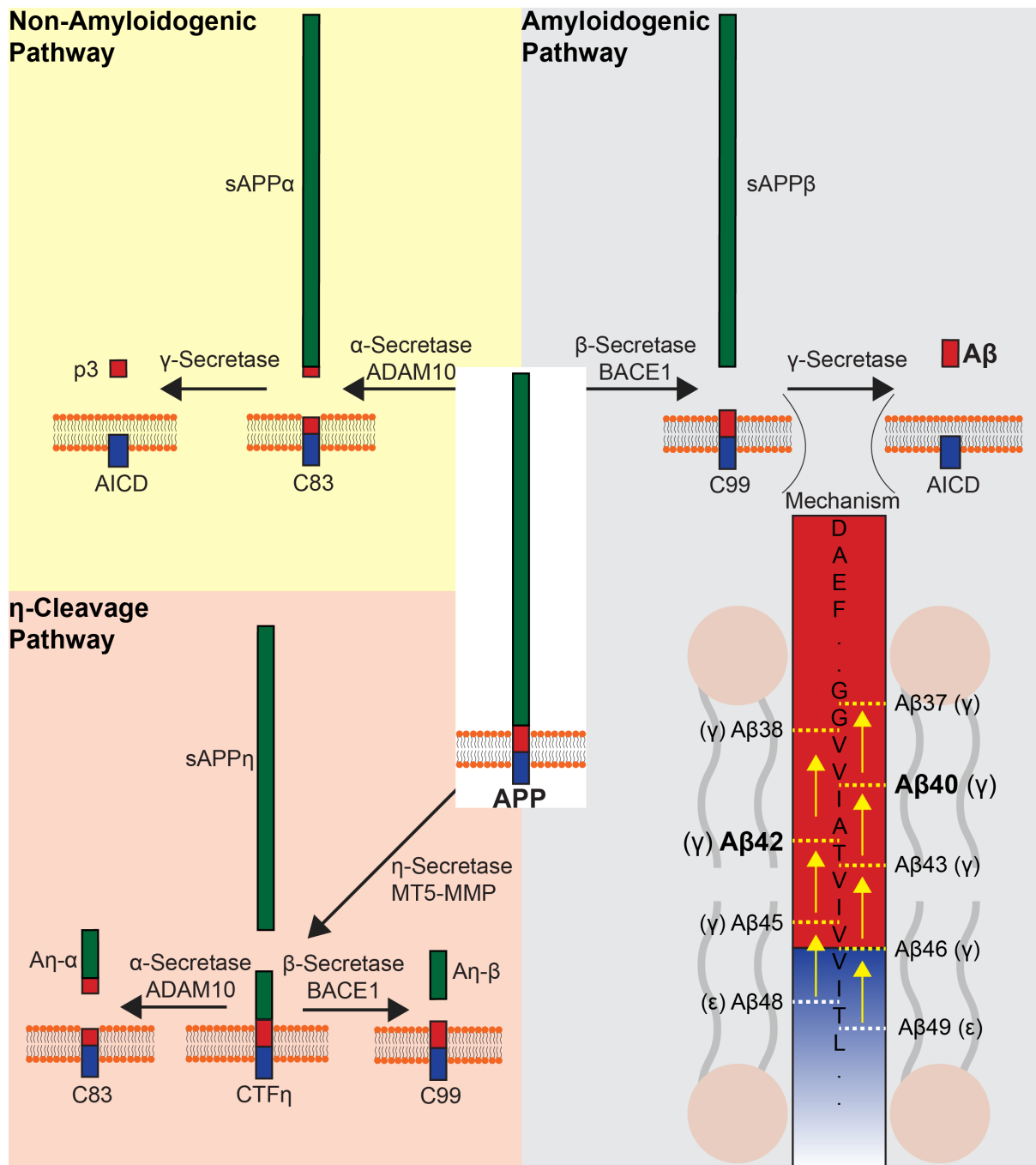


Figure 1. APP cleavage pathways and the mechanism of γ -secretase tripeptide cleavage. The non-amyloidogenic pathway proceeds with α -secretase (ADAM10) cleavage of APP releasing sAPP α , followed by γ -secretase cleavage of C83 to produce AICD and p3. Conversely, the η -cleavage pathway has an initial cleavage of APP by η -secretase (MT5-MMP) that releases sAPP η . The remaining CTF η peptide (approximate peptide length of 190 aa) can be cleaved by either β -secretase (BACE1) or α -secretase that produces A η - β or the neurotoxic A η - α peptide, respectively. The amyloidogenic pathway proceeds with β -secretase cleavage of APP (releasing sAPP β) then γ -secretase cleavage of C99. The γ -secretase complex processes C99 with an initial ϵ -cut (A β 48 or A β 49) and then sequential carboxypeptidase cleavage (γ) in three peptide intervals (tripeptide cleavage). This releases the disease associated A β peptide, where two separate pathways generate A β 40 and A β 42.

Genetics of familial AD

The APP protein and its cleavage has also been linked to AD through dominantly inherited mutations in APP and the PSEN1&2 proteins that lead to the familial form of AD (fAD) (Goate *et al.* 1991; Sherrington *et al.* 1995; Karch and Goate 2015). This class of AD is not common and only explains approximately 1% of all positively identified cases (Alzheimer's Association 2014). In general, all of these mutations have been implicated in altering the processing of APP by the secretases described above (Voytyuk *et al.* 2017). A number of mutations in APP itself cluster around the two cleavage sites in the amyloidogenic pathway for β -secretase and γ -secretase (Goate *et al.* 1991; Murrell *et al.* 1991; Mullan *et al.* 1992). This has been suggested as causing an important alteration in APP cleavage, leading to an increased production of longer isoforms of A β (Szaruga *et al.* 2017; Voytyuk *et al.* 2017). As described above, an increase in A β 42 has been linked to disease given its aggregation prone and neurotoxic nature (Jarrett *et al.* 1993; Haass and Selkoe 2007). Additionally, mutations in the catalytic γ -secretase protein, PSEN1, generally have increased production of A β species in cell assays, and more specifically the longer forms of A β , including A β 42 (Szaruga *et al.* 2015). Recently, a more mechanistic understanding of the effect of mutations in the PSEN proteins has been realized. Specifically, the efficiency of cleavage at the γ -secretase site in APP is decreased in a number of PSEN mutations (Szaruga *et al.* 2015; Szaruga *et al.* 2017). This has implications given the tripeptide cleavage mechanism of γ -secretase, whereby less efficient cutting will lead to a premature release of the substrate (C99) from the substrate-enzyme complex (C99-PSEN) and consequently a longer A β species (Bolduc *et al.* 2015; Szaruga *et al.* 2017). This was similarly shown for APP mutations, where longer A β fragments were released by wildtype PSEN1 (Szaruga *et al.* 2017). This demonstrates the precise mechanism behind many mutations causing fAD and how changes in APP processing are linked to disease.

An interesting parallel to fAD mutations is the increased risk of AD in human subjects with Down's syndrome. This genetic disorder is caused by trisomy of chromosome 21, which leads to distinctive cranial development and mental retardation (Rovelet-Lecrux *et al.* 2006). The APP gene is located on chromosome 21 and the overexpression of APP protein leads to an early presence of A β plaque pathology (Rovelet-Lecrux *et al.* 2006). Consequently, these subjects will commonly develop full-blown AD if an advanced age is reached. As such, both

fAD and Down's syndrome demonstrate that changes in A β physiology within the brain are at the root of AD.

Sporadic AD and risk factors

The other and most common form of AD is known as sporadic AD (sAD) and, as the name suggests, does not have a defined cause. It is considered to be a multi-factorial form of AD with a complex etiology leading to neurodegeneration. Despite the different origin, sAD is still quite similar to fAD in terms of the presence of senile plaques and NFT at autopsy and their disease progression (Day *et al.* 2016). Genome-wide association studies (GWAS) have provided a wealth of information about genetic risk factors for developing AD (Karch and Goate 2015). There are a small number of genes that confer a moderate risk for AD, while at the same time have a moderate abundance in the human population (Karch and Goate 2015). Both TREM2 and ApoE4 are such gene products and have been extensively studied to determine their involvement in AD (Karch and Goate 2015). Physiologically, the ApoE proteins are involved in cholesterol metabolism through binding to low-density and very low-density lipoproteins (LDL and vLDL, respectively) (Mahley *et al.* 1988). From a disease perspective, the ApoE proteins show an affinity for A β binding which has been linked to A β clearance from the brain (Kim *et al.* 2009). A recent study further solidified this link using a novel bioengineered blood vessel model (Robert *et al.* 2017). The ApoE4 variant has also been suggested to facilitate A β aggregation and production (Hashimoto *et al.* 2012; Huang *et al.* 2016). These findings support recent work showing that ApoE4 plays an important role in enhancing the onset of A β plaque deposition (Huynh *et al.* 2017; Liu *et al.* 2017). When considering the TREM2 protein there is also a connection to A β but instead through microglia, the phagocytic immune cells of the brain. Microglia have an activated morphology in AD and cluster around A β plaques, while having the ability to engulf and degrade A β (Bard *et al.* 2000; Bolmont *et al.* 2008; Heneka *et al.* 2015). TREM2 expression on microglia is crucial for these behaviors and consequently limits neuritic injury caused by plaques (Kleinberger *et al.* 2014; Wang *et al.* 2016). Mutations in TREM2 linked to AD also confer a reduced phagocytic capacity of microglia (Schlepckow *et al.* 2017). Recent studies have even implicated TREM2 in mediating the removal of A β after immunotherapy (Xiang *et al.* 2016). Interestingly, a link between TREM2 and ApoE in cerebral β -amyloidosis has been identified through the transcriptional signature of microglia and a mechanism where a TREM2-ApoE complex facilitates A β phagocytosis by microglia (Yeh *et al.* 2016; Krasemann *et al.* 2017).

As is apparent, the clearance of A β from the brain is important for normal brain physiology and as such has been hypothesized as a general cause of sAD (Wang *et al.* 2017). There are a number of degradation pathways that include proteolytic degradation both intracellularly in glial cells of the brain or extracellularly (Heneka *et al.* 2015; Tarasoff-Conway *et al.* 2015). Substantial clearance of the A β peptide also occurs through bulk flow of the interstitial fluid (Tarasoff-Conway *et al.* 2015; Wang *et al.* 2017). The A β within these fluids can then cross to the blood circulation through receptor mediated pathways or absorption (Tarasoff-Conway *et al.* 2015; Wang *et al.* 2017). Once in the periphery, degradation can occur in peripheral immune cells or within the hepatocytes of the liver (Tarasoff-Conway *et al.* 2015; Wang *et al.* 2017). The risks of sAD as briefly shown here, outline that a number of these factors can be directly linked to the A β peptide, similar to fAD.

Amyloid Cascade Hypothesis

One of the most widely accepted mechanistic frameworks for explaining AD pathogenesis is the amyloid cascade hypothesis and is based off the central role that the A β peptide has in the disease, as indicated above (Selkoe and Hardy 2016). In this framework that applies to both fAD and sAD, increased levels of A β in the brain lead to aggregation and the formation of oligomers (Selkoe and Hardy 2016). These A β species eventually deposit in the parenchyma leading to an inflammatory response and changes in synapse biology, such as an increased excitability (Selkoe and Hardy 2016). In later stages of the cascade, hyperphosphorylated tau mislocalizes in the soma of neurons (Selkoe and Hardy 2016). Finally, this tau alteration causes NFT formation and neuronal death occurs, leading to the clinical presentation of cognitive decline in patients (Selkoe and Hardy 2016). Some of the strongest support for this hypothesis lies in the dominantly inherited genetic data, where only mutations affecting the APP protein and its processing are guaranteed to cause AD (Karch and Goate 2015; Selkoe and Hardy 2016). Furthermore, a protective mutation in *APP*, *A673T*, identified in an Icelandic population, lends strong support to the amyloid cascade hypothesis (Jonsson *et al.* 2012). Interestingly, although tau is a pathological hallmark of AD and correlates strongly with cognitive decline, there are no tau mutations linked to AD, suggesting that changes in A β are a crucial event in AD (Karch and Goate 2015; Polanco *et al.* 2018). As outlined in the amyloid cascade hypothesis it seems likely that the temporal occurrence of A β and then tau may also explain the genetic importance of A β in AD (Selkoe and Hardy 2016). Although it is proposed as a rather linear model of disease progression, there is discussion about the

precise order of these steps and how each of these interacts with each other (De Strooper and Karran 2016). It seems likely, that after an initial “hit” caused by A β misfolding, changes in tau and neuroinflammation will interact with A β and each other on multiple levels to cause neuronal death and a feed-forward mechanism. Some alternative hypotheses exist for AD, such as the cholinergic hypothesis and cardiovascular hypothesis. The cholinergic hypothesis focuses on the fact that cholinergic neurons in the basal forebrain degenerate during AD while the cardiovascular hypothesis views AD as a disease centered around impaired circulation and vascular abnormalities (Francis *et al.* 1999; de la Torre 2010). Although these and other hypotheses do focus on an AD related physiological abnormality, they do not have the strength of the amyloid cascade hypothesis in explaining the molecular mechanism leading to brain pathology and dysfunction.

Experimental models of AD

The occurrence of AD is a uniquely human affliction with no other species displaying the full pathologies and typical AD cognitive deficits (Walker and Jucker 2017). Even in non-human primates that reach significantly advanced age there is not the same pairing of A β and tau protein deposits in relevant brain regions (Walker and Jucker 2017). This is an intriguing phenomenon that begs the question of what makes humans so vulnerable to this devastating disease. Research into the mechanisms of AD has aimed at overcoming this hurdle using transgenic mouse models expressing human forms of APP and tau (Gotz and Ittner 2008). A number of the models for AD pathology have focused on a single pathology, namely A β or tau. It must be noted that the transgenic mice developing tau pathology as NFT contain tau mutations that are not associated with AD, questioning the relevance of these models to AD specifically (Gotz and Ittner 2008). However, a number of different mouse models have been developed that demonstrate robust A β plaque pathology. Two well-studied models of cerebral β -amyloidosis are the APP23 and APPPS1 mouse lines (Sturchler-Pierrat *et al.* 1997; Radde *et al.* 2006). Each transgenic model overexpresses the human APP protein (APP23 7-fold; APPPS1 3-fold) containing the Swedish double mutation (*KM670/671NL*) under the control of the Thy1 neuronal promoter (Sturchler-Pierrat *et al.* 1997; Radde *et al.* 2006). In addition, the APPPS1 transgenic line expresses mutated human PSEN1 (*L166P*) under the same Thy1 promoter (Radde *et al.* 2006). The APP23 model demonstrates a late-onset of pathology at approximately 6 months of age with larger parenchymal deposits and cerebral amyloid angiopathy (Sturchler-Pierrat *et al.* 1997). Alternatively, the APPPS1 model

has an early onset of 1.5 months and, with aging, plaques are comparatively smaller and more numerous than in APP23 (Radde *et al.* 2006). These transgenic models, as well as a number of others have been used to learn more about the exclusive effects of A β on the neuronal environment and how immune cells like microglia and astrocytes react to these pathologies (Gotz and Ittner 2008).

Models of cerebral β -amyloidosis are powerful tools for investigating the deposition of A β *in vivo* and the structure of amyloids in tissue, but it is worth noting some of the limitations when investigating physiological effects of A β pathology. For example, a number of these transgenic mice do not have significant neuronal loss (Gotz and Ittner 2008; Sasaguri *et al.* 2017). Furthermore, most of these models overexpress a human protein that is under the control of a non-endogenous promoter (Sturchler-Pierrat *et al.* 1997; Radde *et al.* 2006; Gotz and Ittner 2008; Saito *et al.* 2014; Sasaguri *et al.* 2017). This produces an extra-physiological situation where it can be difficult to distinguish between effects caused directly by the intended transgenic alteration and the unintended alterations caused by disruptions to the host genome during integration or changes to the cellular physiology when a foreign protein is massively produced (Saito *et al.* 2014; Saito *et al.* 2016). Recently a novel model of β -amyloidosis was developed using a knock-in strategy (Saito *et al.* 2014). With this strategy, Saito and colleagues (2014) were able to produce transgenic mice expressing humanized APP at physiological levels and under the control of the endogenous promoter. The study took advantage of different fAD mutations, including the previously mentioned Swedish mutation (*KM670/671NL*) and the Arctic (*E693G*) and Iberian (*I716F*) mutations in *APP* (Saito *et al.* 2014). From a pathology perspective, these transgenic mice harbor A β deposits with associated inflammatory reaction of microglia and astrocytes, demonstrating that these mice can also be used as models of cerebral β -amyloidosis (Saito *et al.* 2014).

Given that AD is a dual pathology disease without any associated dominantly inherited tau mutations, it is important to consider the best strategies to model the full spectrum of AD pathology *in vivo*. A recent study showed that tau pathology could be induced in wild-type mice when intracerebrally inoculated with insoluble tau extracted from AD brains (Guo *et al.* 2016). Tau pathology was shown to spread through functionally connected neuronal networks, providing further support that this model mirrored physiological phenomenon identified in AD (Jucker and Walker 2013; Brettschneider *et al.* 2015; Guo *et al.* 2016). As

an extension of this novel model for AD-relevant tau pathology, a subsequent study paired the introduction of exogenous AD tau with different models of cerebral β -amyloidosis to produce a compelling AD model (He *et al.* 2017). The study determined that the presence of A β plaques resulted in pathological tau in dystrophic neurites initially but later as neurofibrillary tangles and neuropil threads in distal brain areas (He *et al.* 2017). Another recent study was able to demonstrate AD pathology *in vivo* by injecting neurons derived from human stem cells into the brain of APP transgenic mice, resulting in tau hyperphosphorylation and death of human neurons (Espuny-Camacho *et al.* 2017). The further development of AD models will advance our understanding of neurodegeneration in AD and the molecular mechanisms driving disease.

2.1.3 The protein-only hypothesis: a unifying concept of disease

The protein-only hypothesis was first proposed for a perplexing set of disorders called prion diseases that defied explanation for years (Prusiner 1982). Prion diseases are a class of severe neurodegenerative maladies, first identified in sheep with scrapie, a condition named after the excessive scratching phenotype in these animals (Stockman 1913). A number of other species are susceptible to prion diseases or transmissible spongiform encephalopathies (TSE), as they are also known (Collinge 2001). One of the most famous forms of prion disease is that affecting cattle, known as bovine spongiform encephalopathy (BSE) or, more colloquially, mad cow disease (Wilesmith *et al.* 1988). Cattle suffering from the disease present with severe neurological symptoms including abnormal gait, exaggerated motor reactions and in the latest stages an inability to stand (Wilesmith *et al.* 1988). From a pathology standpoint, the brain in TSE-infected organisms has a spongy appearance under the microscope due to massive neuronal death caused by the misfolded prion protein, PrP^{TSE}, which deposits in the brain (Beck and Daniels 1987). This PrP^{TSE} agent is derived from misfolding of the physiological, membrane-associated cellular form of the prion protein termed PrP^C (Borchelt *et al.* 1990; Caughey and Raymond 1991).

Prion diseases have also been identified in the human population and can have a number of origins. The most common form of prion disease is sporadic Creutzfeldt-Jakob Disease (sCJD) and does not have a defined single-factor cause but genetic risk factors have been identified (Palmer *et al.* 1991; Collinge 2001). There are rare genetic forms of prion disease

such as Gerstmann-Straussler-Scheinker syndrome, which are caused by mutations in the PrP^C encoding gene, *PRNP* (Hsiao *et al.* 1989). Additionally, there are forms of CJD that are linked to an exogenous introduction or infection with the PrP^{TSE} agent (Collinge 2001). These are referred to as iatrogenic CJD (iCJD), caused by an exposure to PrP^{TSE}-contaminated medical instruments, and variant CJD (vCJD), which is linked to consumption of beef products tainted with PrP^{TSE} (Collinge *et al.* 1991; Collinge *et al.* 1996; Thomas *et al.* 2013). Kuru is another unique example of prion disease similar to vCJD caused by ritualistic cannibalism in the tribal Fore people of Papua New Guinea (Klatzo *et al.* 1959; Gajdusek *et al.* 1966; Alpers 1987). These last three forms of CJD are central to the controversial history of prion diseases as being infectious but not caused by a classic virus or microorganism.

Initially, prion diseases were thought to be caused by a slow virus, which led to severe neurodegeneration without a correspondingly severe inflammatory response (Gajdusek 1977). Purification of the infectious agent proved challenging for a number of years and puzzled researchers because infectivity was not easily biochemically fractionated (Prusiner 1982; Meyer *et al.* 1986). Additionally, foreign genetic material was never consistently identified (Alper *et al.* 1966; Alper *et al.* 1967; Prusiner 1982). Decades of rigorous experimentation by numerous groups led to the delineation of the protein-only hypothesis, positing that the infectious unit was devoid of nucleic acid and was a misfolded protein (Griffith 1967; Prusiner 1982). Although quite controversial at the time, this hypothesis has been further supported by research in recent years. One of the most important supports of this hypothesis was the generation of infectious PrP^{TSE} from defined synthetic components (Legname *et al.* 2004; Deleault *et al.* 2007; Colby *et al.* 2009; Wang *et al.* 2010). This avoided any confounding factors when purifying the infectious agent from brain material where multiple different molecules are also purified. The exceptional stability of PrP^{TSE} to physicochemical treatments like heat and fixation with formaldehyde was another factor that provided evidence that a bacterial or viral agent was not the culprit for prion disease (Brown *et al.* 1990; Zobeley *et al.* 1999). This recalcitrant phenotype is derived from the structural change that occurs during the transition from α -helical PrP^C to the β -sheet enriched PrP^{TSE} form. The PrP^{TSE} agent has long been known to contain an enriched β -sheet structure and a recent study provided a more detailed view of an organized PrP^{TSE} amyloid fibril (Bolton *et al.* 1982; Vazquez-Fernandez *et al.* 2016). Amyloid is a general quaternary structural motif defined by the ordered stacking of β -sheet segments that extend as an elongated fibril

(Eisenberg and Jucker 2012). Biophysically, this leads to a distinctive x-ray diffraction pattern when the beam is directed perpendicular to the fibril axis with a signal at 4.7Å and 10Å (Eisenberg and Jucker 2012). The mechanism behind the infectious nature of PrP^{TSE} is hypothesized as the ability of PrP^{TSE} to induce PrP^C misfolding (Borchelt *et al.* 1990; Caughey and Raymond 1991). Although the experimental proof of this specific misfolding event at the molecular level is still lacking, experiments using transgenic mice devoid of PrP^C demonstrated that these animals are completely resistant to prion disease, emphasizing the key role of PrP^C as a substrate (Bueler *et al.* 1993).

Expanding prion concepts to neurodegenerative disease

Although the protein-only hypothesis of prion diseases was controversial at its inception, this new concept for a disease-causing agent has gained popularity for other diseases where protein pathologies occur (Prusiner 2013; Walker and Jucker 2015; Collinge 2016; Rasmussen *et al.* 2017a). Indeed, many neurodegenerative diseases characterized by deposits of misfolded proteins like AD are being investigated for prion-like qualities (Walker and Jucker 2015). A number of studies working with autopsy tissue from individuals of varying age and disease status (healthy to severe disease) have facilitated models for staging neurodegenerative diseases based on the location of protein deposits (Brettscheider *et al.* 2015). Pathologies in a number of diseases were determined to spread in a stereotypical manner, rather than appearing randomly, suggesting that a common mechanism, similar to the prion model of induced misfolding could exist (Jucker and Walker 2013; Brettschneider *et al.* 2015).

When specifically considering A β , there have been quite some parallels drawn to the protein-only hypothesis of PrP^{TSE} that have resulted in a prion-like definition (Rasmussen *et al.* 2017a). In the case of AD, cross-sectional human studies have demonstrated A β pathology spreading, which has led to a staging rubric along with tau pathology, but investigations in transgenic mice have more clearly demonstrated that pathology spreads through the brain along functionally connected networks (Clavaguera *et al.* 2009; Nath *et al.* 2012; Domert *et al.* 2014; Brettschneider *et al.* 2015; Calafate *et al.* 2015; Ye *et al.* 2015). Extending the prion-like moniker even further, A β has well documented amyloid tendencies and traditional staining methods for A β plaques include the amyloid specific dye, Congo Red (Divry *et al.* 1927). However, it is worth mentioning that both PrP^{TSE} and A β can form aggregated species

that are not in an ordered amyloid assembly but are still disease associated (Langer *et al.* 2011; Philipson *et al.* 2012; Alibhai *et al.* 2016; Rasmussen *et al.* 2017a). Aggregated A β is also extremely stable when exposed to proteases, fixatives, heat and denaturants, which parallels the PrP^{TSE} agent (Meyer-Luehamann *et al.* 2006; Langer *et al.* 2011; Fritschi *et al.* 2014b; Watts *et al.* 2014).

The parallels drawn between AD and prion diseases spawning the prion-like definition has provided an invaluable road map for investigating molecular features of neurodegeneration (Walker and Jucker 2015; Rasmussen *et al.* 2017a). Using these principles, the role of A β in initiating disease and influencing phenotypic diversity has been advanced in recent studies to further validate targeting this misfolded protein for the development of therapeutic interventions.

2.2 Heterogeneity of β -amyloid aggregates in Alzheimer's disease

2.2.1 Fibrillar β -amyloid structures and deposits

The assembly of proteins into fibrillar amyloid aggregates is a well-defined phenomenon that occurs both in health and disease for multiple proteins but this quaternary structural motif can have varied characteristics (Riek and Eisenberg 2016). The β -sheet rich structures are typically arranged into extended fibrils at later stages of aggregation and can be classified based on the orientation of β -sheets (Tycko 2015; Riek and Eisenberg 2016). Namely, β -sheets can be oriented in a parallel, anti-parallel or β -hairpin anti-parallel fashion and in all of these cases, the side groups of the β -sheet interdigitate and form a stable steric zipper (**Figure 2**; Eisenberg and Jucker 2012; Tycko 2015). The A β peptide is capable of both parallel and anti-parallel orientations *in vitro* and *in vivo* (Qiang *et al.* 2012; Lu *et al.* 2013; Xu *et al.* 2016). At the mesoscopic level, A β fibrils also vary based on their width, crossover rate and fibril mass per length, which can be distinguished by electron microscopy (Petkova *et al.* 2005). These experiments largely rely on *in vitro* fibrillization of A β , where different conditions of fibril growth, like agitation and salt concentration, lead to different fibril characteristics (Qiang *et al.* 2012; Tycko *et al.* 2015;). Interestingly, it has been shown for a different protein (β -endorphin) that amyloid fibrils can have distinct mesoscopic properties, like the presence of crossovers while having the same atomic structure (Seuring *et al.* 2017). However, these subtle differences in A β fibril structure within a sample provide a hurdle to

gaining structural information from a fibril sample, as homogeneity is required for most structural biology techniques (Meier *et al.* 2017).

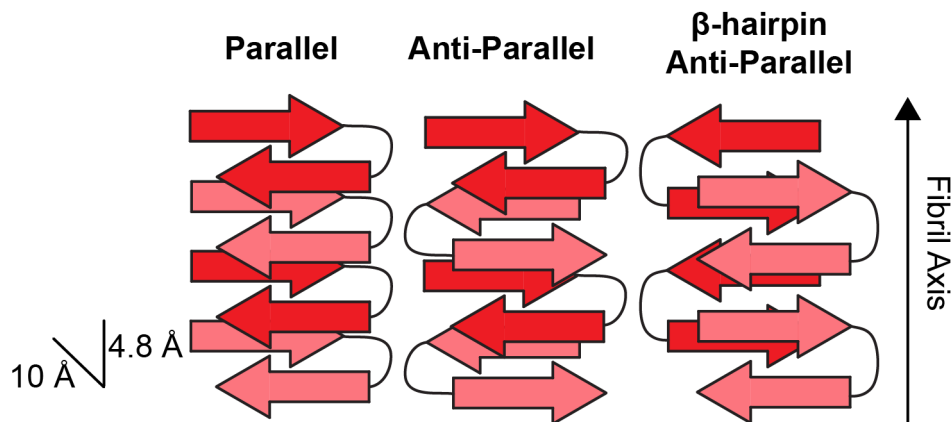


Figure 2. Various orientations of β -sheet organization within a fibril. A peptide with two β -sheet segments can organize as parallel, anti-parallel or β -hairpin anti-parallel in an amyloid fibril, which is determined by the stacking of β -sheets and the direction of adjacent β -sheets along the fibril axis.

A β fibril structure

The detailed structure of A β in pathogenic aggregates is a central focus of AD research in order to better understand the complexity of these pathologies. However, an accurate elucidation of A β structural information is hindered by the insoluble nature of the aggregated protein complexes. Therefore, methods have been developed in order to gain high-resolution information from amyloid fibrils. Solid-state nuclear magnetic resonance (ssNMR) is one of these methods, where detailed information can be gained about the structure of amyloids through the interaction of carbon and nitrogen nuclei (Meier *et al.* 2017). Additionally, scanning electron microscopy (SEM) and the more recent method cryo-electron microscopy (cryo-EM) have been used to determine the structure of A β using visual information obtained from an electron beam (Schmidt *et al.* 2009; Schmidt *et al.* 2015; Gremer *et al.* 2017). A significant problem with determining the structure of A β is that fibrils need to have a high concentration but also need to be of suitable purity and homogeneity. Therefore, the methods for obtaining high-resolution information rely either on purely *in vitro* made fibrils or *in vitro* amplified brain derived A β . In recent years, the structure of *in vitro* A β 40 was shown with SEM to be constructed from two dimer protofilaments, with the C-terminus being involved in the fibril core and the N-terminus having a less defined structure (Schmidt *et al.* 2009). Conversely, in the same study the structure of an *in vitro* A β 42 fibril contained only a single dimer protofilament but the C-terminus also populated the fibril core (Schmidt *et al.* 2009).

In a subsequent study using cryo-EM, A β 42 again showed a single dimer protofilament unit, however there was an extended interface between dimers in the fibril core due to a kinked C-terminus (Schmidt *et al.* 2015). In all of these cases the A β peptide is oriented as a “U” shape with two β -sheet segments adjacent to each other. Other structures of *in vitro* A β 42 have suggested that the peptide has an “S” shape with three β -sheets in a single peptide and a single dimer protofilament in the fibril (Xiao *et al.* 2015; Walti *et al.* 2016; Gremer *et al.* 2017). In two of these structures, the use of ssNMR revealed that the N-terminus was not involved in the fibril core similar to previous studies (Xiao *et al.* 2015; Walti *et al.* 2016). Surprisingly, one structure of *in vitro* A β 42 using both cryo-EM and ssNMR has suggested that the entire peptide length is involved in the fibril core (Gremer *et al.* 2017). It has been suggested that these differences in atomic structure for A β 40 and A β 42 lead to a single A β species creating a homogeneous fibril composition (Xiao *et al.* 2015). Although some of these studies demonstrated that fibrils were cytotoxic in neuronal culture and contained structural features similar to *in vivo* pathology, they were generated with purely *in vitro* A β (Walti *et al.* 2016; Gremer *et al.* 2017). The pathogenic potential of *in vitro* A β has been questioned in previous research studies using *in vivo* derived A β aggregates (Meyer-Luehmann *et al.* 2006; Novotny *et al.* 2016). In an effort to resolve the structure of *in vivo* A β , fibrils grown from patient brain material have been analysed with ssNMR, avoiding the need for complex purification methods (Lu *et al.* 2013). This innovative method revealed that the structure of A β fibrils were different when derived from *in vivo* samples compared to traditional *in vitro* fibrils (Lu *et al.* 2013). One caveat to the *in vitro* propagation of *in vivo* A β is that it is unclear how representative these structures are within the brain and it is possible that a selection bias occurs. This is a well-described methodological issue for structural biology when using *in vitro* A β fibrils, where strict growth conditions must be used to produce a homogeneous fibril morphology that can then be resolved (Meier *et al.* 2017). Thus, growth conditions for fibrils can heavily influence the atomic structure and result in the selection of a single morphotype. The structural analysis of fibrils has provided atomic level detail but the pathological deposits of A β at the tissue level are also important to consider.

A β pathologies

In the progression of AD, it is well known that A β pathology can present in different forms. The earliest histological analysis of AD brain material described senile plaques, which were later identified as being made up of A β primarily (Alzheimer 1907; Divry *et al.* 1927; Wong

et al. 1985; Masters *et al.* 1985). Additionally, A β can be deposited within the vasculature and is referred to as cerebral amyloid angiopathy or CAA, which can cause brain hemorrhaging (Glenner and Wong 1984). Distinguishing CAA from plaques is straightforward given their distinct locations, however neuropathologists have classified senile plaques into different categories using A β specific antibodies and amyloid dyes. Plaques can generally be classified as either dense-cored or diffuse (Thal *et al.* 2006; Serrano-Pozo *et al.* 2011). As the name suggests, dense core plaques have a core which is positive for amyloid dyes like Congo Red or Thioflavin T, indicative of an ordered amyloid arrangement, while diffuse plaques lack this amyloid positive staining (Thal *et al.* 2006; Serrano-Pozo *et al.* 2011). Diffuse plaques are considered to be less important for AD progression and are more associated with a general aging phenotype (Thal *et al.* 2006; Serrano-Pozo *et al.* 2011). Conversely, dense-cored plaques are considered to be specific for AD and are also the site of severe inflammation with activated microglia and reactive astrocytes (Serrano-Pozo *et al.* 2011; Heneka *et al.* 2015). Abnormal neuronal processes called dystrophic neurites, which are thought to be the main cytotoxic consequence of senile plaques, also surround these dense-cored plaques (Thal *et al.* 2006; Serrano-Pozo *et al.* 2011). Dystrophic neurites can be identified by a number of different markers, one of which being hyperphosphorylated tau, the main component of NFTs (Serrano-Pozo *et al.* 2011). A β deposits have been further distinguished based on the location and the morphology of A β staining (Tagliavini *et al.* 1988; Yamaguchi *et al.* 1988; Ikeda *et al.* 1989; Wisniewski *et al.* 1989; Dickson and Vickers 2001; Maarouf *et al.* 2008). In addition to these extracellular pathologies of A β , it is also now clear that intracellular deposits can exist (LaFerla *et al.* 2007). However, the exact role of intracellular A β aggregates in disease is unclear, with some debate over whether this pathology occurs before or after extracellular deposits (LaFerla *et al.* 2007). The above classification of A β neuropathology has provided an overview of how pathology can appear in AD but bridging this information with detailed structural studies has been a challenge.

Recently, classes of amyloid binding dyes called luminescent conjugated oligothiophenes (LCO) have provided an additional, unique tool for investigating aggregated protein deposits. These dyes contain multiple aromatic rings and bind to the repetitive β -sheet backbone in amyloids (Aslund *et al.* 2009). The specificity of this binding interaction can be further tailored by changing the number of rings in the LCO (Aslund *et al.* 2009; Herrmann *et al.* 2015). This strong and specific binding is derived by the interaction between anionic side

groups of the LCO and the cationic amyloid residues, as the LCO lies parallel to the fibril axis (Herrmann *et al.* 2015; Schütz *et al.* 2017). Interestingly, the binding site of LCOs is distinct from the radiographic A β imaging compound Pittsburgh compound B (PiB) but is similar to X-34, an analogue of Congo Red (Bäck *et al.* 2016). The binding potential of LCOs has also been investigated from a therapeutic perspective for prion disease where LCOs were designed based on the structure of amyloid structures (Hermann *et al.* 2015). Perhaps one of the most powerful aspects of LCOs is that upon binding to the amyloid backbone there is a shift in the fluorescent emission spectra, which can distinguish between different amyloid deposits (Aslund *et al.* 2009). This additional information gained from histological staining has provided an opportunity to investigate the implication of pathology conformation on disease.

2.2.2 Prion-like strains and clouds of conformation

In reference to:

Rasmussen J*, Mahler J*, Beschorner N*, Kaeser SA, Häsler LM, Baumann F, Nyström S, Portelius E, Blennow K, Lashley T, Fox NC, Sepulveda-Falla D, Glatzel M, Oblak AL, Ghetti B, Nilsson KPR, Hammarström P, Staufenbiel M, Walker LC, Jucker M. Amyloid polymorphisms constitute distinct clouds of conformational variants in different etiological subtypes of Alzheimer's disease. *Proc Natl Acad Sci U S A* 2017b; 114: 13018-13023.

(doi:10.1073/pnas.1713215114)

*equal contribution

Although a number of different prion diseases have been identified in animals, not all PrP^{TSE} sources are able to cause disease when introduced into a new species (Aguzzi *et al.* 2007; Collinge 2010). This species barrier effect as it has been defined, suggests there is an interaction between the PrP^{TSE} agent and host PrP^C where some level of compatibility is required to advance disease (Bruce *et al.* 1994; Aguzzi *et al.* 2007; Collinge 2010). It has been shown that the amino acid sequence of PrP^C, and in particular polymorphisms at amino acid 129, can strongly influence the susceptibility of a host to prion disease (Palmer *et al.* 1991; Collinge *et al.* 1996; Wadsworth *et al.* 2004; Collinge 2010). Astonishingly, with serial passaging of brain material into the same host species, the incubation period of prion disease can be drastically reduced as the species barrier is overcome (Aguzzi *et al.* 2007). This

phenomenon suggests some adaptation of PrP^{TSE} structure occurs to enhance its infectious nature. This adaptation upon passaging has been hypothesized as occurring through two different mechanisms. The mutated selection scenario suggests that a new and mutated form of PrP^{TSE} is formed during amplification that is more potent upon subsequent passage in a naïve host (**Figure 3**; Collinge 2010). More recently the idea of PrP^{TSE} quasi-species was put forward that suggests multiple structures of PrP^{TSE} exist in the brain, which are then selected for with passaging into a naïve host (**Figure 3**; Collinge 2010; Li *et al.* 2010). PrP^{TSE} from different animals of the same species have also been demonstrated as having unique disease characteristics when inoculated into naïve hosts with PrP^{TSE} (Pattison and Millson 1961; Fraser and Dickson 1973; Aguzzi *et al.* 2007). This is known as the strain concept, where different forms of PrP^{TSE} exist while having an identical amino acid sequence, but distinct structural features that encode a biological activity (Collinge 2010). A number of different methods can be used to assess the strain properties of PrP^{TSE} upon passage into a naïve host (Aguzzi *et al.* 2007). Most notably, strains can be distinguished by their pathobiology in a host (Aguzzi *et al.* 2007). A classic example is hamster-adapted transmissible mink encephalopathy (TME) where “hyper” and “drowsy” strains were described when hamsters were inoculated with TME PrP^{TSE} (Bessen and Marsh 1992a; Bessen and Marsh 1992b; Bessen and Marsh 1994; Marsh and Bessen 1994). These two strains, as their name describes, led to opposite disease phenotypes with distinct deposition patterns and incubation times (Bessen and Marsh 1992b). Often the biochemical features can also differ between PrP^{TSE} strains including post-translational glycosylation, resistance to proteolytic degradation or protein unfolding caused by detergents (Bessen and Marsh 1994; Collinge *et al.* 1996; Safar *et al.* 1998; Colby *et al.* 2009). An exemplary study identified eight different prion strains in hamsters based on their sensitivity to denaturing using a conformation-dependent immunoassay (Safar *et al.* 1998). These methods for identifying different strains of PrP^{TSE} were also crucial in connecting the development of vCJD to the consumption of tainted beef and solidifying prion diseases as transmissible through environmental exposure (Collinge *et al.* 1996). The link between biochemical features of PrP^{TSE} and their distinct properties in a new host is not only a fascinating biological phenomenon but also strong evidence for the protein-only hypothesis.

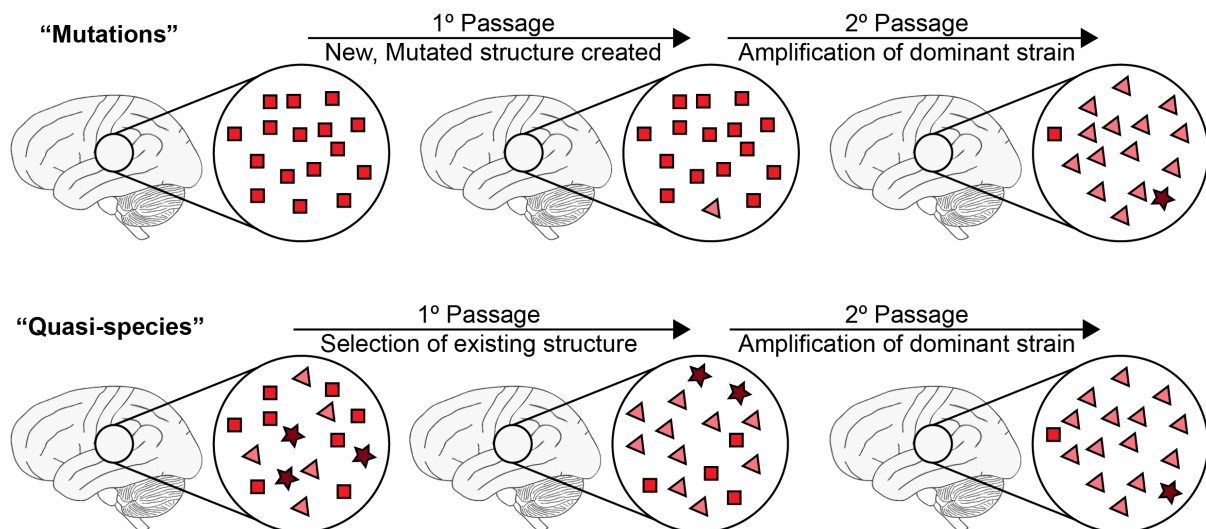


Figure 3. Two hypotheses for the evolving properties of prion agents upon experimental passage into a naïve host. In the “mutations” hypothesis, a new prion structure is formed in a new host, which is more pathogenic upon subsequent experimental passage and becomes the dominant amplified strain. Conversely, the “quasi-species” hypothesis suggests that multiple prion structures exist within a brain and that one structure is more pathogenic in a new host and becomes the dominant strain through amplification.

Strain-like features of A β

Similar to prion disease research, the investigation of strain-like properties of A β involves the inoculation of aggregates into transgenic mice to then investigate the features of induced pathology. This experimental paradigm is referred to as seeded nucleation, where structural features are amplified in a new host by templated misfolding (Jucker and Walker 2013; described in detail in 2.3.1). A seminal study utilized this model to investigate A β in the two transgenic mouse lines, APP23 and APPS1, that have low and high ratios of brain A β 42/40, respectively (Meyer-Luehmann *et al.* 2006). After intracerebral inoculation of brain extracts in young transgenic mice, different plaque morphologies developed (Meyer-Luehmann *et al.* 2006). It was proposed that these strain-like morphotypes were encoded by the ratio of A β species produced in each mouse line (Meyer-Luehmann *et al.* 2006). Indeed, similar strain-like features have been identified for *in vitro* seeded A β fibrils where distinct fibril structures could be propagated (Petkova *et al.* 2005). In a separate study, *in vitro* A β fibrils made using either A β 40 or A β 42 produced distinct pathologies *in vivo* (Stöhr *et al.* 2014). This distinct induced pathology was abolished when A β 42 fibrils were grown in the presence of a denaturant to suggest the induced pathology was controlled by the structure of aggregates (Stöhr *et al.* 2014).

The previously described class of amyloid binding spectral dyes, known as LCOs, can also be used to identify structural differences between pathologies. Spectral discrimination of amyloid structure occurs through the twisting of the flexible LCO backbone upon binding to the β -sheet backbone resulting in a shifted emission spectrum (Nilsson *et al.* 2005). These distinct spectral properties were apparent when using an early version of LCOs to analyze different mouse-adapted prion strains (Magnusson *et al.* 2014). Similarly, the structure-discriminating properties of LCOs also apply to the A β peptide. Using *in vitro* fibrillized A β 40, the extent of fibril bundling as confirmed with atomic force microscopy was distinguished by the emission spectra of LCOs (Psonka-Antonczyk *et al.* 2016). As an extension of previous work investigating the strain-like features of *in vivo* A β pathology from APP23 and APPPS1 transgenic mice, LCOs were used to determine if the plaque core structure was also different in the induced pathology (Heilbronner *et al.* 2011). Distinct spectral emissions were identified in the induced pathology from the two mouse extracts, suggesting that these features are not only influencing the plaque morphology but also the amyloid core plaque structure (Heilbronner *et al.* 2011).

Although the presence of strain-like A β aggregates is an interesting finding for *in vitro* or transgenic mouse material, it is important to determine whether such varied structures could exist in human AD. Distinct A β biochemical features have been identified in human AD patients with a unique disease progression characterized by rapid cognitive decline (Cohen *et al.* 2015). This rapid AD subtype is commonly referred to prion disease reference centers given the similar aggressive clinical phenotype but at autopsy standard AD pathology is observed (Schmidt *et al.* 2011). The conformation of A β 42 in these rapid AD brains was quite heterogeneous and had abundant medium sized aggregates compared to sAD (Cohen *et al.* 2015). These biochemical distinctions were then speculated as being a potential reason for a different clinical presentation for disease (Cohen *et al.* 2015). However, it is important to note that these biochemical features were not propagated in an *in vitro* or transgenic mouse model, which is important for determining their strain-like properties (Aguzzi *et al.* 2007). A separate study satisfied this criteria by demonstrating that A β derived from patients harboring the Arctic mutation (E693G), which results in an amino acid change within the A β peptide sequence, displayed high susceptibility to denaturation and induced distinct, diffuse deposition in the vessels of transgenic mice compared to other AD extracts (Watts *et al.* 2014). Additionally, the deposition of A β 38 was prominent in mice inoculated with Arctic

A β (Watts *et al.* 2014). Two related studies also identified that distinct structures of A β could be propagated *in vitro* from different AD brain tissue samples (Lu *et al.* 2013; Qiang *et al.* 2017). Similar to work by Cohen *et al.* (2015), rapid AD brain tissue contained different A β fibril structures than typical sAD and the posterior cortical atrophy variant of AD (PCA) (Qiang *et al.* 2017). Surprisingly, all samples showed fibril structure diversity when A β 42 was used as an *in vitro* substrate (Qiang *et al.* 2017). These studies provide evidence that atomic structural features propagated by brain derived A β can differ between subtypes of AD. However, as mentioned earlier, it is unclear how *in vitro* propagation may influence the selection and amplification of different A β structures, given that *in vitro* growth conditions can greatly influence the structure of A β and the heterogeneity of structures (Meier *et al.* 2017).

In order to further advance the knowledge surrounding A β structural variation in AD brain tissue, our recent study investigated a large cohort of patients with various etiologies using LCO spectral dyes (Rasmussen *et al.* 2017b). Specifically, both fAD (*APP-V717I*, *PSEN1-A431E*, *E280A*, *F105L*) and sAD cases were investigated in addition to the PCA variant of AD. This diverse cohort of patient subtypes was also interrogated for regional brain differences, with temporal, occipital and frontal cortex samples being included. A previously established staining method for discerning A β pathology structure using the two LCOs, h-FTAA and q-FTAA, was used to stain plaques in human tissue (Nyström *et al.* 2013). The collected fluorescent emission spectra indicated that certain fAD patients (*APP-V717I* and *PSEN1-A431E*) had obviously distinct plaques, both when considering the entire emission spectrum as well as using a ratio-metric analysis of fluorescent emission peaks for the two LCOs (502 nm/588 nm) (Rasmussen *et al.* 2017b). Subtle, but significant, differences were also seen between other groups of fAD and sAD patients, and notably between PCA and sAD patients (Rasmussen *et al.* 2017b). In agreement with other studies, there was no difference seen between brain regions for the spectral emission of amyloid plaque cores (Lu *et al.* 2013; Cohen *et al.* 2015; Qiang *et al.* 2017). Furthermore, while the mean plaque core structure was distinct between AD subtypes, it was observed that the spectral signature of single plaques did vary within a patient brain in a region-independent manner (Rasmussen *et al.* 2017b). This variation was referred to as clouds of amyloid core conformation and demonstrated that plaque structure has overlapping properties between AD etiologies and, notably, that there was substantial variation in the plaque conformation for sAD (Rasmussen *et al.* 2017b). This

observation drew parallels to prion studies where clouds of PrP^{TSE} conformation were hypothesized as being responsible for strain adaptation with chemical treatment (**Figure 3**; Li *et al.* 2010; Collinge 2010). Spectral signatures for sAD and PCA cases were compared to clinical information (ApoE status, age and post-mortem interval) and A β biochemistry (A β amount, A β 42/40 and protease resistance) but all of these factors were independent from the plaque spectral signature (Rasmussen *et al.* 2017b). Therefore, by inoculating the same amount of A β derived from *APP-V717I*, *PSEN1-A431E* and sAD brain extracts into transgenic APP23 mice, the ability of A β plaque structures to propagate was assessed similar to previous studies (Meyer-Luehmann *et al.* 2006; Heilbronner *et al.* 2011; Watts *et al.* 2014; Rasmussen *et al.* 2017b). In addition, a unique human sAD case with low affinity PiB binding and divergent LCO spectral characteristics compared to typical AD was also injected into APP23 mice (Rosen *et al.* 2010). The amount and spectral signature of induced pathology differed between the injection groups to suggest different strain-like properties of AD derived A β (Rasmussen *et al.* 2017b). However, the induced amyloid core spectra did not perfectly mirror the difference seen in human tissue; a discrepancy that may be explained by the influence that host A β has on pathology (Meyer-Luehmann *et al.* 2006; Mahler *et al.* 2015).

This study was the first to investigate structural features of A β pathology in its native tissue environment and has provided insight into how subtypes of AD may be distinct at a molecular level. Astonishingly, these spectral differences were acquired from plaque cores that are indistinguishable using traditional staining methods (Rasmussen *et al.* 2017b). It is tempting to speculate that these differences in A β plaque structure could explain differences in clinical phenotype, especially for PCA and traditional sAD where distinct clinical phenotypes exist (Crutch *et al.* 2017). A more conservative interpretation of this data, which has direct implications to patients, is that this variation in plaque structure could decrease the efficacy of A β therapeutics (monoclonal antibodies) or diagnostic imaging, as indicated by the PiB negative sAD case (Condello and Stöhr 2018; Rasmussen *et al.* 2017b). The identification of conformational clouds is intriguing and is further supported by x-ray microdiffraction studies on human tissue samples, where plaque polymorphisms were identified within the same brain section (Liu *et al.* 2016). Another recent study identified A β structural variation within an AD brain using fluorescent dyes but even more variation between sAD patients, which aligns with our findings (Condello *et al.* 2018). However, it

will be important for future studies to isolate A β fibril structures from the brain that can then be used in structural studies as was recently reported for pathological tau in AD (Fitzpatrick *et al.* 2017). This would clarify if spectral properties correlate with atomic level structural variation in A β .

The identification of A β plaque variation within AD that can be propagated is an intriguing finding whose relevance to the biology of disease still needs to be investigated. All samples used in the above study were collected from end-stage post-mortem AD patients where the disease is obviously at an advanced stage (McDade and Bateman 2017). As postulated by the amyloid cascade hypothesis, a perturbation in A β metabolism is the earliest event in disease (Selkoe and Hardy 2016). Some have even suggested that the involvement of A β in AD at later stages of disease is minor, as A β physiological changes reach a plateau late in disease (Holtzman *et al.* 2011; McDade and Bateman 2017). It follows that a perfect extension of these findings in end-stage human tissue would be to investigate the characteristics of A β over the course of maturing pathology.

2.3 β -amyloid seeds

2.3.1 *The seeding paradigm*

As described earlier, multiple neurodegenerative diseases are characterized by the spreading of pathology throughout the brain (Jucker and Walker 2013; Brettschneider *et al.* 2015). An explanation for this spreading is a seeded nucleation model where pathologies spread along functionally connected networks of neurons through templated protein misfolding (Lee *et al.* 2011; Jucker and Walker 2013). Characterizing the ability of misfolded forms of proteins to induce the conversion of naïve protein has strengthened the seeded nucleation model for prion-like proteins including A β and has led to a better understanding of the mechanism behind disease progression (Jarrett and Lansbury 1993; Jucker and Walker 2013; Walker and Jucker 2015).

Numerous *in vitro* studies investigating A β fibrillization mirror the results found for PrP^{TSE}. The ability of PrP^{TSE} to seed aggregation of monomeric PrP^C has been adapted into a number of *in vitro* methodologies. Specifically, these include protein misfolding cyclic amplification (PMCA), an amyloid seeding assay (ASA) and real-time quaking induced conversion (RT-

QuIC) (Saborio *et al.* 2001; Colby *et al.* 2007; Atarashi *et al.* 2008). PMCA uses sonication to seed the aggregation of brain-derived PrP^C with a test sample, and subsequent rounds are seeded with an aliquot of the previous cycle to amplify misfolded PrP^{TSE}, which is detected by protease resistance (Saborio *et al.* 2001). Conversely, the principles of RT-QuIC and ASA utilize recombinant forms of PrP^C (Colby *et al.* 2007; Atarashi *et al.* 2008). In these methods, the fluorescence of thioflavin T (ThT) is used to monitor protein aggregation while a sample is intermittently agitated (Colby *et al.* 2007; Atarashi *et al.* 2008). A number of ThT assays have been developed to investigate the aggregation of A β (Cohen *et al.* 2012; Morgado *et al.* 2012; Nagarathinam *et al.* 2013). In general, these assays have clearly defined A β aggregation proceeding in a sigmoidal fashion with a slow nucleating or lag phase, followed by rapid fibril growth and finally, a plateau phase when the system is saturated (**Figure 4**; Knowles *et al.* 2014; Meisl *et al.* 2014). These assays have been particularly valuable in defining the kinetics of aggregation and determining different mechanisms by which seeded nucleation can occur (**Figure 4**; Knowles *et al.* 2014; Meisl *et al.* 2014). The two main mechanisms defined by these assays are primary and secondary nucleation, which are distinguished by the aggregation curve rate constant (Knowles *et al.* 2014; Meisl *et al.* 2014). From an atomic scale, primary nucleation occurs when a seed forms and a fibril grows from this seed, while secondary nucleation occurs when a new seed is formed at the surface of an already existing fibril which leads to a second, separate extending fibril (Knowles *et al.* 2014; Meisl *et al.* 2014). Additionally, ThT assays identified that fragmentation of fibrils produces more surfaces for extension of amyloid growth and, consequently, a distinct aggregation curve (Knowles *et al.* 2014). ThT assays have also been used to investigate the ability of different A β samples to induce aggregation of recombinant A β by analyzing the duration of the lag phase. The lipid membrane has been demonstrated as a site of potent A β seed generation capable of rapidly causing fibril extension in samples from a novel transgenic mouse model with membrane anchored A β species (Nagarathinam *et al.* 2013). A subsequent study used the same methodology to further elucidate that mitochondrial membrane associated A β is an efficient seed of aggregation (Marzesco *et al.* 2016). The controlled environment of *in vitro* ThT assays has added invaluable mechanistic insights into the seeding ability of A β but further *in vivo* evidence has solidified the relevance of this paradigm to disease.

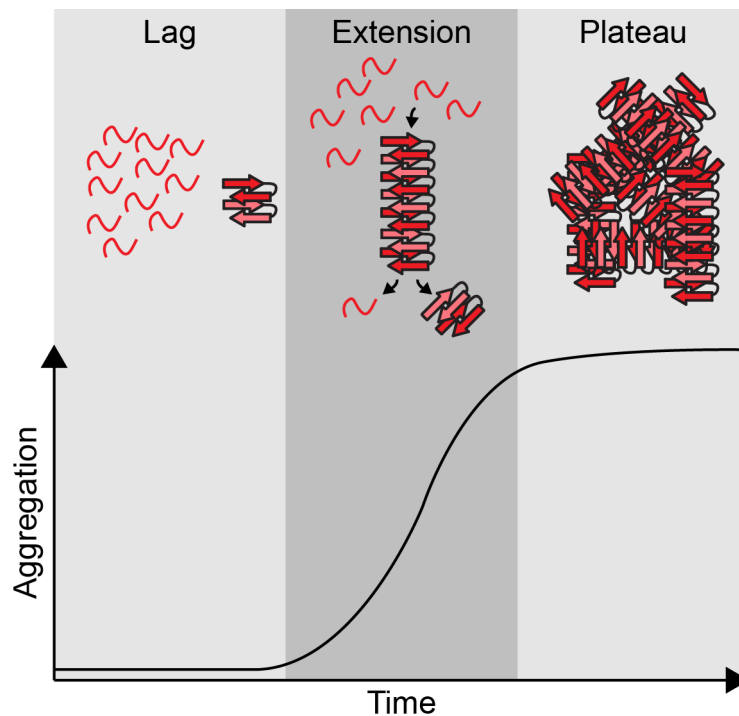


Figure 4. *Amyloid aggregation proceeds in three phases.* During the lag phase, monomeric peptide is in solution and there is little to no aggregation. Upon formation of a nucleus or seed, aggregation of monomeric protein occurs in ordered β -sheet rich fibrils, which elongate in the extension phase. The extension phase is quite dynamic with monomers being added to fibrils but also fragmentation of the fibril and the release of monomeric peptide. The final plateau phase is characteristic of a saturated system where many aggregates are present.

In vivo seeding

Using transgenic models of cerebral β -amyloidosis, the concept of seeded aggregation has been elegantly demonstrated as a robust mechanism for amyloid pathology onset. As mentioned earlier, the APP23 and APPS1 models have been used to demonstrate that A β laden brain extracts can induce pathology within the hippocampus of APP transgenic mice while control WT extracts do not induce deposition (Meyer-Luehmann *et al.* 2006). Similar findings of seeded induction of A β pathology were also reported using a novel transgenic mouse with a bioluminescence reporter for astrocytic gliosis (Watts *et al.* 2011; Stöhr *et al.* 2012). In these mice, an increased bioluminescent signal represents A β pathology induced gliosis, and with this tool the injection of A β -laden brain extracts was confirmed to spur A β deposition (Watts *et al.* 2011; Stöhr *et al.* 2012). The earlier onset of A β deposition caused by misfolded A β strongly supports the seeded nucleation of pathology, but subsequent studies added to this by using transgenic models where endogenous pathology does not occur in the transgenic hosts (Morales *et al.* 2012; Rosen *et al.* 2002). This *de novo* induction of A β pathology through injection of AD brain extracts in transgenic rodents was crucial to showing

that aggregated A β can seed the deposition of endogenous A β (Morales *et al.* 2012; Rosen *et al.* 2002). Further, seeded deposition of A β was demonstrated in a hippocampal slice culture model, where pathology could be induced with the application of an aged transgenic brain extract (Novotny *et al.* 2016). Although the seeded deposition of A β *in vivo* is a robust phenomenon, it is unclear which mechanism identified *in vitro*, namely primary nucleation or secondary nucleation, is dominant in a tissue environment (Knowles *et al.* 2014). These mechanisms likely occur simultaneously for endogenous pathology in transgenic models of cerebral β -amyloidosis, perhaps with primary nucleation being dominant early in pathology, but secondary nucleation being more prevalent later. It is also interesting to speculate that, in a seeding paradigm where a brain extract containing aggregated A β is focally injected, secondary nucleation may preferentially occur at the surface of these injected aggregates. A number of other factors not accounted for in *in vitro* experiments like inflammation, A β production and the tissue environment itself, would likely heavily influence A β aggregation kinetics.

The above *in vitro* and *in vivo* models have supported the seeding abilities of A β but whether this is a relevant mechanism within AD remains unclear (Selkoe and Hardy 2016; Rasmussen *et al.* 2017a). Recent evidence from human post-mortem brain tissue has provided some of the most convincing data thus far for A β pathology being transmissible in humans in a seeded nucleation model (Jaunmuktane *et al.* 2015; Frontzek *et al.* 2016; Hamaguchi *et al.* 2016; Kovacs *et al.* 2016; Ritchie *et al.* 2017; Cali *et al.* 2018). A seminal study found that human cases of CJD caused by the injection of growth hormone prepared from PrP^{TSE}-contaminated pituitary extracts had substantial A β pathology (Jaunmuktane *et al.* 2015). The amount of A β could not be explained by other factors, such as age or genetic status and thus, it was proposed that the pituitary extracts containing PrP^{TSE} also harbored A β aggregates that induced pathology (Jaunmuktane *et al.* 2015). A series of later studies identified that CJD caused by dura mater grafts contaminated with PrP^{TSE} also resulted in some cases displaying A β pathology above the expected level (Frontzek *et al.* 2016; Hamaguchi *et al.* 2016; Kovacs *et al.* 2016; Cali *et al.* 2018). This ruled out that A β pathology was spurred by injection of growth hormone and corroborated the interpretation that A β pathology may indeed be transmitted. Finally, similar unexpectedly high levels of A β pathology were found in patients that received growth hormone treatment but did not have CJD, removing any confounding possibility of PrP^{TSE} causing A β pathology (Ritchie *et al.* 2017). This series of studies on

human post-mortem tissue has provided credible evidence for the prion-like features of A β in humans and its central role in causing pathology. It is important to note that robust tau pathology was not seen in these cases, meaning that these patients did not reach the pathological or cognitive criteria required for the AD classification. However, it is possible that the incubation period was not long enough for tau pathology to develop, which normally follows A β deposition in AD. It will be crucial for future work to determine whether A β alone can induce full-blown AD with tau pathology in either an appropriate model system or in humans where environmental exposure to A β occurred very early in life.

The seeding paradigm has provided a valuable construct for understanding A β pathology and the likely mechanism behind its appearance in disease. Relying on the above paradigm and methods, recent work has aimed to better understand the abilities of different A β sources to seed deposition in a naïve host.

2.3.2 The age-dependency of β -amyloid seeding potency

In reference to:

Ye L*, Rasmussen J*, Kaeser SA, Marzesco A, Obermueller U, Mahler J, Schelle J, Odenthal J, Krueger C, Fritschi SK, Walker LC, Staufenbiel M, Baumann F, Jucker M. A β seeding potency peaks in the early stages of cerebral β -amyloidosis. *EMBO Rep* 2017; 18: 1536-1544.

(doi:10.15252/embr.201744067)

*equal contribution

Indeed, not all aggregated A β samples harbor the same ability to seed aggregation of monomeric A β . In the first investigations of A β seeding properties *in vivo* it was found that while brain derived A β seeds were very efficient at inducing deposition, *in vitro* A β fibrils were poor seeds (Meyer-Luehmann *et al.* 2006). This was some of the first evidence that aggregated A β can have varying seeding properties. Astonishingly, the ability of *in vitro* A β to seed deposition *in vivo* was greatly enhanced using a slice culture assay to amplify amyloid prior to injection (Novotny *et al.* 2016). This suggests that a tissue environment can play a central role in forming potent seeds. It has since been demonstrated that *in vitro* A β aggregates can seed deposition *in vivo* if large amounts are injected and the aggregation

conditions are altered (Stöhr *et al.* 2014). The seeding potency of *in vivo* derived A β was further investigated using ultracentrifugation to separate soluble and insoluble fractions (Langer *et al.* 2011). While the soluble A β fraction contained substantially less A β than the insoluble fraction (>1000-fold), both extracts induced a comparable amount of A β pathology in APP23 mice (Langer *et al.* 2011). Additionally, the soluble A β seeds were sensitive to digestion by a protease but the same digestion protocol did not completely remove the seeding ability of the total extract (Langer *et al.* 2011). Similarly, potent soluble A β seeds were identified in the human AD brain, where extremely low levels of A β (<10⁻¹⁸ moles) seeded A β deposition in APP23 mice (Fritschi *et al.* 2014a). Conversely, A β aggregates obtained from the cerebrospinal fluid of AD patients did not seed A β deposition *in vivo* (Fritschi *et al.* 2014a). This difference in seeding ability was attributed to the smaller size of aggregates in CSF compared to the soluble AD brain fraction (Fritschi *et al.* 2014a). As mentioned earlier, A β formed in different lipid environments can also greatly increase the potency of seeding both using ThT aggregation assays and *in vivo* inoculations (Marzesco *et al.* 2016).

The infectious titer of a disease agent is a crucial characteristic for assessing its risk for a population. This has been achieved for decades using *in vivo* bioassays where the titration of a sample determines its potency (Reed and Munch 1938). Typically, the inoculation of naïve hosts with a dilution series of the infectious agent allows for the determination of the dilution at which 50% of inoculated animals die, also known as the lethal dose 50 or LD₅₀ (Reed and Munch 1938). In this way, different isolates can be compared for their pathogenicity. Bioassays are also used extensively in prion diseases to determine how infectious certain PrP^{TSE} isolates are (Prusiner *et al.* 1982). When considering models of A β seeded deposition, an obvious hurdle for determining potency of a sample is that the transgenic animals used in a seeding paradigm do not have robust symptoms associated with pathology (Meyer-Luehmann *et al.* 2006). Indeed *in vivo* A β can be extensively diluted while still producing seeded deposition of A β in transgenic mice but the potency of A β extracts has not been addressed (Fritschi *et al.* 2015; Morales *et al.* 2015).

In an effort to simultaneously design a precise A β seeding bioassay and also determine how A β seeding properties evolve over the course of cerebral amyloidosis, our recent study used two models of A β deposition, namely, APP23 and APPPS1 (Ye *et al.* 2017). The maximum

life span was assessed for each mouse line and age groups were defined in order to have six time points for each transgenic model (Ye *et al.* 2017). Histological and ELISA measurements of A β 40 and A β 42 determined that pathology and protein levels increase during aging for both lines as expected (Ye *et al.* 2017). Intriguingly, the ratio of A β 42/40 was not constant over the course of aging and peaked in both lines at the earliest time point where pathology was detected with histology (Ye *et al.* 2017). Pooled brain extracts from the different age groups of mice were then serially diluted and injected into young transgenic APP23 mice. In this standard seeding paradigm, mice were aged for a fixed six-month period and subsequently sacrificed to assess A β pathology in the hippocampus. The numbers of mice with induced pathology were recorded for each extract age and dilution, similar to the number of dead mice in a bioassay for a lethal agent, and the seeding dose 50 (SD₅₀) was calculated in order to assess the seeding activity (Ye *et al.* 2017). While the seeding activity plateaued for both mouse lines at later time points, the specific seeding activity (calculated by taking into account the amount of A β present within the extract) displayed a peak in both lines (Ye *et al.* 2017). Astonishingly, this peak coincided with the age where A β 42/40 was highest (Ye *et al.* 2017). This simultaneous change in A β biochemistry and specific seeding activity near the onset of pathology provides an interesting perspective about A β deposition and perhaps even AD onset.

The robust nature of this finding in two models both with early and late onsets suggests that targeting these unique A β species at the earliest stages is likely crucial for successful disease mitigation (McDade and Bateman 2017). Designing a therapeutic treatment directed against A β at the earliest stages of AD will require exquisite biomarkers to identify when A β pathology first develops. Likely these biomarkers could then be assessed in at risk populations of people based on thorough genetic testing, allowing for accurate prediction of disease onset and thus, appropriate therapeutic intervention (McDade and Bateman 2017). The targeting of A β seeds is an enticing strategy but further analysis of the exact nature of these A β aggregates will be crucial for designing potent therapeutics.

2.4 Isolating bioactive *in vivo* A β seeds

2.4.1 The varied forms of aggregated β -amyloid

While larger amyloid structures have been discussed thus far, a number of different A β multimers with various properties have also been identified. Following the cleavage of APP in the amyloidogenic pathway, monomeric A β is then free to aggregate into higher order structures. As outlined in the amyloid cascade hypothesis, this misfolding of A β is believed to be responsible for subsequent alterations in brain physiology and finally neurodegeneration (Selkoe and Hardy 2016).

The monomeric form of A β has not been clearly identified as having a biological effect in the brain but even at the level of dimer formation this changes. Early reports found that stable small oligomers such as dimers and trimers are produced by living cells (Podlisny *et al.* 1995; Walsh *et al.* 2000; Walsh *et al.* 2002). When isolated from cells, cerebrospinal fluid and even the brain, A β dimers were capable of inhibiting long-term potentiation (Walsh *et al.* 2002; Klyubin *et al.* 2008; Shankar *et al.* 2008). These and similar reports were key in producing interest in soluble oligomers of A β to complement the body of research on the pathological hallmark of senile plaques (Haass and Selkoe 2007). A soluble dodecamer of A β , termed A β *56, identified in transgenic mice has also been associated with memory impairment in a number of studies (Lesne *et al.* 2006; Lesne *et al.* 2008; Lesne *et al.* 2013; Liu *et al.* 2015; Amar *et al.* 2017). Structurally, A β *56 is assembled from A β trimers while existing in membrane-associated fractions (Lesne *et al.* 2006). In human subjects, A β dimers, trimers and A β *56 all increase with age and in disease, but A β *56 correlated best with synaptic deficits and pathological tau (Lesne *et al.* 2013). This distinct A β *56 assembly has been hypothesized as an off-pathway aggregate, separate from A β fibrillar structures, based on its unique structural properties, temporal occurrence early in disease and location within in the brain (Lesne *et al.* 2013; Liu *et al.* 2015). A recent study has implicated A β *56 as eliciting its neuron altering effects by interacting with N-methyl-D-aspartate receptors, increasing intracellular calcium concentration and finally inducing tau phosphorylation and missorting within neurons (Amar *et al.* 2017).

In addition to the *in vivo*-derived oligomers mentioned above, A β -derived diffusible ligands (ADDL) are an oligomeric preparation from *in vitro* studies that also have suggested

neurotoxic effects (Lambert *et al.* 1998; Wang *et al.* 2002; Gong *et al.* 2003). ADDLs are composed of A β 42 and have since been identified as a subpopulation of multiple A β assemblies, as opposed to a single multimeric aggregate (Hepler *et al.* 2006). In a separate study, a slightly different A β oligomer preparation showed similar neurotoxicity in cell culture but an antibody specific for medium sized oligomers abolished this toxicity, suggesting that moderately sized oligomers are the toxic entity (Kayed *et al.* 2003). A slightly larger version of ADDLs have also been identified *in vitro* with a similar “doughnut” appearance under an electron microscope that are referred to as annular assemblies (Lashuel *et al.* 2002; Bitan *et al.* 2003;). These annular species have an intermediate size when compared to larger fibrils and lack a fibrillar ultrastructure (Haass and Selkoe 2007). Small but fibrillar A β assemblies, known as protofibrils, are also described as stable A β assemblies (Hartley *et al.* 1999; Walsh *et al.* 1999). These protofibril structures have a more ordered β -sheet structure and have the ability to continue fibrillization and become mature amyloid fibrils (Harper *et al.* 1999; Walsh *et al.* 1999). There has been conflicting information about whether protofibrils are toxic and impair neuron function or are rather benign structures (Hartley *et al.* 1999; Walsh *et al.* 1999; Liu *et al.* 2015). The role of these different A β populations and the end-stage A β fibrils/deposits has been a central debate in AD research, with some arguing oligomers should be a focus of research since senile plaques do not correlate with neurodegeneration (Giannakopoulos *et al.* 2003; Haass and Selkoe 2007). However, it is worth mentioning that the extensive inflammatory reaction and neuritic injury surrounding dense-cored plaques is damaging to the tissue environment and thus senile plaques are also detrimental, at least indirectly, as opposed to only oligomeric A β (Serrano-Pozo *et al.* 2011; Heneka *et al.* 2015). While the physiological effect of A β on neurons is important to consider when describing A β subpopulations, the ability of different structures to induce fibrillization should be investigated, given that this is the first event of AD (Selkoe and Hardy 2016). As mentioned previously, brain extracts containing extensive aggregated A β are capable of inducing deposition *in vivo* (Rasmussen *et al.* 2017b; Ye *et al.* 2017). Interestingly, soluble fractions of these brain extracts are extremely potent inducers of A β deposition (Langer *et al.* 2011; Fritschi *et al.* 2014a). This could suggest that certain oligomeric species of A β outlined above may play a particularly important role in inducing A β pathology.

The presence of aggregated A β is indeed a central characteristic of AD and is thus a potential target of disease modifying therapy. Given the various A β species outlined above, it is important to identify how different therapies can target specific A β assemblies *in vivo* and whether such subpopulations are more efficacious at slowing disease.

2.4.2 Finding a suitable target for Alzheimer's disease therapies

In reference to:

Rasmussen J, Bühler A, Baumann F, Jucker M. An agarose gel fractionation method for enriching brain derived proteopathic seeds. *in preparation*

The successful treatment of AD progression has been elusive to researchers and clinicians thus far (Karran and Hardy 2014). Early treatments were based on observations that there were low levels of the choline acetyltransferase enzyme, a crucial enzyme in the production of the neurotransmitter acetylcholine, in AD patients with associated cholinergic neuron death (Bowen *et al.* 1976; Perry *et al.* 1977; Francis *et al.* 1999). Unfortunately, these treatments have not slowed the progression of disease but rather treated symptoms in AD patients.

Based on the amyloid cascade hypothesis, a number of strategies for modulating A β production/clearance have been developed to target the earliest trigger of disease (Karran and DeStrooper 2016). When targeting the production of A β , inhibitors of secretases have been used in order to alter APP processing (Voytyuk *et al.* 2017). Early identification of small molecules that reduced A β release in cell culture were found to act on the γ -secretase complex (Karran and De Strooper 2016). However, off-target effects of these γ -secretase inhibitors were identified during *in vivo* testing due to the many substrates that the γ -secretase acts on (Doody *et al.* 2013; Voytyuk *et al.* 2017). Recent work has even suggested, that a now defunct γ -secretase inhibitor, semagacestat, which failed in Phase 3 testing, may not completely inhibit APP cleavage, but rather alter A β subcellular localization (Doody *et al.* 2013; Tagami *et al.* 2017). There are now suggestions for targeting γ -secretase at the level of modifying cleavage of APP to reduce A β 42 production rather than completely inhibiting enzyme activity, which produces undesirable side effects (Voytyuk *et al.* 2017). There is evidence that instability of the γ -secretase complex may be at the root of changes in APP

cleavage and, as such, a treatment that stabilizes this complex may be a suitable disease modifying strategy (Szaruga *et al.* 2017). Similar targeting of the β -secretase, BACE1, with small molecules has produced promising results (Vassar *et al.* 2014). Complete inhibition of this enzyme complex has produced less severe side effects and has subsequently been vigorously pursued as an AD treatment (Vassar *et al.* 2014; Shimshek *et al.* 2016). In animal models, BACE1 inhibitors have demonstrated a potent reduction in A β (Vassar *et al.* 2014; Kennedy *et al.* 2016; Schelle *et al.* 2016; Villarreal *et al.* 2017). However, recent failure of a BACE1 inhibitor, verubecestat in Phase 2/3 human trials was again a troubling set back for AD therapeutics (Hawkes 2017). Additionally, a recent study highlighted that inhibition of BACE1 can shift APP processing towards η -cleavage and produce neurotoxic peptides (Willem *et al.* 2015). Although targeting secretases for modification holds some promise for reducing A β and treating AD, a critique of this strategy is that already formed A β aggregates and pathology are not targeted.

Another main focus of AD therapeutics is improving the clearance of A β (Karran and De Strooper 2016). Indeed, after A β is produced, it can leave the brain through bulk flow in the interstitial fluid where it is later degraded in the periphery, but this is a challenging target for therapies (Wang *et al.* 2017). Early work spurred interest in specifically targeting the A β peptide by showing that vaccination with A β (active immunization) reduced A β levels in APP transgenic mice (Schenk *et al.* 1999; Morgan *et al.* 2000). Another seminal study was instrumental in showing that A β can be cleared through phagocytosis by microglia after passive immunization with an A β -specific antibody (Bard *et al.* 2000). These results in transgenic mouse models were also confirmed in human studies where A β immunotherapy was shown to reduce A β pathology (Rinne *et al.* 2010; Ostrowitzki *et al.* 2012; Sevigny *et al.* 2016). A number of different immunotherapies are in various phases of clinical trials, each with slightly different binding properties to the different forms of A β mentioned above (Ostrowitzki *et al.* 2012; Doody *et al.* 2014; Sevigny *et al.* 2016). Solanezumab is an antibody developed by Eli Lilly & Co. with affinities toward monomeric A β and small soluble oligomers that was first produced in mice by immunizing with an N-terminal A β epitope (Doody *et al.* 2014). In Phase 3 trials, slowed cognitive decline was suggested with solanezumab infusion but only in subjects with mild symptoms (Doody *et al.* 2014). This significant effect was then lost in patients with more advanced stages of disease (Doody *et al.* 2014). Another A β form has been targeted in AD trials with both aducanumab and

gantenerumab (Biogen and Roche, respectively), which are selective for A β aggregates (Ostrowitzki *et al.* 2012; Sevigny *et al.* 2016). Interestingly, aducanumab was identified by screening B-cell clones isolated from cognitively normal aged humans while gantenerumab was developed more traditionally through screening a humanized phage library for binding to aggregated A β (Ostrowitzki *et al.* 2012; Sevigny *et al.* 2016). A study in human subjects has demonstrated that gantenerumab can reduce A β load within the brain; however, effects on cognition have not been clear (Ostrowitzki *et al.* 2012). Excitingly, results from both transgenic mouse models and human clinical trials have suggested that aducanumab reduces A β levels in the brain and moderately slows cognitive decline (Sevigny *et al.* 2016). This immunotherapy research has demonstrated that even aggregated A β can be targeted for removal, suggesting that AD progression could be stopped and perhaps even slight improvements made. There are two current ideas about how to improve the efficacy of A β immunotherapies even further, one is to intervene as early as possible in AD to stop the cascade of neurodegeneration, and the other is to ensure that therapies are targeting the most bioactive populations of A β (Haass and Selkoe 2007; McDade and Bateman 2017; Ye *et al.* 2017). Thus, it is important to develop therapeutics that target A β species that have a well defined biological role in disease.

We recently developed a new methodology that shows promise for isolating subpopulations of A β from *in vivo* sources using gel fractionation, which in turn can be used in downstream applications (Rasmussen *et al.*, *in preparation*). This agarose gel electrophoresis method for resolving larger aggregates of amyloid proteins was adapted for a finer analysis of aggregates within the gel matrix by isolating different agarose fractions (Bagriantsev *et al.* 2006). Different *in vitro* preparations of A β , namely monomers, ADDLs and fibrils, migrated in an expected manner, with progressively higher molecular weight migration patterns, respectively (Rasmussen *et al.* *in preparation*). For *in vivo*-derived brain extracts rich in aggregated A β , it was determined that A β migrated differently from *in vitro* samples with the majority of A β being found in the highest and lowest molecular weight fractions across many age groups (Rasmussen *et al.* *in preparation*). Such discrepancies between *in vitro* and *in vivo* A β could represent the reason that these two forms have substantially different *in vivo* seeding activities (Meyer-Luehmann *et al.* 2006; Novotny *et al.* 2016). A crucial advance of this new methodology was the liberation of A β from the solid agar fractions through enzymatic digestion (Rasmussen *et al.* *in preparation*). A β migrating at a high molecular

weight from an aged APP23 brain extract even retained quaternary structure, as shown by binding to a conformational amyloid-specific antibody and inducing seeded deposition in APP23 mice after intracerebral inoculation (Rasmussen *et al. in preparation*).

Considering the above studies on immunotherapy in AD, the agarose fractionation methodology can have a number of applications. Perhaps most exciting would be the comparison of candidate antibodies in their binding profile to native *in vivo* A β samples as performed by immunoprecipitation on different fractions (Rasmussen *et al., in preparation*). This would greatly enhance our understanding of how exactly therapeutic antibody candidates differentially recognize the various subpopulations of A β outlined above (Haass and Selkoe 2007). Additionally, this novel methodology can be used to generate immunogens composed of distinct A β aggregate sizes, which can then be used for the generation of novel therapeutics. These distinct fractions of A β can also be analyzed for seeding potency to determine the size fraction where the most potent seeds are present (Ye *et al.* 2017). The use of agarose fractionation could immediately advance our understanding of A β seeding and help to target the most bioactive species and subsequently neutralize this initial trigger of AD. Such rational and targeted disease intervention may provide the strategy necessary for slowing the cognitive decline that plagues AD patients.

2.5 Conclusions and outlook

The amyloid cascade hypothesis has had a dominant influence on the research strategies surrounding AD in recent decades (Karran and De Strooper 2016; Selkoe and Hardy 2016). This focus on A β misfolding and seeded nucleation as the seminal event responsible for setting off a cascade culminating with neurodegeneration has led to an enhanced understanding of A β production, clearance and physiological effects. Within this dissertation, it has been demonstrated that A β plaque core morphology is distinct between AD subtypes and can be propagated, but also that plaque core conformation varies within a single AD brain (Rasmussen *et al.* 2017b). Working on this conclusion of A β -related differences late in disease, a subsequent investigation used APP transgenic mice to focus on pathology onset, which has been implicated as a crucial point in AD (McDade and Bateman 2017; Ye *et al.* 2017). It was conclusively shown that A β at the earliest stages of pathology possesses a different specific seeding activity and distinct biochemical features, compared to advanced

disease (Ye *et al.* 2017). These two studies outlined that A β structures can vary within AD and likely over the course of disease as well, emphasizing that a method is needed to further analyze these aggregates from *in vivo* sources. Finally, the use of agarose fractionation was shown to adequately separate A β by size while retaining structural and biological features to facilitate downstream application for sample analysis and therapeutic development (Rasmussen *et al.*, *in preparation*).

When considering this body of work as a whole, it is clear that future research will need to determine how these principles overlap on multiple levels. A central question out of the first study is whether A β plaque core structural variation meaningfully alters the course of AD. Particularly, the substantial variation in plaque conformation for sAD patients begs the question whether the diverse symptomology in AD may be encoded in A β structure. In line with this, it would be interesting to investigate A β pathology with LCOs in brains from rapid AD and individuals with high A β burden but normal cognition as two ends of the spectrum for cognitive function (Schmidt *et al.* 2011). If there was a distinction between these extreme groups of neurodegeneration with A β pathology it would further suggest that conformational variation influences disease. It is also important to determine whether structural variation in oligomeric A β can distinguish patient groups given its hypothesized active role in AD (Haass and Selkoe 2007). This question could be answered by using agarose fractionation to isolate oligomeric fractions for structural analysis (Rasmussen *et al.* *in preparation*). If multiple forms of aggregated A β were distinct at a structural level in different AD etiologies at the end-stage of disease it could suggest that this structural variation has a role in determining AD progression and symptoms.

The variation in A β pathology conformation at the end-stage of disease was striking, but whether this is also found at early stages of disease remains unknown (Rasmussen *et al.* 2017b). If A β aggregates were distinct between AD patients with different clinical presentations early in disease, it could suggest that this conformational variation influences disease progression as opposed to being an artifact produced late in disease. The findings in transgenic models of cerebral β -amyloidosis have demonstrated that A β aggregates do change with aging but the strain-like morphotypes produced after seeding from different models are preserved throughout aging (Ye *et al.* 2017). Thus, it could be that early versions

of pathogenic A β would also be distinct between certain patients with disparate end-stage pathology.

Given that most interventions targeting A β are moving to primary prevention, emphasis should be placed on A β features during this early stage of pathophysiology (McDade and Bateman 2017). Although investigating early populations of A β has been possible with transgenic mice (Ye *et al.* 2017), this is obviously a difficult human sample to obtain. More explicitly: Which young individuals without cognitive symptoms have pathogenic A β that would set off a cascade leading to AD decades later? It would be of interest to investigate A β in biological fluids by different conformational means to determine whether distinctions can still be made for patients, both with advanced AD and earlier stages of mild-cognitive impairment. Although still a challenge, the collection of CSF from people at risk of developing AD is possible, for example with ApoE4 carriers or fAD mutation carriers like those enrolled in the Dominantly Inherited Alzheimer's Network (DIAN) (Bateman *et al.* 2012; Karch and Goate 2015). Although, CSF and brain derived A β have different seeding capabilities and aggregate sizes, it could be that A β in the CSF retains some structural elements to distinguish patients (Fritschi *et al.* 2014a). The application of LCOs or other conformation sensitive methods to such biological fluids could prove invaluable for this strategy and is an obvious avenue for continued research.

From a translational perspective, the A β structural variations described in human brain tissue with LCO dyes have immediate implications for the treatment of AD (Rasmussen *et al.* 2017b; Condello and Stöhr 2018). One method for assessing the disease status of suspected AD patients is the retention of the PiB compound or similar radioligands within the brain, which identify A β based on amyloid conformation (Klunk *et al.* 2004; Clark *et al.* 2012; Wolk *et al.* 2012). It has already been demonstrated that a unique case with sAD had a reduced retention of PiB, despite the brain being populated with plaques (Rosen *et al.* 2010). Although PiB and other PET ligands have proven an accurate indication of A β burden within the brain across the human population, it is important to note that structural variation of A β plaques identified here could complicate these findings (Klunk *et al.* 2004; Wolk *et al.* 2012; Clark *et al.* 2012; Rasmussen *et al.* 2017b).

Perhaps one of the more striking speculations based on the above results is that variation in A β plaque conformation could impact the efficacy of an anti-A β immunotherapy (Rasmussen *et al.* 2017b). The somewhat underwhelming results of immunotherapy in AD could be partially explained by this variation (Condello and Strohr 2018). In order to answer this question and determine whether antibodies against A β vary in their binding to individual patients, agarose fractionation could be applied (Rasmussen *et al.* *in preparation*). As demonstrated for commercial antibodies, immunoprecipitation from different size fractions could be used to assess a variety of patient samples with current A β immunotherapy candidates using *in vivo* material under physiological conditions (Rasmussen *et al.* *in preparation*). This could be used to confirm the efficacy of antibody-binding to amyloid aggregates present in a broad range of patients before initiating immunotherapy trials.

Another extension of the agarose fractionation methodology is that after enriching a potent A β seed fraction, perhaps generated with early-stage A β aggregates (Ye *et al.* 2017), structural analysis with methods like cryo-electron microscopy could be pursued. Combining structural analysis with drug design could yield a potent treatment as was recently shown for PrP^{TSE} and LCOs (Herrmann *et al.* 2015). More traditional methods like active immunization in a naïve animal could also be pursued to generate novel immunotherapies. Alternatively, the more recent use of humanized phage libraries has allowed for high-throughput, *in vitro* screening of samples to identify binding partners of A β (Droste *et al.* 2015; Munke *et al.* 2017). Such a strategy using either a naïve library or an A β -primed library paired with screening specific size fractions of potent *in vivo* A β seeds would likely identify a novel immunotherapy. The advantage of utilizing agarose fractionation is that a disease-relevant immunogen could be isolated from a desired biological sample that can be thoroughly characterized with other biochemical and biological methods in parallel with the development of a therapy.

In conclusion, A β has long been identified as a central player in AD pathology, but more recently as a hypothesized trigger of disease itself (Selkoe and Hardy 2016). The prion-like properties of A β have further intensified focus on the mechanism by which amyloidogenic misfolding occurs and elicits neurodegeneration (Jucker and Walker 2013). The diverse methods and models used in this dissertation have provided evidence for A β conformational and biological characteristics being unique depending on disease status (Rasmussen *et al.*

2017b; Ye *et al.* 2017). A powerful tool was also proposed to advance the search for an A β species that can be targeted for the treatment of AD (Rasmussen et al, *in preparation*). These findings have significantly added to our understanding of AD and will undoubtedly provide a platform for further investigations into this devastating disease.

2.6 References

- Aguzzi A, Heikenwalder M, Polymenidou M. Insights into prion strains and neurotoxicity. *Nat Rev Mol Cell Biol* 2007; 8: 552-61.
- Alibhai J, Blanco RA, Barria MA, Piccardo P, Caughey B, Perry VH, *et al.* Distribution of misfolded prion protein seeding activity alone does not predict regions of neurodegeneration. *Plos Biol* 2016; 14: e1002579.
- Alper T, Haig DA, Clarke MC. The exceptionally small size of the scrapie agent. *Biochem Biophys Res Commun* 1966; 22: 278-84.
- Alper T, Cramp WA, Haig DA, Clarke MC. Does the agent of scrapie replicate without nucleic acid? *Nature* 1967; 214: 764-66.
- Alpers MP. Epidemiology and clinical aspects of kuru. Prions: Novel infectious pathogens causing scrapie and Creutzfeldt-Jakob Disease, 1987; (eds Prusiner SB, McKinley MP) Academic Press, San Diego: 451-65.
- Alzheimer A. Über eine eigenartige Erkrankung der Hirnrinde. *Allgemeine Zeitschrift für Psychiatrie und psychisch-gerichtliche Medizin* 1907; 64: 146-8.
- Alzheimer A. Über eigenartige Krankheitsfälle des späteren Alters. *Zeitschrift für die Gesamte Neurologie und Psychiatrie* 1911; 4: 356-85.
- Alzheimer's Association. 2014 Alzheimer's disease facts and figures. *Alzheimers Dement* 2014; 10: e47-92.
- Amar F, Sherman MA, Rush T, Larson M, Boyle G, Chang L, *et al.* The amyloid-beta oligomer A β *56 induces specific alterations in neuronal signaling that lead to tau phosphorylation and aggregation. *Sci Signal* 2017; 10: eaal2021.
- Aslund A, Sigurdson CJ, Klingstedt T, Grathwohl S, Bolmont T, Dickstein DL, *et al.* Novel pentameric thiophene derivatives for in vitro and in vivo optical imaging of a plethora of protein aggregates in cerebral amyloidoses. *ACS Chem Biol* 2009; 4: 673-84.
- Atarashi R, Wilham JM, Christensen L, Hughson AG, Moore RA, Johnson LM, *et al.* Simplified ultrasensitive prion detection by recombinant PrP conversion with shaking. *Nat Methods* 2008; 5: 211-2.
- Bäck M, Appelqvist H, LeVine H, 3rd, Nilsson KP. Anionic oligothiophenes compete for binding of X-34 but not PiB to recombinant A β amyloid fibrils and Alzheimer's disease brain-derived A β . *Chemistry* 2016; 22: 18335-8.
- Bagriantsev SN, Kushnirov VV, Liebman SW. Analysis of amyloid aggregates using agarose gel electrophoresis. *Methods Enzymol* 2006; 412: 33-48.
- Bard F, Cannon C, Barbour R, Burke RL, Games D, Grajeda H, *et al.* Peripherally administered antibodies against amyloid-beta peptide enter the central nervous system and reduce pathology in a mouse model of Alzheimer disease. *Nat Med* 2000; 6: 916-9.
- Bateman RJ, Xiong C, Benzinger TL, Fagan AM, Goate A, Fox NC, *et al.* Clinical and biomarker changes in dominantly inherited Alzheimer's disease. *N Engl J Med* 2012; 367: 795-804.
- Beck E, Daniel PM. Neuropathology of transmissible Spongiform Encephalopathies. Prions: Novel infectious pathogens causing scrapie and Creutzfeldt-Jakob Disease, 1987; (eds Prusiner SB, McKinley MP) Academic Press, San Diego: 331-85.
- Bessen RA, Marsh RF. Biochemical and physical properties of the prion protein from two strains of the transmissible mink encephalopathy agent. *J Virol* 1992a; 66: 2096-101.
- Bessen RA, Marsh RF. Identification of two biologically distinct strains of transmissible mink encephalopathy in hamsters. *J Gen Virol* 1992b; 73: 329-34.
- Bessen RA, Marsh RF. Distinct PrP properties suggest the molecular basis of strain variation in transmissible mink encephalopathy. *J Virol* 1994; 68: 7859-68.

- Bitan G, Kirkitadze MD, Lomakin A, Vollers SS, Benedek GB, Teplow DB. Amyloid-beta protein (Abeta) assembly: Abeta 40 and Abeta 42 oligomerize through distinct pathways. *Proc Natl Acad Sci U S A* 2003; 100: 330-5.
- Bolduc DM, Montagna DR, Seghers MC, Wolfe MS, Selkoe DJ. The amyloid-beta forming tripeptide cleavage mechanism of gamma-secretase. *Elife* 2016; 5: e17578.
- Bolmont T, Haiss F, Eicke D, Radde R, Mathis CA, Klunk WE, *et al.* Dynamics of the microglia/amyloid interaction indicate a role in plaque maintenance. *J Neurosci* 2008; 28: 4283-92.
- Bolton DC, McKinley MP, Prusiner SB. Identification of a protein that purifies with the scrapie prion. *Science* 1982; 218: 1309-11.
- Borchelt DR, Scott M, Taraboulos A, Stahl N, Prusiner SB. Scrapie and cellular prion proteins differ in their kinetics of synthesis and topology in cultured cells. *J Cell Biol* 1990; 110:743-52.
- Bowen DM, Smith CB, White P, Davison AN. Neurotransmitter-related enzymes and indices of hypoxia in senile dementia and other abiotrophies. *Brain* 1976; 99: 459-96.
- Brettschneider J, Del Tredici K, Lee VM, Trojanowski JQ. Spreading of pathology in neurodegenerative diseases: a focus on human studies. *Nat Rev Neurosci* 2015; 16: 109-20.
- Brier MR, Gordon B, Friedrichsen K, McCarthy J, Stern J, Christensen J, *et al.* Tau, Abeta imaging, CSF measures, and cognition in Alzheimer's disease. *Sci Transl Med* 2016; 8: 338ra66.
- Brown P, Liberski PP, Wolff A, Gajdusek DC. Resistance of scrapie infectivity to steam autoclaving after formaldehyde fixation and limited survival after ashing at 360°C. *J Infect Dis* 1990; 161: 467-72.
- Bruce M, Chree A, McConnell I, Foster J, Pearson G, Fraser H. Transmission of bovine spongiform encephalopathy and scrapie to mice: strain variation and the species barrier. *Philos Trans R Soc Lond B Biol Sci* 1994; 343: 405-11.
- Buchhave P, Minthon L, Zetterberg H, Wallin AK, Blennow K, Hansson O. Cerebrospinal fluid levels of beta-amyloid 1-42, but not of tau, are fully changed already 5 to 10 years before the onset of Alzheimer dementia. *Arch Gen Psychiatry* 2012; 69: 98-106.
- Bueler H, Aguzzi A, Sailer A, Greiner RA, Autenried P, Aguet M, *et al.* Mice devoid of PrP are resistant to scrapie. *Cell* 1993; 73: 1339-47.
- Calafate S, Buist A, Miskiewicz K, Vijayan V, Daneels G, de Strooper B, *et al.* Synaptic contacts enhance cell-to-cell tau pathology propagation. *Cell Rep* 2015; 11: 1176-83.
- Cali I, Cohen ML, Haik S, Parchi P, Giaccone G, Collins SJ, *et al.* Iatrogenic Creutzfeldt-Jakob disease with Amyloid-beta pathology: an international study. *Acta Neuropathol Commun* 2018; 6: 5.
- Cao X, Sudhof TC. A transcriptionally active complex of APP with Fe65 and histone acetyltransferase Tip60. *Science* 2001; 293: 115-20.
- Caughey B, Raymond GJ. The scrapie associated form of PrP is made from a cell surface precursor that is both protease and phospholipase-sensitive. *J Biol Chem* 1991; 266: 18217-23.
- Clark CM, Pontecorvo MJ, Beach TG, Bedell BJ, Coleman RE, Doraiswamy PM, *et al.* Cerebral PET with florbetapir compared with neuropathology at autopsy for detection of neuritic amyloid-beta plaques: a prospective cohort study. *Lancet Neurol* 2012; 11: 669-78.
- Clavaguera F, Bolmont T, Crowther RA, Abramowski D, Frank S, Probst A, *et al.* Transmission and spreading of tauopathy in transgenic mouse brain. *Nat Cell Biol* 2009; 11: 909-13.

- Cohen ML, Kim C, Haldiman T, ElHag M, Mehndiratta P, Pichet T, *et al.* Rapidly progressive Alzheimer's disease features distinct structures of amyloid-beta. *Brain* 2015; 138: 1009-22.
- Cohen SI, Linse S, Luheshi LM, Hellstrand E, White DA, Rajah L, *et al.* Proliferation of amyloid-beta42 aggregates occurs through a secondary nucleation mechanism. *Proc Natl Acad Sci U S A* 2013; 110: 9758-63.
- Colby DW, Giles K, Legname G, Wille H, Baskakov IV, DeArmond SJ, *et al.* Design and construction of diverse mammalian prion strains. *Proc Natl Acad Sci U S A* 2009; 106: 20417-22.
- Colby DW, Zhang Q, Wang S, Groth D, Legname G, Riesner D, *et al.* Prion detection by an amyloid seeding assay. *Proc Natl Acad Sci U S A* 2007; 104: 20914-9.
- Collinge J, Palmer MS, Dryden AJ. Genetic predisposition to iatrogenic Creutzfeldt-Jakob disease. *Lancet* 1991; 337: 1441-42.
- Collinge J. Prion diseases of humans and animals: their causes and molecular basis. *Annu Rev Neurosci* 2001; 24: 519-50.
- Collinge J. Prion strain mutation and selection. *Science* 2010; 328: 1111-2.
- Collinge J. Mammalian prions and their wider relevance in neurodegenerative diseases. *Nature* 2016; 539: 217-26.
- Collinge J, Sidle KC, Meads J, Ironside J, Hill AF. Molecular analysis of prion strain variation and the aetiology of 'new variant' CJD. *Nature* 1996; 383: 685-90.
- Condello C, Lemmin T, Stöhr J, Nick M, Wu Y, Maxwell AM, *et al.* Structural heterogeneity and intersubject variability of Abeta in familial and sporadic Alzheimer's disease. *Proc Natl Acad Sci U S A* 2018; 115: e782-91.
- Condello C, Stöhr J. Abeta propagation and strains: Implications for the phenotypic diversity in Alzheimer's disease. *Neurobiol Dis* 2018; 109: 191-200.
- Crutch SJ, Schott JM, Rabinovici GD, Murray M, Snowden JS, van der Flier WM, *et al.* Consensus classification of posterior cortical atrophy. *Alzheimers Dement* 2017; 13: 870-84.
- Day GS, Musiek ES, Roe CM, Norton J, Goate AM, Cruchaga C, *et al.* Phenotypic similarities between late-onset autosomal dominant and sporadic Alzheimer disease: A single-family case-control study. *JAMA Neurol* 2016; 73: 1125-32.
- de la Torre JC. The vascular hypothesis of Alzheimer's disease: bench to bedside and beyond. *Neurodegener Dis* 2010; 7: 116-21.
- De Strooper B, Karran E. The cellular phase of Alzheimer's disease. *Cell* 2016; 164: 603-15.
- De Strooper B, Saftig P, Craessaerts K, Vanderstichele H, Guhde G, Annaert W, *et al.* Deficiency of presenilin-1 inhibits the normal cleavage of amyloid precursor protein. *Nature* 1998; 391: 387-90.
- Deleault NR, Harris BT, Rees JR, Supattapone S. Formation of native prions from minimal components in vitro. *Proc Natl Acad Sci U S A* 2007; 104: 9741-6.
- Dickson TC, Vickers JC. The morphological phenotype of beta-amyloid plaques and associated neuritic changes in Alzheimer's disease. *Neuroscience* 2001; 105: 99-107.
- Divry P. Etude histochemique des plaques seniles. *J Belge Neurol Psychiat* 1927; 27: 643-57.
- Domert J, Rao SB, Agholme L, Brorsson AC, Marcusson J, Hallbeck M, *et al.* Spreading of amyloid-beta peptides via neuritic cell-to-cell transfer is dependent on insufficient cellular clearance. *Neurobiol Dis* 2014; 65: 82-92.
- Doody RS, Raman R, Farlow M, Iwatsubo T, Vellas B, Joffe S, *et al.* A phase 3 trial of semagacestat for treatment of Alzheimer's disease. *N Engl J Med* 2013; 369: 341-50.
- Doody RS, Thomas RG, Farlow M, Iwatsubo T, Vellas B, Joffe S, *et al.* Phase 3 trials of solanezumab for mild-to-moderate Alzheimer's disease. *N Engl J Med* 2014; 370: 311-21.

- Droste P, Frenzel A, Steinwand M, Pelat T, Thullier P, Hust M, *et al.* Structural differences of amyloid-beta fibrils revealed by antibodies from phage display. *BMC Biotechnol* 2015; 15: 57.
- Dubois B, Hampel H, Feldman HH, Scheltens P, Aisen P, Andrieu S, *et al.* Preclinical Alzheimer's disease: Definition, natural history, and diagnostic criteria. *Alzheimers Dement* 2016; 12: 292-323.
- Eisenberg D, Jucker M. The amyloid state of proteins in human diseases. *Cell* 2012; 148: 1188-203.
- Espuny-Camacho I, Arranz AM, Fiers M, Snellinx A, Ando K, Munck S, *et al.* Hallmarks of Alzheimer's disease in stem-cell-derived human neurons transplanted into mouse brain. *Neuron* 2017; 93: 1066-81.
- Fagan AM, Roe CM, Xiong C, Mintun MA, Morris JC, Holtzman DM. Cerebrospinal fluid tau/beta-amyloid42 ratio as a prediction of cognitive decline in nondemented older adults. *Arch Neurol* 2007; 64: 343-9.
- Fitzpatrick AWP, Falcon B, He S, Murzin AG, Murshudov G, Garringer HJ, *et al.* Cryo-EM structures of tau filaments from Alzheimer's disease. *Nature* 2017; 547: 185-90.
- Francis PT, Palmer AM, Snape M, Wilcock GK. The cholinergic hypothesis of Alzheimer's disease: a review of progress. *J Neurol Neurosurg Psychiatry* 1999; 66: 137-47.
- Fraser H, Dickinson AG. Scrapie in mice. Agent-strain differences in the distribution and intensity of grey matter vacuolation. *J Comp Pathol* 1973; 83: 29-40.
- Fritschi SK, Cintron A, Ye L, Mahler J, Buhler A, Baumann F, *et al.* Abeta seeds resist inactivation by formaldehyde. *Acta Neuropathol* 2014a; 128: 477-84.
- Fritschi SK, Langer F, Kaeser SA, Maia LF, Portelius E, Pinotsi D, *et al.* Highly potent soluble amyloid-beta seeds in human Alzheimer brain but not cerebrospinal fluid. *Brain* 2014b; 137: 2909-15.
- Frontzek K, Lutz MI, Aguzzi A, Kovacs GG, Budka H. Amyloid-beta pathology and cerebral amyloid angiopathy are frequent in iatrogenic Creutzfeldt-Jakob disease after dural grafting. *Swiss Med Wkly* 2016; 146: w14287.
- Gajdusek DC, Gibbs CJ Jr, Alpers MP. Experimental transmission of a kuru-like syndrome to chimpanzees. *Nature* 1966; 209: 794-96.
- Gajdusek DC. Unconventional viruses and the origin and disappearance of kuru. *Science* 1977; 197: 943-60.
- Gao Y, Pimplikar S. The gamma-secretase-cleaved C-terminal fragment of amyloid precursor protein mediates signaling to the nucleus. *Proc Natl Acad Sci U S A* 2001; 98: 14979-84.
- Giannakopoulos P, Herrmann FR, Bussiere T, Bouras C, Kovari E, Perl DP, *et al.* Tangle and neuron numbers, but not amyloid load, predict cognitive status in Alzheimer's disease. *Neurology* 2003; 60: 1495-500.
- Glenner GG, Wong CW. Alzheimer's disease: initial report of the purification and characterization of a novel cerebrovascular amyloid protein. *Biochem Biophys Res Commun* 1984; 120: 885-90.
- Goate A, Chartier-Harlin MC, Mullan M, Brown J, Crawford F, Fidani L, *et al.* Segregation of a missense mutation in the amyloid precursor protein gene with familial Alzheimer's disease. *Nature* 1991; 349: 704-6.
- Goedert M, Wischik CM, Crowther RA, Walker JE, Klug A. Cloning and sequencing of the cDNA encoding a core protein of the paired helical filament of Alzheimer disease: identification as the microtubule-associated protein tau. *Proc Natl Acad Sci U S A* 1988; 85: 4051-5.

- Goldgaber D, Lerman MO, McBride OW, Saffiontti U, Gajdusek DC. Characterization and chromosomal localization of a cDNA encoding brain amyloid of Alzheimer's disease. *Science* 1987; 235: 877-80.
- Gong Y, Chang L, Viola KL, Lacor PN, Lambert MP, Finch CE, *et al.* Alzheimer's disease-affected brain: presence of oligomeric Abeta ligands (ADDLs) suggests a molecular basis for reversible memory loss. *Proc Natl Acad Sci U S A* 2003; 100: 10417-22.
- Gotz J, Ittner LM. Animal models of Alzheimer's disease and frontotemporal dementia. *Nat Rev Neurosci* 2008; 9: 532-44.
- Gremer L, Scholzel D, Schenk C, Reinartz E, Labahn J, Ravelli RBG, *et al.* Fibril structure of amyloid-beta(1-42) by cryo-electron microscopy. *Science* 2017; 358: 116-9.
- Griffith JS. Self-replication and scrapie. *Nature* 1967; 215: 1043-44.
- Guo JL, Narasimhan S, Changolkar L, He Z, Stieber A, Zhang B, *et al.* Unique pathological tau conformers from Alzheimer's brains transmit tau pathology in nontransgenic mice. *J Exp Med* 2016; 213: 2635-54.
- Haass C, Schlossmacher MG, Hung AY, Vigo-Pelfrey C, Mellon A, Ostaszewski BL, *et al.* Amyloid-beta peptide is produced by cultured cells during normal metabolism. *Nature* 1992; 359: 322-5.
- Haass C, Selkoe DJ. Soluble protein oligomers in neurodegeneration: lessons from the Alzheimer's amyloid-beta peptide. *Nat Rev Mol Cell Biol* 2007; 8: 101-12.
- Hamaguchi T, Taniguchi Y, Sakai K, Kitamoto T, Takao M, Murayama S, *et al.* Significant association of cadaveric dura mater grafting with subpial Abeta deposition and meningeal amyloid angiopathy. *Acta Neuropathol* 2016; 132: 313-5.
- Harper JD, Wong SS, Lieber CM, Lansbury PT, Jr. Assembly of Abeta amyloid protofibrils: an in vitro model for a possible early event in Alzheimer's disease. *Biochemistry* 1999; 38: 8972-80.
- Hartley DM, Walsh DM, Ye CP, Diehl T, Vasquez S, Vassilev PM, *et al.* Protofibrillar intermediates of amyloid-beta protein induce acute electrophysiological changes and progressive neurotoxicity in cortical neurons. *J Neurosci* 1999; 19: 8876-84.
- Hashimoto T, Serrano-Pozo A, Hori Y, Adams KW, Takeda S, Banerji AO, *et al.* Apolipoprotein E, especially apolipoprotein E4, increases the oligomerization of amyloid-beta peptide. *J Neurosci* 2012; 32: 15181-92.
- Hawkes N. Merck ends trial of potential Alzheimer's drug verubecestat. *BMJ* 2017; 356: j845.
- He Z, Guo JL, McBride JD, Narasimhan S, Kim H, Changolkar L, *et al.* Amyloid-beta plaques enhance Alzheimer's brain tau-seeded pathologies by facilitating neuritic plaque tau aggregation. *Nature Med* 2017; 24: 29-38.
- Heilbronner G, Eisele YS, Langer F, Kaeser SA, Novotny R, Nagarathinam A, *et al.* Seeded strain-like transmission of beta-amyloid morphotypes in APP transgenic mice. *EMBO Rep* 2013; 14: 1017-22.
- Heneka MT, Carson MJ, El Khoury J, Landreth GE, Brosseron F, Feinstein DL, *et al.* Neuroinflammation in Alzheimer's disease. *Lancet Neurol* 2015; 14: 388-405.
- Hepler RW, Grimm KM, Nahas DD, Breese R, Dodson EC, Acton P, *et al.* Solution state characterization of amyloid-beta-derived diffusible ligands. *Biochemistry* 2006; 45: 15157-67.
- Herrmann US, Schütz AK, Shirani H, Huang D, Saban D, Nuvolone M, *et al.* Structure-based drug design identifies polythiophenes as antiprion compounds. *Sci Transl Med* 2015; 7: 299ra123.
- Holtzman DM, Morris JC, Goate AM. Alzheimer's disease: the challenge of the second century. *Sci Transl Med* 2011; 3: 77sr1.

- Hsiao K, Baker HF, Crow TJ, Poulter M, Owen F, Terwillinger JD, *et al.* Linkage of a prion protein missense variant to Gerstmann-Sträussler syndrome. *Nature* 1989; 338: 342-5.
- Huang YWA, Zhou B, Wernig M, Sudhof TC. ApoE2, ApoE3, and ApoE4 differentially stimulate APP transcription and A β secretion. *Cell* 2017; 168: 427-41.
- Huynh TV, Liao F, Francis CM, Robinson GO, Serrano JR, Jiang H, *et al.* Age-dependent effects of ApoE reduction using antisense oligonucleotides in a model of beta-amyloidosis. *Neuron* 2017; 96: 1013-23.
- Ikeda S, Allsop D, Glenner GG. Morphology and distribution of plaque and related deposits in the brains of Alzheimer's disease and control cases. An immunohistochemical study using amyloid-beta protein antibody. *Lab Invest* 1989; 60: 113-22.
- Jack CR, Jr., Holtzman DM. Biomarker modeling of Alzheimer's disease. *Neuron* 2013; 80: 1347-58.
- Jarrett JT, Berger EP, Lansbury PT, Jr. The carboxy terminus of the beta-amyloid protein is critical for the seeding of amyloid formation: implications for the pathogenesis of Alzheimer's disease. *Biochemistry* 1993; 32: 4693-7.
- Jarrett JT, Lansbury PT, Jr. Seeding "one-dimensional crystallization" of amyloid: a pathogenic mechanism in Alzheimer's disease and scrapie? *Cell* 1993; 73: 1055-8.
- Jaunmuktane Z, Mead S, Ellis M, Wadsworth JD, Nicoll AJ, Kenny J, *et al.* Evidence for human transmission of amyloid-beta pathology and cerebral amyloid angiopathy. *Nature* 2015; 525: 247-50.
- Jonsson T, Atwal JK, Steinberg S, Snaedal J, Jonsson PV, Bjornsson S, *et al.* A mutation in APP protects against Alzheimer's disease and age-related cognitive decline. *Nature* 2012; 488: 96-9.
- Jucker M, Walker LC. Self-propagation of pathogenic protein aggregates in neurodegenerative diseases. *Nature* 2013; 501: 45-51.
- Kakuda N, Miyasaka T, Iwasaki N, Nirasawa T, Wada-Kakuda S, Takahashi-Fujigasaki J, *et al.* Distinct deposition of amyloid-beta species in brains with Alzheimer's disease pathology visualized with MALDI imaging mass spectrometry. *Acta Neuropathol Commun* 2017; 5: 73.
- Kang J, Lemaire HG, Unterbeck A, Salbaum JM, Masters CL, Grzeschik KH, *et al.* The precursor of Alzheimer's disease amyloid A β protein resembles a cell-surface receptor. *Nature* 1987; 325: 733-36.
- Karch CM, Goate AM. Alzheimer's disease risk genes and mechanisms of disease pathogenesis. *Biol Psychiatry* 2015; 77: 43-51.
- Karran E, De Strooper B. The amyloid cascade hypothesis: are we poised for success or failure? *J Neurochem* 2016; 139 Suppl 2: 237-52.
- Karran E, Hardy J. A critique of the drug discovery and phase 3 clinical programs targeting the amyloid hypothesis for Alzheimer disease. *Ann Neurol* 2014; 76: 185-205.
- Kayed R, Head E, Thompson JL, McIntire TM, Milton SC, Cotman CW, *et al.* Common structure of soluble amyloid oligomers implies common mechanism of pathogenesis. *Science* 2003; 300: 486-9.
- Kennedy ME, Stamford AW, Chen X, Cox K, Cumming JN, Dockendorf MF, *et al.* The BACE1 inhibitor verubecestat (MK-8931) reduces CNS beta-amyloid in animal models and in Alzheimer's disease patients. *Sci Transl Med* 2016; 8: 363ra150.
- Kim J, Basak JM, Holtzman DM. The role of apolipoprotein E in Alzheimer's disease. *Neuron* 2009; 63: 287-303.
- Klatzo I, Gajdusek DC, Zigas V. Pathology of kuru. *Lab Invest* 1959; 8: 799-847.
- Kleinberger G, Yamanishi Y, Suarez-Calvet M, Czirr E, Lohmann E, Cuyvers E, *et al.* TREM2 mutations implicated in neurodegeneration impair cell surface transport and phagocytosis. *Sci Transl Med* 2014; 6: 243ra86.

- Klunk WE, Engler H, Nordberg A, Wang Y, Blomqvist G, Holt DP, *et al.* Imaging brain amyloid in Alzheimer's disease with Pittsburgh Compound-B. *Ann Neurol* 2004; 55: 306-19.
- Klyubin I, Betts V, Welzel AT, Blennow K, Zetterberg H, Wallin A, *et al.* Amyloid-beta protein dimer-containing human CSF disrupts synaptic plasticity: prevention by systemic passive immunization. *J Neurosci* 2008; 28: 4231-7.
- Knowles TP, Vendruscolo M, Dobson CM. The amyloid state and its association with protein misfolding diseases. *Nat Rev Mol Cell Biol* 2014; 15: 384-96.
- Kondo J, Honda T, Mori H, Hamada Y, Miura R, Ogawara M, *et al.* The carboxyl third of tau is tightly bound to paired helical filaments. *Neuron* 1988; 1: 827-34.
- Kovacs GG, Lutz MI, Ricken G, Strobel T, Hofberger R, Preusser M, *et al.* Dura mater is a potential source of Aβ seeds. *Acta Neuropathol* 2016; 131: 911-23.
- Krasemann S, Madore C, Cialic R, Baufeld C, Calcagno N, El Fatimy R, *et al.* The TREM2-APOE pathway drives the transcriptional phenotype of dysfunctional microglia in neurodegenerative diseases. *Immunity* 2017; 47: 566-81.
- Kuhn PH, Wang H, Dislich B, Colombo A, Zeitschel U, Ellwart JW, *et al.* ADAM10 is the physiologically relevant, constitutive α-secretase of the amyloid precursor protein in primary neurons. *EMBO J* 2010; 29: 3020-32.
- LaFerla FM, Green KN, Oddo S. Intracellular amyloid-beta in Alzheimer's disease. *Nat Rev Neurosci* 2007; 8: 499-509.
- Lambert MP, Barlow AK, Chromy BA, Edwards C, Freed R, Liosatos M, *et al.* Diffusible, nonfibrillar ligands derived from Aβ₁₋₄₂ are potent central nervous system neurotoxins. *Proc Natl Acad Sci U S A* 1998; 95: 6448-53.
- Langer F, Eisele YS, Fritsch SK, Staufenbiel M, Walker LC, Jucker M. Soluble Aβ seeds are potent inducers of cerebral beta-amyloid deposition. *J Neurosci* 2011; 31: 14488-95.
- Lashuel HA, Hartley D, Petre BM, Walz T, Lansbury PT, Jr. Neurodegenerative disease: amyloid pores from pathogenic mutations. *Nature* 2002; 418: 291.
- Lathuiliere A, Laversenne V, Astolfo A, Kopetzki E, Jacobsen H, Stampanoni M, *et al.* A subcutaneous cellular implant for passive immunization against amyloid-beta reduces brain amyloid and tau pathologies. *Brain* 2016; 139: 1587-604.
- Lee J, Culyba EK, Powers ET, Kelly JW. Amyloid-beta forms fibrils by nucleated conformational conversion of oligomers. *Nat Chem Biol* 2011; 7: 602-9.
- Legname G, Baskakov IV, Nguyen HO, Riesner D, Cohen FE, DeArmond SJ, *et al.* Synthetic mammalian prions. *Science* 2004; 305: 673-6.
- Lesne S, Koh MT, Kotilinek L, Kaye R, Glabe CG, Yang A, *et al.* A specific amyloid-beta protein assembly in the brain impairs memory. *Nature* 2006; 440: 352-7.
- Lesne S, Kotilinek L, Ashe KH. Plaque-bearing mice with reduced levels of oligomeric amyloid-beta assemblies have intact memory function. *Neuroscience* 2008; 151: 745-9.
- Lesne SE, Sherman MA, Grant M, Kuskowski M, Schneider JA, Bennett DA, *et al.* Brain amyloid-beta oligomers in ageing and Alzheimer's disease. *Brain* 2013; 136: 1383-98.
- Li J, Browning S, Mahal SP, Oelschlegel AM, Weissmann C. Darwinian evolution of prions in cell culture. *Science* 2010; 327: 869-72.
- Liu CC, Zhao N, Fu Y, Wang N, Linares C, Tsai CW, *et al.* ApoE4 accelerates early seeding of amyloid pathology. *Neuron* 2017; 96: 1024-32.
- Liu J, Costantino I, Venugopalan N, Fischetti RF, Hyman BT, Frosch MP, *et al.* Amyloid structure exhibits polymorphism on multiple length scales in human brain tissue. *Sci Rep* 2016; 6: 33079.

- Liu P, Reed MN, Kotilinek LA, Grant MK, Forster CL, Qiang W, *et al.* Quaternary structure defines a large class of amyloid-beta oligomers neutralized by sequestration. *Cell Rep* 2015; 11: 1760-71.
- Lu JX, Qiang W, Yau WM, Schwieters CD, Meredith SC, Tycko R. Molecular structure of beta-amyloid fibrils in Alzheimer's disease brain tissue. *Cell* 2013; 154: 1257-68.
- Maarouf CL, Dausgs ID, Spina S, Vidal R, Kokjohn TA, Patton RL, *et al.* Histopathological and molecular heterogeneity among individuals with dementia associated with Presenilin mutations. *Mol Neurodegener* 2008; 3: 20.
- Magnusson K, Simon R, Sjolander D, Sigurdson CJ, Hammarstrom P, Nilsson KP. Multimodal fluorescence microscopy of prion strain specific PrP deposits stained by thiophene-based amyloid ligands. *Prion* 2014; 8: 319-29.
- Mahler J, Morales-Corraliza J, Stolz J, Skodras A, Radde R, Duma CC, *et al.* Endogenous murine Abeta increases amyloid deposition in APP23 but not in APPPS1 transgenic mice. *Neurobiol Aging* 2015; 36: 2241-7.
- Mahley RW. Apolipoprotein E: cholesterol transport protein with expanding role in cell biology. *Science* 1988; 240: 622-30.
- Marsh RF, Bessen RA. Physicochemical and biological characterizations of distinct strains of the transmissible mink encephalopathy agent. *Philos Trans R Soc Lond B Biol Sci* 1994; 343: 413-4.
- Marzesco AM, Flotenmeyer M, Buhler A, Obermuller U, Staufenbiel M, Jucker M, *et al.* Highly potent intracellular membrane-associated Abeta seeds. *Sci Rep* 2016; 6: 28125.
- Masters CL, Simms G, Weinman NA, Multhaup G, McDonald BL, Beyreuther K. Amyloid plaque core protein in Alzheimer disease and Down syndrome. *Proc Natl Acad Sci U S A* 1985; 82: 4245-9.
- McDade E, Bateman RJ. Stop Alzheimer's before it starts. *Nature* 2017; 547: 153-5.
- Meier BH, Riek R, Bockmann A. Emerging structural understanding of amyloid fibrils by solid-state NMR. *Trends Biochem Sci* 2017; 42: 777-87.
- Meisl G, Yang X, Hellstrand E, Frohm B, Kirkegaard JB, Cohen SI, *et al.* Differences in nucleation behavior underlie the contrasting aggregation kinetics of the Abeta40 and Abeta42 peptides. *Proc Natl Acad Sci U S A* 2014; 111: 9384-9.
- Meyer RK, McKinley MP, Bowman KA, Braunfeld MB, Barry RA, Prusiner SB. Separation and properties of cellular and scrapie prion proteins. *Proc Natl Acad Sci U S A* 1986; 83: 2310-4.
- Meyer-Luehmann M, Coomaraswamy J, Bolmont T, Kaeser S, Schaefer C, Kilger E, *et al.* Exogenous induction of cerebral beta-amyloidogenesis is governed by agent and host. *Science* 2006; 313: 1781-4.
- Morales R, Bravo-Alegria J, Duran-Aniotz C, Soto C. Titration of biologically active amyloid-beta seeds in a transgenic mouse model of Alzheimer's disease. *Sci Rep* 2015; 5: 9349.
- Morales R, Duran-Aniotz C, Castilla J, Estrada LD, Soto C. De novo induction of amyloid-beta deposition in vivo. *Mol Psych* 2012; 17: 1347-53.
- Morgado I, Wieligmann K, Bereza M, Ronicke R, Meinhardt K, Annamalai K, *et al.* Molecular basis of beta-amyloid oligomer recognition with a conformational antibody fragment. *Proc Natl Acad Sci U S A* 2012; 109: 12503-8.
- Morgan D, Diamond DM, Gottschall PE, Ugen KE, Dickey C, Hardy J, *et al.* Abeta peptide vaccination prevents memory loss in an animal model of Alzheimer's disease. *Nature* 2000; 408: 982-5.
- Mori H, Takio K, Ogawara M, Selkoe DJ. Mass spectrometry of purified amyloid-beta protein in Alzheimer's disease. *J Biol Chem* 1992; 267: 17082-6.

- Mullan M, Crawford F, Axelman K, Houlden H, Lilius L, Winblad B, *et al.* A pathogenic mutation for probable Alzheimer's disease in the APP gene at the N-terminus of beta-amyloid. *Nat Genet* 1992; 1: 345-7.
- Muller UC, Deller T, Korte M. Not just amyloid: physiological functions of the amyloid precursor protein family. *Nat Rev Neurosci* 2017; 18: 281-98.
- Munke A, Persson J, Weiffert T, De Genst E, Meisl G, Arosio P, *et al.* Phage display and kinetic selection of antibodies that specifically inhibit amyloid self-replication. *Proc Natl Acad Sci U S A* 2017; 114: 6444-9.
- Murrell J, Farlow M, Ghetti B, Benson MD. A mutation in the amyloid precursor protein associated with hereditary Alzheimer's disease. *Science* 1991; 254: 97-9.
- Nagarathinam A, Hoflinger P, Buhler A, Schafer C, McGovern G, Jeffrey M, *et al.* Membrane-anchored Abeta accelerates amyloid formation and exacerbates amyloid-associated toxicity in mice. *J Neurosci* 2013; 33: 19284-94.
- Naslund J, Schierhorn A, Hellman U, Lannfelt L, Roses AD, Tjernberg LO, *et al.* Relative abundance of Alzheimer Abeta amyloid peptide variants in Alzheimer disease and normal aging. *Proc Natl Acad Sci U S A* 1994; 91: 8378-82.
- Nath S, Agholme L, Kurudenkandy FR, Granseth B, Marcusson J, Hallbeck M. Spreading of neurodegenerative pathology via neuron-to-neuron transmission of beta-amyloid. *J Neurosci* 2012; 32: 8767-77.
- Nilsson KP, Herland A, Hammarstrom P, Inganas O. Conjugated polyelectrolytes: conformation-sensitive optical probes for detection of amyloid fibril formation. *Biochemistry* 2005; 44: 3718-24.
- Novotny R, Langer F, Mahler J, Skodras A, Vlachos A, Wegenast-Braun BM, *et al.* Conversion of synthetic Abeta to in vivo active seeds and amyloid plaque formation in a hippocampal slice culture model. *J Neurosci* 2016; 36: 5084-93.
- Nyström S, Psonka-Antonczyk KM, Ellingsen PG, Johansson LBG, Reitan N, Handrick S, *et al.* Evidence for age-dependent in vivo conformational rearrangement within Abeta amyloid deposits. *ACS Chem Biol* 2013; 8: 1128-33.
- Olsen O, Kallop DY, McLaughlin T, Huntwork-Rodriguez S, Wu Z, Duggan CD, *et al.* Genetic analysis reveals that amyloid precursor protein and death receptor 6 function in the same pathway to control axonal pruning independent of beta-secretase. *J Neurosci* 2014; 34: 6438-47.
- Ostrowitzki S, Deptula D, Thurfjell L, Barkhof F, Bohrmann B, Brooks DJ, *et al.* Mechanism of amyloid removal in patients with Alzheimer disease treated with gantenerumab. *Arch Neurol* 2012; 69: 198-207.
- Palmer MS, Dryden AJ, Hughes JT, Collinge J. Homozygous prion protein genotype predisposes to sporadic Creutzfeldt-Jakob disease. *Nature* 1991; 352: 340-2.
- Pattison IH, Millson GC. Scrapie produced experimentally in goats with special reference to the clinical syndrome. *J Comp Pathol* 1961; 71: 101-9.
- Perry EK, Gibson PH, Blessed G, Perry RH, Tomlinson BE. Neurotransmitter enzyme abnormalities in senile dementia. Choline acetyltransferase and glutamic acid decarboxylase activities in necropsy brain tissue. *J Neurol Sci* 1977; 34: 247-65.
- Petkova AT, Leapman RD, Guo Z, Yau WM, Mattson MP, Tycko R. Self-propagating, molecular-level polymorphism in Alzheimer's beta-amyloid fibrils. *Science* 2005; 307: 262-5.
- Philipson O, Lord A, Lalowski M, Soliymani R, Baumann M, Thyberg J, *et al.* The Arctic amyloid-beta precursor protein (AbetaPP) mutation results in distinct plaques and accumulation of N- and C-truncated Abeta. *Neurobiol Aging* 2012; 33: 1010 e1-13.

- Podlisny MB, Ostaszewski BL, Squazzo SL, Koo EH, Rydell RE, Teplow DB, *et al.*
Aggregation of secreted amyloid-beta protein into sodium dodecyl sulfate-stable oligomers in cell culture. *J Biol Chem* 1995; 270: 9564-70.
- Polanco JC, Li C, Bodea LG, Martinez-Marmol R, Meunier FA, Gotz J. Amyloid-beta and tau complexity - towards improved biomarkers and targeted therapies. *Nat Rev Neurol* 2018; 14: 22-39.
- Pontecorvo MJ, Devous MD, Sr., Navitsky M, Lu M, Salloway S, Schaerf FW, *et al.*
Relationships between flortaucipir PET tau binding and amyloid burden, clinical diagnosis, age and cognition. *Brain* 2017; 140: 748-63.
- Portelius E, Bogdanovic N, Gustavsson MK, Volkman I, Brinkmalm G, Zetterberg H, *et al.*
Mass spectrometric characterization of brain amyloid-beta isoform signatures in familial and sporadic Alzheimer's disease. *Acta Neuropathol* 2010; 120: 185-93.
- Prusiner SB. Novel proteinaceous infectious particles cause scrapie. *Science* 1982; 216: 136-44.
- Prusiner SB. Biology and genetics of prions causing neurodegeneration. *Annu Rev Genet* 2013; 47: 601-23.
- Prusiner SB, Cochran SP, Groth DF, Downey DE, Bowman KA, Martinez HM.
Measurement of the scrapie agent using an incubation time interval assay. *Ann Neurol* 1982; 11: 353-8.
- Psonka-Antonczyk KM, Hammarstrom P, Johansson LB, Lindgren M, Stokke BT, Nilsson KP, *et al.* Nanoscale structure and spectroscopic probing of Abeta1-40 fibril bundle formation. *Front Chem* 2016; 4: 44.
- Qiang W, Yau WM, Lu JX, Collinge J, Tycko R. Structural variation in amyloid-beta fibrils from Alzheimer's disease clinical subtypes. *Nature* 2017; 541: 217-21.
- Qiang W, Yau WM, Luo Y, Mattson MP, Tycko R. Antiparallel beta-sheet architecture in Iowa-mutant beta-amyloid fibrils. *Proc Natl Acad Sci U S A* 2012; 109: 4443-8.
- Radde R, Bolmont T, Kaeser SA, Coomaraswamy J, Lindau D, Stoltze L, *et al.* Abeta42-driven cerebral amyloidosis in transgenic mice reveals early and robust pathology. *EMBO Rep* 2006; 7: 940-6.
- Rasmussen J, Jucker M, Walker LC. Abeta seeds and prions: How close the fit? *Prion* 2017a; 11: 215-25.
- Rasmussen J, Mahler J, Beschorner N, Kaeser SA, Hasler LM, Baumann F, *et al.* Amyloid polymorphisms constitute distinct clouds of conformational variants in different etiological subtypes of Alzheimer's disease. *Proc Natl Acad Sci U S A* 2017b; 114: 13018-23.
- Rasmussen J, Bühler A, Baumann F, Jucker M. An agarose gel fractionation method for enriching brain derived proteopathic seeds. *in preparation*.
- Reed LJ, Muench H. A simple method of estimating fifty per cent endpoints. *Am J Epidemiol* 1938; 27: 493-7.
- Riek R, Eisenberg DS. The activities of amyloids from a structural perspective. *Nature* 2016; 539: 227-35.
- Ring S, Weyer SW, Kilian SB, Waldron E, Pietrzik CU, Filippov MA, *et al.* The secreted beta-amyloid precursor protein ectodomain sAPP-alpha is sufficient to rescue the anatomical, behavioral, and electrophysiological abnormalities of APP-deficient mice. *J Neurosci* 2007; 27: 7817-26.
- Rinne JO, Brooks DJ, Rossor MN, Fox NC, Bullock R, Klunk WE, *et al.* 11C-PiB PET assessment of change in fibrillar amyloid-beta load in patients with Alzheimer's disease treated with bapineuzumab: a phase 2, double-blind, placebo-controlled, ascending-dose study. *Lancet Neurol* 2010; 9: 363-72.

- Ritchie DL, Adlard P, Peden AH, Lowrie S, Le Grice M, Burns K, *et al.* Amyloid-beta accumulation in the CNS in human growth hormone recipients in the UK. *Acta Neuropathol* 2017; 134: 221-40.
- Robert J, Button EB, Yuen B, Gilmour M, Kang K, Bahrabadi A, *et al.* Clearance of beta-amyloid is facilitated by apolipoprotein E and circulating high-density lipoproteins in bioengineered human vessels. *Elife* 2017; 6.
- Rocca WA, Petersen RC, Knopman DS, Hebert LE, Evans DA, Hall KS, *et al.* Trends in the incidence and prevalence of Alzheimer's disease, dementia, and cognitive impairment in the United States. *Alzheimers Dement* 2011; 7: 80-93.
- Rosen RF, Ciliax BJ, Wingo TS, Gearing M, Dooyema J, Lah JJ, *et al.* Deficient high-affinity binding of Pittsburgh compound B in a case of Alzheimer's disease. *Acta Neuropathol* 2010; 119: 221-33.
- Rosen RF, Fritz JJ, Dooyema J, Cintron AF, Hamaguchi T, Lah JJ, *et al.* Exogenous seeding of cerebral beta-amyloid deposition in betaAPP-transgenic rats. *J Neurochem* 2012; 120: 660-6.
- Rovelet-Lecrux A, Hannequin D, Raux G, Le Meur N, Laquerriere A, Vital A, *et al.* APP locus duplication causes autosomal dominant early-onset Alzheimer disease with cerebral amyloid angiopathy. *Nat Genet* 2006; 38: 24-6.
- Saborio GP, Permanne B, Soto C. Sensitive detection of pathological prion protein by cyclic amplification of protein misfolding. *Nature* 2001; 411: 810-3.
- Safar J, Wille H, Itri V, Groth D, Serban H, Torchia M, *et al.* Eight prion strains have PrP(Sc) molecules with different conformations. *Nat Med* 1998; 4: 1157-65.
- Saido TC, Yamao-Harigaya W, Iwatsubo T, Kawashima S. Amino- and carboxyl-terminal heterogeneity of beta-amyloid peptides deposited in human brain. *Neurosci Lett* 1996; 215: 173-6.
- Saint-Aubert L, Lemoine L, Chiotis K, Leuzy A, Rodriguez-Vieitez E, Nordberg A. Tau PET imaging: present and future directions. *Mol Neurodegener* 2017; 12: 19.
- Saito T, Matsuba Y, Mihira N, Takano J, Nilsson P, Itohara S, *et al.* Single APP knock-in mouse models of Alzheimer's disease. *Nat Neurosci* 2014; 17: 661-3.
- Saito T, Matsuba Y, Yamazaki N, Hashimoto S, Saido TC. Calpain Activation in Alzheimer's model mice is an artifact of APP and Presenilin overexpression. *J Neurosci* 2016; 36: 9933-6.
- Sannerud R, Esselens C, Ejsmont P, Mattera R, Rochin L, Tharkeshwar AK, *et al.* Restricted location of PSEN2/gamma-secretase determines substrate specificity and generates an intracellular A β pool. *Cell* 2016; 166: 193-208.
- Sasaguri H, Nilsson P, Hashimoto S, Nagata K, Saito T, De Strooper B, *et al.* APP mouse models for Alzheimer's disease preclinical studies. *EMBO J* 2017; 36: 2473-87.
- Satizabal CL, Beiser AS, Chouraki V, Chene G, Dufouil C, Seshadri S. Incidence of dementia over three decades in the Framingham Heart Study. *N Engl J Med* 2016; 374: 523-32.
- Schelle J, Hasler LM, Gopfert JC, Joos TO, Vanderstichele H, Stoops E, *et al.* Prevention of tau increase in cerebrospinal fluid of APP transgenic mice suggests downstream effect of BACE1 inhibition. *Alzheimers Dement* 2017; 13: 701-9.
- Schenk D, Barbour R, Dunn W, Gordon G, Grajeda H, Guido T, *et al.* Immunization with amyloid-beta attenuates Alzheimer-disease-like pathology in the PDAPP mouse. *Nature* 1999; 400: 173-7.
- Schlepckow K, Kleinberger G, Fukumori A, Feederle R, Lichtenthaler SF, Steiner H, *et al.* An Alzheimer-associated TREM2 variant occurs at the ADAM cleavage site and affects shedding and phagocytic function. *EMBO Mol Med* 2017; 9: 1356-65.

- Schmidt C, Wolff M, Weitz M, Bartlau T, Korth C, Zerr I. Rapidly progressive Alzheimer disease. *Arch Neurol* 2011; 68: 1124-30.
- Schmidt M, Rohou A, Lasker K, Yadav JK, Schiene-Fischer C, Fandrich M, *et al.* Peptide dimer structure in an Aβ(1-42) fibril visualized with cryo-EM. *Proc Natl Acad Sci U S A* 2015; 112: 11858-63.
- Schmidt M, Sachse C, Richter W, Xu C, Fandrich M, Grigorieff N. Comparison of Alzheimer Aβ(1-40) and Aβ(1-42) amyloid fibrils reveals similar protofilament structures. *Proc Natl Acad Sci U S A* 2009; 106: 19813-8.
- Schütz AK, Hornemann S, Walti MA, Greuter L, Tiberi C, Cadalbert R, *et al.* Binding of polythiophenes to amyloids: Structural mapping of the pharmacophore. *ACS Chem Neurosci* 2017.
- Selkoe DJ, Hardy J. The amyloid hypothesis of Alzheimer's disease at 25 years. *EMBO Mol Med* 2016; 8: 595-608.
- Serrano-Pozo A, Frosch MP, Masliah E, Hyman BT. Neuropathological alterations in Alzheimer disease. *Cold Spring Harb Perspect Med* 2011; 1: a006189.
- Seuring C, Verasdonck J, Ringler P, Cadalbert R, Stahlberg H, Bockmann A, *et al.* Amyloid fibril polymorphism: Almost identical on the atomic level, mesoscopically very different. *J Phys Chem B* 2017; 121: 1783-92.
- Sevigny J, Chiao P, Bussiere T, Weinreb PH, Williams L, Maier M, *et al.* The antibody aducanumab reduces Aβ plaques in Alzheimer's disease. *Nature* 2016; 537: 50-6.
- Shankar GM, Li S, Mehta TH, Garcia-Munoz A, Shepardson NE, Smith I, *et al.* Amyloid-beta protein dimers isolated directly from Alzheimer's brains impair synaptic plasticity and memory. *Nature Med* 2008; 14: 837-42.
- Shaw LM, Vanderstichele H, Knapik-Czajka M, Clark CM, Aisen PS, Petersen RC, *et al.* Cerebrospinal fluid biomarker signature in Alzheimer's disease neuroimaging initiative subjects. *Ann Neurol* 2009; 65: 403-13.
- Sherrington R, Rogaev EI, Liang Y, Rogaeva EA, Levesque G, Ikeda M, *et al.* Cloning of a gene bearing missense mutations in early-onset familial Alzheimer's disease. *Nature* 1995; 375: 754-60.
- Shimshak DR, Jacobson LH, Kolly C, Zamurovic N, Balavenkatraman KK, Morawiec L, *et al.* Pharmacological BACE1 and BACE2 inhibition induces hair depigmentation by inhibiting PMEL17 processing in mice. *Sci Rep* 2016; 6: 21917.
- Soba P, Eggert S, Wagner K, Zentgraf H, Siehl K, Kreger S, *et al.* Homo- and heterodimerization of APP family members promotes intercellular adhesion. *EMBO J* 2005; 24: 3624-34.
- Stockman S. Scrapie: An obscure disease of sheep. *J Comp Pathol Ther* 1913; 26: 317-27.
- Stöhr J, Condello C, Watts JC, Bloch L, Oehler A, Nick M, *et al.* Distinct synthetic Aβ prion strains producing different amyloid deposits in bigenic mice. *Proc Natl Acad Sci U S A* 2014; 111: 10329-34.
- Stöhr J, Watts JC, Mensinger ZL, Oehler A, Grillo SK, DeArmond SJ, *et al.* Purified and synthetic Alzheimer's amyloid-beta (Aβ) prions. *Proc Natl Acad Sci U S A* 2012; 109: 11025-30.
- Sturchler-Pierrat C, Abramowski D, Duke M, Wiederhold KH, Mistl C, Rothacher S, *et al.* Two amyloid precursor protein transgenic mouse models with Alzheimer disease-like pathology. *Proc Natl Acad Sci U S A* 1997; 94: 13287-92.
- Szaruga M, Munteanu B, Lismont S, Veugelen S, Horre K, Mercken M, *et al.* Alzheimer's-causing mutations shift Aβ length by destabilizing gamma-secretase-Aβ interactions. *Cell* 2017; 170: 443-56 e14.

- Szaruga M, Veugelen S, Benurwar M, Lismont S, Sepulveda-Falla D, Lleo A, *et al.* Qualitative changes in human gamma-secretase underlie familial Alzheimer's disease. *J Exp Med* 2015; 212: 2003-13.
- Tagami S, Yanagida K, Kodama TS, Takami M, Mizuta N, Oyama H, *et al.* Semagacestat is a pseudo-inhibitor of gamma-secretase. *Cell Rep* 2017; 21: 259-73.
- Tagliavini F, Giaccone G, Frangione B, Bugiani O. Preamyloid deposits in the cerebral cortex of patients with Alzheimer's disease and nondemented individuals. *Neurosci Lett* 1988; 93: 191-6.
- Takagi-Niidome S, Sasaki T, Osawa S, Sato T, Morishima K, Cai T, *et al.* Cooperative roles of hydrophilic loop 1 and the C-terminus of presenilin 1 in the substrate-gating mechanism of gamma-secretase. *J Neurosci* 2015; 35: 2646-56.
- Takami M, Nagashima Y, Sano Y, Ishihara S, Morishima-Kawashima M, Funamoto S, *et al.* gamma-Secretase: successive tripeptide and tetrapeptide release from the transmembrane domain of beta-carboxyl terminal fragment. *J Neurosci* 2009; 29: 13042-52.
- Tanzi RE, Gusella JF, Watkins PC, Bruns GA, St George-Hyslop P, van Keuren ML, *et al.* Amyloid beta protein gene: cDNA, mRNA distribution, and genetic linkage near the Alzheimer locus. *Science* 1987; 235: 880-84.
- Tarasoff-Conway JM, Carare RO, Osorio RS, Glodzik L, Butler T, Fieremans E, *et al.* Clearance systems in the brain-implications for Alzheimer disease. *Nat Rev Neurol* 2015; 11: 457-70.
- Taylor CJ, Ireland DR, Ballagh I, Bourne K, Marechal NM, Turner PR, *et al.* Endogenous secreted amyloid precursor protein-alpha regulates hippocampal NMDA receptor function, long-term potentiation and spatial memory. *Neurobiol Dis* 2008; 31: 250-60.
- Thal DR, Rüb U, Orantes M, Braak H. Phases of Aβ-deposition in the human brain and its relevance for the development of AD. *Neurology* 2002; 58: 1791-1800.
- Thal DR, Capetillo-Zarate E, Del Tredici K, Braak H. The development of amyloid-beta protein deposits in the aged brain. *Sci Aging Knowledge Environ* 2006; 2006: re1.
- Thal DR, Beach TG, Zanette M, Heurling K, Chakrabarty A, Ismail A, *et al.* [(18)F] flutemetamol amyloid positron emission tomography in preclinical and symptomatic Alzheimer's disease: specific detection of advanced phases of amyloid-beta pathology. *Alzheimers Dement* 2015; 11: 975-85.
- Thomas JG, Chenoweth CE, Sullivan SE. Iatrogenic Creutzfeldt-Jakob disease via surgical instruments. *J Clin Neurosci* 2013; 20: 1207-12.
- Tycko R. Amyloid polymorphism: Structural basis and neurobiological relevance. *Neuron* 2015; 86: 632-45.
- van Harten AC, Visser PJ, Pijnenburg YAL, Teunissen CE, Blankenstein MA, Scheltens P, *et al.* Cerebrospinal fluid Aβ42 is the best predictor of clinical progression in patients with subjective complaints. *Alzheimer Dement* 2013; 9: 481-7.
- Vassar R, Kuhn PH, Haass C, Kennedy ME, Rajendran L, Wong PC, *et al.* Function, therapeutic potential and cell biology of BACE proteases: current status and future prospects. *J Neurochem* 2014; 130: 4-28.
- Vazquez-Fernandez E, Vos MR, Afanasyev P, Cebey L, Sevillano AM, Vidal E, *et al.* The structural architecture of an infectious mammalian prion using electron cryomicroscopy. *Plos Pathog* 2016; 12: e1005835.
- Villarreal S, Zhao F, Hyde LA, Holder D, Forest T, Sondey M, *et al.* Chronic Verubecestat treatment suppresses amyloid accumulation in advanced aged Tg2576-AβPPswe mice without inducing microhemorrhage. *J Alzheimers Dis* 2017; 59: 1393-413.
- Voytyuk I, De Strooper B, Chavez-Gutierrez L. Modulation of gamma- and beta-secretases as early prevention against Alzheimer's disease. *Biol Psychiatry* 2017; 83: 320-7.

- Wadsworth JD, Asante EA, Desbruslais M, Linehan JM, Joiner S, Gowland I, *et al.* Human prion protein with valine 129 prevents expression of variant CJD phenotype. *Science* 2004; 306: 1793-6.
- Walker LC, Jucker M. Neurodegenerative diseases: Expanding the prion concept. *Annu Rev Neurosci* 2015; 38: 87-103.
- Walker LC, Jucker M. The Exceptional vulnerability of humans to Alzheimer's disease. *Trends Mol Med* 2017; 23: 534-45.
- Walsh DM, Hartley DM, Kusumoto Y, Fezoui Y, Condron MM, Lomakin A, *et al.* Amyloid-beta protein fibrillogenesis. Structure and biological activity of protofibrillar intermediates. *J Biol Chem* 1999; 274: 25945-52.
- Walsh DM, Klyubin I, Fadeeva JV, Cullen WK, Anwyl R, Wolfe MS, *et al.* Naturally secreted oligomers of amyloid-beta protein potently inhibit hippocampal long-term potentiation in vivo. *Nature* 2002; 416: 535-9.
- Walsh DM, Tseng BP, Rydel RE, Podlisny MB, Selkoe DJ. The oligomerization of amyloid-beta protein begins intracellularly in cells derived from human brain. *Biochemistry* 2000; 39: 10831-9.
- Walti MA, Ravotti F, Arai H, Glabe CG, Wall JS, Bockmann A, *et al.* Atomic-resolution structure of a disease-relevant Abeta(1-42) amyloid fibril. *Proc Natl Acad Sci U S A* 2016; 113: E4976-84.
- Wang F, Wang X, Yuan CG, Ma J. Generating a prion with bacterially expressed recombinant prion protein. *Science* 2010; 327: 1132-5.
- Wang HW, Pasternak JF, Kuo H, Ristic H, Lambert MP, Chromy B, *et al.* Soluble oligomers of beta-amyloid (1-42) inhibit long-term potentiation but not long-term depression in rat dentate gyrus. *Brain Res* 2002; 924: 133-40.
- Wang J, Gu BJ, Masters CL, Wang YJ. A systemic view of Alzheimer disease - insights from amyloid-beta metabolism beyond the brain. *Nat Rev Neurol* 2017; 13: 612-23.
- Wang Y, Ulland TK, Ulrich JD, Song W, Tzaferis JA, Hole JT, *et al.* TREM2-mediated early microglial response limits diffusion and toxicity of amyloid plaques. *J Exp Med* 2016; 213: 667-75.
- Watts JC, Condello C, Stöhr J, Oehler A, Lee J, DeArmond SJ, *et al.* Serial propagation of distinct strains of Abeta prions from Alzheimer's disease patients. *Proc Natl Acad Sci U S A* 2014; 111: 10323-8.
- Watts JC, Giles K, Grillo SK, Lemus A, DeArmond SJ, Prusiner SB. Bioluminescence imaging of Abeta deposition in bigenic mouse models of Alzheimer's disease. *Proc Natl Acad Sci U S A* 2011; 108: 2528-33.
- Westergard L, Christensen HM, Harris DA. The cellular prion protein (PrP(C)): its physiological function and role in disease. *Biochim Biophys Acta* 2007; 1772: 629-44.
- Wilesmith JW, Wells GA, Cranwell MP, Ryan JB. Bovine spongiform encephalopathy: epidemiological studies. *Vet Rec* 1988; 123: 638-44.
- Willem M, Tahirovic S, Busche MA, Ovsepian SV, Chafai M, Kootar S, *et al.* eta-Secretase processing of APP inhibits neuronal activity in the hippocampus. *Nature* 2015; 526: 443-7.
- Wischik CM, Novak M, Thogersen HC, Edwards PC, Runswick MJ, Jakes R, *et al.* Isolation of a fragment of tau derived from the core of the paired helical filament of Alzheimer disease. *Proc Natl Acad Sci U S A* 1988; 85: 4506-10.
- Wisniewski HM, Bancher C, Barcikowska M, Wen GY, Currie J. Spectrum of morphological appearance of amyloid deposits in Alzheimer's disease. *Acta Neuropathol* 1989; 78: 337-47.

- Wolfe MS, Xia W, Ostaszewski BL, Diehl TS, Kimberly WT, Selkoe DJ. Two transmembrane aspartates in presenilin-1 required for presenilin endoproteolysis and gamma-secretase activity. *Nature* 1999; 398: 513-7.
- Wolk DA, Zhang Z, Boudhar S, Clark CM, Pontecorvo MJ, Arnold SE. Amyloid imaging in Alzheimer's disease: comparison of florbetapir and Pittsburgh compound-B positron emission tomography. *J Neurol Neurosurg Psychiatry* 2012; 83: 923-6.
- Wong CW, Quaranta V, Glenner GG. Neuritic plaques and cerebrovascular amyloid in Alzheimer disease are antigenically related. *Proc Natl Acad Sci U S A* 1985; 82: 8729-32.
- World Alzheimers Report 2015. The Global Impact of Dementia: An analysis of prevalence, incidence, cost and trends. *Alzheimer's Disease International* 2015; 1-82
- Xiang X, Werner G, Bohrmann B, Liesz A, Mazaheri F, Capell A, *et al.* TREM2 deficiency reduces the efficacy of immunotherapeutic amyloid clearance. *EMBO Mol Med* 2016; 8: 992-1004.
- Xiao Y, Ma B, McElheny D, Parthasarathy S, Long F, Hoshi M, *et al.* Abeta(1-42) fibril structure illuminates self-recognition and replication of amyloid in Alzheimer's disease. *Nat Struct Mol Biol* 2015; 22: 499-505.
- Xu F, Fu Z, Dass S, Kotarba AE, Davis J, Smith SO, *et al.* Cerebral vascular amyloid seeds drive amyloid-beta protein fibril assembly with a distinct anti-parallel structure. *Nat Commun* 2016; 7: 13527.
- Yamaguchi H, Hirai S, Morimatsu M, Shoji M, Ihara Y. A variety of cerebral amyloid deposits in the brains of the Alzheimer-type dementia demonstrated by beta protein immunostaining. *Acta Neuropathol* 1988; 76: 541-9.
- Ye L, Hamaguchi T, Fritschi SK, Eisele YS, Obermuller U, Jucker M, *et al.* Progression of seed-induced Abeta deposition within the limbic connectome. *Brain Pathol* 2015; 25: 743-52.
- Ye L, Rasmussen J, Kaeser SA, Marzesco AM, Obermuller U, Mahler J, *et al.* Abeta seeding potency peaks in the early stages of cerebral beta-amyloidosis. *EMBO Rep* 2017; 18: 1536-44.
- Yeh FL, Wang Y, Tom I, Gonzalez LC, Sheng M. TREM2 binds to apolipoproteins, including APOE and CLU/APOJ, and thereby facilitates uptake of Amyloid-beta by microglia. *Neuron* 2016; 91: 328-40.
- Zhang Y, Kim MS, Jia B, Yan J, Zuniga-Hertz JP, Han C, *et al.* Hypothalamic stem cells control ageing speed partly through exosomal miRNAs. *Nature* 2017; 548: 52-7.
- Zheng H, Jiang M, Trumbauer ME, Sirinathsinghji DJ, Hopkins R, Smith DW, *et al.* beta-amyloid precursor protein-deficient mice show reactive gliosis and decreased locomotor activity. *Cell* 1995; 81: 525-31.
- Zobeley E, Flechsig E, Cozzio A, Enari M, Weissmann C. Infectivity of scrapie prions bound to a stainless steel surface. *Mol Med* 1999; 5: 240-3.

3. Publications

3.1 Description of personal contribution

I. *Amyloid polymorphisms constitute distinct clouds of conformational variants in different etiological subtypes of Alzheimer's disease.*

Rasmussen J*, Mahler J*, Beschorner N*, Kaeser SA, Häsler LM, Baumann F, Nyström S, Portelius E, Blennow K, Lashley T, Fox NC, Sepulveda-Falla D, Glatzel M, Oblak AL, Ghetti B, Nilsson KPR, Hammarström P, Staufenbiel M, Walker LC, Jucker M.

*equal contribution

Published in: *Proceedings of the National Academy of Sciences of the United States of America*

Personal Contribution: Experimental design and planning of the study (together with JM, NB, KPRN, PH, MS, LCW and MJ); Homogenization of human tissue; Proteinase K digestions; Mouse injections, histology and stereology (together with NB); Data analysis and statistical analysis (together with JM and NB); Figure design and preparation (together with NB); Writing manuscript (together with all the other authors).

Others: JM, NB, LMH, EP, TL, DSF and ALO performed the experimental work. JM, NB, SAK, LMH, FB, SN, EP, KB, TL, NCF, DSF, MG, ALO and BG carried out the analysis. JM, NB, KPRN, PH, MS, LCW and MJ designed the experiments and wrote the manuscript with help from all other authors.

II. *A β seeding potency peaks in the early stages of cerebral β -amyloidosis.*

Ye L*, **Rasmussen J***, Kaeser SA, Marzesco A, Obermueller U, Mahler J, Schelle J, Odenthal J, Krueger C, Fritschi SK, Walker LC, Staufenbiel M, Baumann F, Jucker M.

*equal contribution

Published in: *EMBO Reports*

Personal Contribution: Dot blotting; Histology image acquisition (together with LY); Data analysis and statistical analysis (together with LY, SAK and AM); Figure design and preparation (together with LY); Writing manuscript (together with all the other authors).

Others: LY, AM, UO, JM, JS, JO, CK and SKF performed the experimental work. LY, SAK, AM, JM, JS, JO, SKF and FB carried out the analysis. LY, SAK, AM, LCW, MS, FB and MJ designed the experiments and wrote the manuscript with help from all other authors.

III. An agarose gel fractionation method for enriching brain derived proteopathic seeds.

Rasmussen J, Bühler A, Baumann F, Jucker M.

in preparation

Personal Contribution: Experimental design and planning of the study (together with AB, FB and MJ); *In vitro* and *in vivo* A β sample preparation; Agarose fractionation, immunoprecipitation and blotting (together with AB); Mouse injections and histology; Figure design and preparation; Writing manuscript (together with all the other authors).

Others: AB performed the experimental work. AB carried out the analysis. AB, FB and MJ designed the experiments and wrote the manuscript with help from all other authors.

3.2 Amyloid polymorphisms constitute distinct clouds of conformational variants in different etiological subtypes of Alzheimer's disease

Rasmussen J*, Mahler J*, Beschorner N*, Kaeser SA, Häsler LM, Baumann F, Nyström S, Portelius E, Blennow K, Lashley T, Fox NC, Sepulveda-Falla D, Glatzel M, Oblak AL, Ghetti B, Nilsson KPR, Hammarström P, Staufenbiel M, Walker LC, Jucker M.

Proc Natl Acad Sci U S A 2017b; 114: 13018-13023.

(doi:10.1073/pnas.1713215114)

*equal contribution



Amyloid polymorphisms constitute distinct clouds of conformational variants in different etiological subtypes of Alzheimer's disease

Jay Rasmussen^{a,b,c,1}, Jasmin Mahler^{a,c,1}, Natalie Beschoner^{a,c,1}, Stephan A. Kaeser^{a,b}, Lisa M. Häslér^{a,b}, Frank Baumann^{a,b}, Sofie Nyström^d, Erik Portelius^{e,f}, Kaj Blennow^{e,f}, Tammaryn Lashley^g, Nick C. Fox^h, Diego Sepulveda-Falla^{i,j,k}, Markus Glatzel^l, Adrian L. Oblak^l, Bernardino Ghetti^l, K. Peter R. Nilsson^d, Per Hammarström^d, Matthias Staufenbiel^a, Lary C. Walker^{m,n}, and Mathias Jucker^{a,b,2}

^aDepartment of Cellular Neurology, Hertie Institute for Clinical Brain Research, University of Tübingen, 72076 Tübingen, Germany; ^bGerman Center for Neurodegenerative Diseases, 72076 Tübingen, Germany; ^cGraduate School of Cellular and Molecular Neuroscience, University of Tübingen, 72074 Tübingen, Germany; ^dDepartment of Physics, Chemistry and Biology, Division of Chemistry, Linköping University, SE-581 83 Linköping, Sweden; ^eInstitute of Neuroscience and Physiology, Department of Psychiatry and Neurochemistry, University of Gothenburg, SE-431 80 Mölndal, Sweden; ^fClinical Neurochemistry Laboratory, Sahlgrenska University Hospital, SE-431 80 Mölndal, Sweden; ^gQueen Square Brain Bank for Neurological Diseases, Department of Molecular Neuroscience, Institute of Neurology, University College London, London WC1N 1PJ, United Kingdom; ^hDementia Research Centre, University College London, London WC1N 3BG, United Kingdom; ⁱInstitute of Neuropathology, University Medical Center Hamburg-Eppendorf, 20246 Hamburg, Germany; ^jNeuroscience Group of Antioquia, University of Antioquia, 1226 Medellín, Colombia; ^kFaculty of Medicine, University of Antioquia, 1226 Medellín, Colombia; ^lDepartment of Pathology and Laboratory Medicine, Indiana University School of Medicine, Indianapolis, IN 46202; ^mDepartment of Neurology, Emory University, Atlanta, GA 30322; and ⁿYerkes National Primate Research Center, Emory University, Atlanta, GA 30329

Edited by Stephen M. Strittmatter, Yale University School of Medicine, New Haven, CT, and accepted by Editorial Board Member Solomon H. Snyder October 24, 2017 (received for review July 26, 2017)

The molecular architecture of amyloids formed *in vivo* can be interrogated using luminescent conjugated oligothiophenes (LCOs), a unique class of amyloid dyes. When bound to amyloid, LCOs yield fluorescence emission spectra that reflect the 3D structure of the protein aggregates. Given that synthetic amyloid- β peptide (A β) has been shown to adopt distinct structural conformations with different biological activities, we asked whether A β can assume structurally and functionally distinct conformations within the brain. To this end, we analyzed the LCO-stained cores of β -amyloid plaques in post-mortem tissue sections from frontal, temporal, and occipital neocortices in 40 cases of familial Alzheimer's disease (AD) or sporadic (idiopathic) AD (sAD). The spectral attributes of LCO-bound plaques varied markedly in the brain, but the mean spectral properties of the amyloid cores were generally similar in all three cortical regions of individual patients. Remarkably, the LCO amyloid spectra differed significantly among some of the familial and sAD subtypes, and between typical patients with sAD and those with posterior cortical atrophy AD. Neither the amount of A β nor its protease resistance correlated with LCO spectral properties. LCO spectral amyloid phenotypes could be partially conveyed to A β plaques induced by experimental transmission in a mouse model. These findings indicate that polymorphic A β -amyloid deposits within the brain cluster as clouds of conformational variants in different AD cases. Heterogeneity in the molecular architecture of pathogenic A β among individuals and in etiologically distinct subtypes of AD justifies further studies to assess putative links between A β conformation and clinical phenotype.

Alzheimer | amyloid | neurodegeneration | prion | strains

Despite a common origin in the structural corruption and accumulation of specific proteins, the clinical and pathological phenotype of Alzheimer's disease (AD) exhibits conspicuous variability within and among patients (1–4). The amyloid cascade hypothesis posits that the seminal event in the pathogenesis of AD is the misfolding and aggregation of the amyloid- β peptide (A β) (5, 6). *In vitro* investigations have found that A β can aggregate into diverse amyloid structures that can impose their conformational characteristics onto naive synthetic forms of the protein (7, 8). In A β precursor protein (APP)-transgenic mouse models, polymorphisms of aggregated A β have been demonstrated that subsequently could be propagated to naive and susceptible host mice (9–11).

Recent work in humans suggests that A β can aggregate into structural variants with distinct pathobiological traits. One such

study used extracted fibrils from AD brains to seed the aggregation of synthetic A β *in vitro*. The resulting synthetic descendants of aggregated A β from brain samples provided indirect evidence for structural heterogeneity of A β among AD brains; in addition, the findings suggested that A β assumes a single, dominant conformation within a given brain (12, 13). Another investigation has shown that the biophysical features of aggregated A β differ significantly in patients with rapidly progressive AD compared with those with normally progressive disease, indicative of distinct molecular structures of A β (14). In an exceptional example of A β aggregate structural variation in AD, a patient was described as having an extraordinarily high A β burden but a paucity of high-affinity Pittsburgh compound B (PiB) binding sites (15). More recently, X-ray microdiffraction analysis of

Significance

The clinical and pathological variability among patients with Alzheimer's disease (AD) remains largely unexplained. Evidence is growing that this heterogeneity may be influenced by the heterogeneous molecular architecture of misfolded amyloid- β peptide (A β) in the brain. To test this hypothesis, we used unique fluorescent ligands to interrogate the molecular structure of A β in amyloid plaques from patients who had died with etiologically distinct subtypes of AD. We found that A β -amyloid plaques in the brain cluster as clouds of conformational variants that differ among certain subtypes of AD. The conformational features of AD plaques were partially transmissible to transgenic mice in a seeding paradigm, suggesting a mechanism whereby different molecular strains of A β propagate their features within the brain.

Author contributions: K.B., N.C.F., M.G., B.G., K.P.R.N., P.H., M.S., L.C.W., and M.J. designed research; and J.R., J.M., N.B., S.A.K., L.M.H., F.B., S.N., E.P., T.L., D.S.-F., and A.L.O. performed research.

The authors declare no conflict of interest.

This article is a PNAS Direct Submission. S.M.S. is a guest editor invited by the Editorial Board.

Published under the PNAS license.

¹J.R., J.M., and N.B. contributed equally to this work.

²To whom correspondence should be addressed. Email: mathias.jucker@uni-tuebingen.de.

This article contains supporting information online at www.pnas.org/lookup/suppl/doi:10.1073/pnas.1713215114/-DCSupplemental.

individual AD brain tissue samples indicated that the amyloid arrangement of A β is polymorphic within and among plaques (16).

Morphologically at the light-microscopic level, it is well documented that amyloid plaques in AD brains present with phenotypic variation that typically ranges from diffuse to dense-core plaques (17–24). How such morphotypes are linked to the molecular conformation of the amyloid has not been established.

The characterization of amyloid has been facilitated by a new class of dyes known as luminescent conjugated oligothiophenes (LCOs; or luminescent conjugated polythiophenes) (25, 26). LCO dyes bind to the repetitive cross- β -sheet structures of amyloid fibrils and display spectral differences based on the twisting of the flexible LCO backbone (25, 27). Additionally, it was found that certain LCOs compete with a Congo red analog (X-34) for binding to recombinant A β -amyloid fibrils as well as AD brain-derived A β , but they do not compete for the PiB binding site (28). It has been demonstrated that LCOs can detect molecular differences in A β plaque structure in different APP-transgenic mouse models (10), and in A β aggregated in vitro at different stages of fibrillization (25, 29, 30).

We hypothesized that the phenotypic and histopathological variability of AD results, at least in part, from variation in the molecular architecture of aggregated A β . To this end, we used LCOs and biochemical analyses to evaluate the variation and structural properties of amyloid in the plaques of patients with AD from different etiological backgrounds [familial forms; sporadic forms, including the posterior cortical atrophy (PCA) variant of AD (PCA-AD); and a unique PiB-negative AD case]. Our results provide evidence for the existence of heterogeneous A β -amyloid structures that cluster as clouds across different patients with AD while encoding conformational characteristics that can be biologically propagated.

Results

Spectral Characteristics of Plaque Amyloid in AD Brains. We evaluated plaque amyloid in tissue sections from a cohort of patients with AD of various etiologies, including familial mutation carriers for *APP* (V717I) and *PSEN1* (A431E, F105L, and E280A), as well as cases of typical sporadic AD (sAD) and sporadic PCA-AD (Table S1). A double-stain combination with two LCOs, quadro-formyl thiophene acetic acid (qFTAA) and hepta-formyl thiophene acetic acid (hFTAA) (29, 30) (Methods), was used to label amyloid plaques in fresh-frozen brain sections. Subsequently, the dense (conophilic) cores of amyloid plaques were spectrally analyzed for fluorescence emission characteristics (Figs. S1 and S2). Three brain regions, the midtemporal gyrus (temporal), pericalcarine gyri (occipital), and midfrontal gyrus (frontal), were investigated for each patient (Fig. 1A). Preliminary visual inspection under the fluorescence microscope revealed obvious variation in plaque appearance even within a tissue section (Fig. 1B).

To determine how the molecular structure of plaque amyloid varies among brains and brain regions, the mean emission spectra were calculated for all plaques in each brain region of all subjects. Pairwise comparisons between individual patients were then performed using a Euclidean distance calculation (Fig. 1C and D). This analysis revealed that the spectral signatures of plaque amyloid in familial *APP* V717I and *PSEN1* A431E mutation carriers were most different from the other groups (Fig. 1C). Statistical analysis of the ratio of the emission peaks for qFTAA (502 nm) and hFTAA (588 nm) in individual plaque cores confirmed that the *APP* V717I and *PSEN1* A431E groups were significantly different from most other groups (Fig. 1E). A difference was also found between sAD and PCA-AD cases (Fig. 1E). Of note, however, was the striking variability within the sAD group (Fig. 1C and E), with one of the samples with a high LCO spectral ratio being a previously described case with reduced high-affinity binding of PiB (Fig. 1C and E).

To further interrogate the variability in LCO spectra among the groups, all data points from the analysis based on the correlation of fluorescence intensity at 502 nm and 588 nm were examined (Fig. 1F). Again, the spectral signatures of plaque amyloid in the different patient groups segregated into noticeable clouds that partially overlapped each other (Fig. 1F).

Amyloid Plaque Spectral Characteristics Compared with Other Metrics. To determine whether the results from the LCO spectral analysis of plaques could be explained by factors that affect amyloid deposition in the brain, LCO ratios were related to apolipoprotein E (ApoE) genotype, subject age at death, and postmortem interval (PMI) (Fig. 2). Only sAD and PCA-AD samples were used to remove obvious confounding effects that the familial mutations might have on the comparison (e.g., younger mean age at death). No correlation was found between spectral ratio and ApoE status or subject age at death (Fig. 2A–C). The correlation found between the spectral ratio and the PMI disappeared when sAD cases and PCA-AD cases were analyzed separately, reflecting the overall longer PMI for the PCA-AD samples (Fig. 2C). Thus, ApoE, age at death, and PMI are not crucial factors for the observed LCO spectral differences.

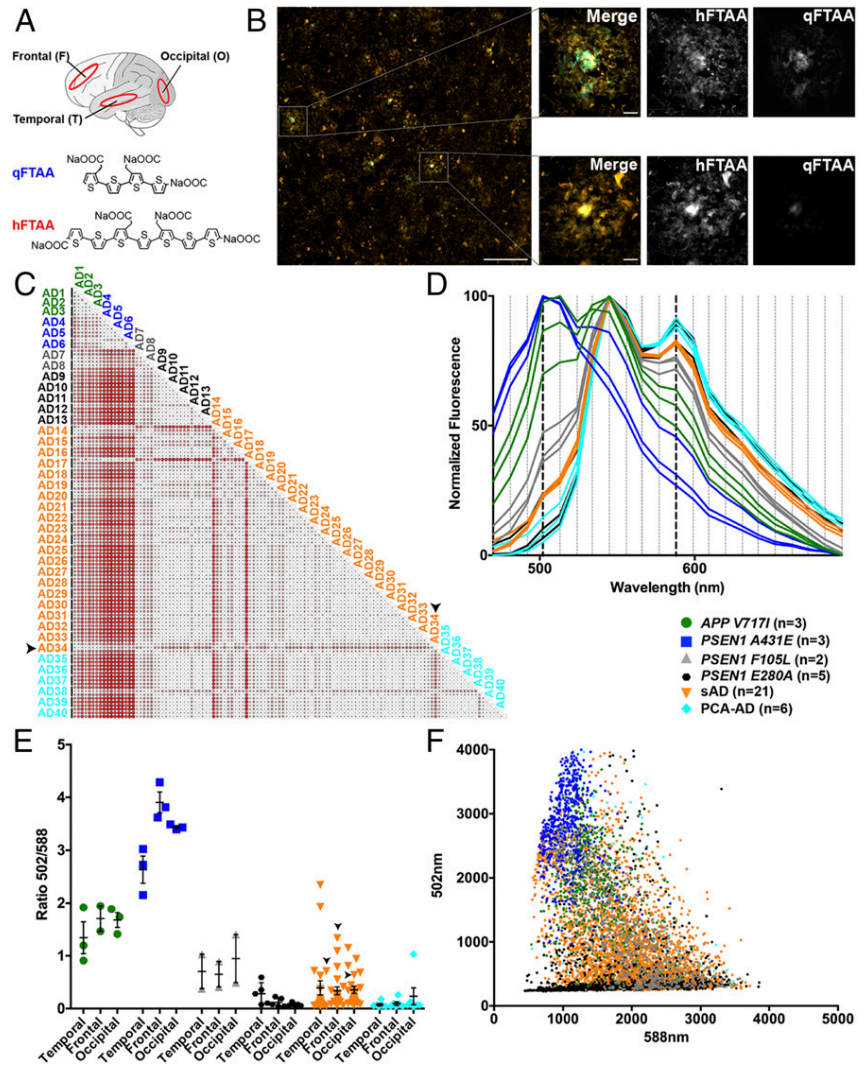
To assess whether the LCO results are related to the total A β load or the deposited A β species, A β was analyzed biochemically (Fig. S2). Overall, samples from the *PSEN1* A431E group had higher A β levels than all other groups. The ratio of A β 42/40 was higher in the *APP* V717I familial mutation carriers compared with the *PSEN1* mutation carriers (Fig. S2). Neither the amount of A β nor the A β 42/40 ratio differed significantly across the three neocortical regions; furthermore, the LCO spectra were not significantly associated with either total A β or the A β 42/40 ratio when the analysis was confined to sAD and PCA-AD samples (Fig. 2D and E).

Proteinase K (PK) resistance has been linked to pathogenic conformations of A β in mouse models and AD brains (11, 31, 32). To determine whether the LCO spectral signatures of the plaque cores are associated with protease sensitivity, the resistance of aggregated A β to proteolysis over time was evaluated (Fig. S2). No differences among patient groups were observed (Fig. S2). Furthermore, when only sAD and PCA-AD cases were considered, there was no significant correlation between the plaque spectral ratio and A β PK resistance (Fig. 2F).

Amyloid Plaque Spectral Characteristics Are Transmissible to Experimental Mouse Models. We next asked whether the LCO spectral properties of amyloid plaques can be propagated in vivo by the prion-like process of molecular conformational templating. To this end, cortical extracts from AD groups showing the most distinct LCO spectra, namely, *APP* V717I, *PSEN1* A431E, and sAD, in addition to the unique PiB-negative sAD case, were injected into the hippocampus of young APP23-transgenic mice (Fig. 3). APP23 mice were used for this analysis because they have recently been characterized in a seeding activity bioassay in which the precise biological activity of brain extracts was assessed (33). Before injection, all extracts were pooled for each AD group and the A β concentration was adjusted to 7.5 pg/ μ L. Since we found that the LCO spectral characteristics of plaques did not differ significantly among the three brain regions, we arbitrarily chose temporal cortical samples as the source of A β seeds.

Inoculated APP23 mice were analyzed 6 mo after injection (Fig. 3A). In all mice, A β deposition was induced in the hippocampus (primarily the dentate gyrus) as reported previously (9, 33). While this regional pattern of induction was not discernibly different among the groups, the amount of induction showed remarkable differences, with mice injected with *APP* V717I and typical sAD extracts manifesting at least twice as much induced A β deposition as mice injected with material from *PSEN1* A431E donors or from the PiB-refractory sAD donor (Fig. 3A and B).

Fig. 1. Subtypes of AD display distinguishable clouds of amyloid conformational variants. (A) Combination of two LCOs, qFTAA and hFTAA, was used to stain A β plaques in three different neocortical regions (temporal: midtemporal gyrus, T; occipital: pericalcarine gyri, O; frontal: midfrontal gyrus, F) of postmortem brain tissue from familial AD (*APP V717I*, *PSEN1 A431E*, *PSEN1 F105L*, and *PSEN1 E280A*), typical sAD, and sporadic PCA-AD cases. (B) Shown is an LCO-stained section of the temporal cortex from a patient with sAD (AD16; also patient information in Table S1). Note that a variety of different fluorescence emission patterns are present in a single brain sample. (Scale bars: Left, 200 μ m; Right, 20 μ m.) (C and D) Plaques were randomly selected, and for each plaque core, the fluorescence intensity was measured at 22 wavelengths to produce a continuous fluorescence spectrum (40–60 plaques were analyzed per region for each brain sample; also Fig. S1). Each line in D represents the mean spectrum for a particular brain area in all patients in a given subgroup. A heat map depicting the difference of Euclidean distances between the mean spectra (of all 22 fluorescence measurements) for brain regions of individual patients is shown in C. Larger and more darkly colored circles represent more dissimilar spectra. The labels represent patient numbers with the temporal, occipital, and frontal regions repeating as sets of three (from top to bottom). Note the variability within the sAD group, with some regions yielding emission spectra more similar to those of the familial groups (for AD2, only temporal and occipital cortex tissue was available for analysis). (E) For statistical analysis, the fluorescence intensity at 502 nm and 588 nm (which represent the fluorescence emission peaks of qFTAA and hFTAA, respectively; Fig. S1C) was analyzed for each region of each patient. Two-way ANOVA (brain region \times AD subtype) revealed a significant effect for subtype [$F_{(5,101)} = 33.07$, $P < 0.0001$], but not for brain region [$F_{(2,101)} = 0.0681$, $P = 0.9343$] or interaction between region and subtype [$F_{(10,101)} = 0.7829$, $P = 0.6451$]. Tukey's multiple comparisons revealed significant differences between *APP V717I* vs. *PSEN1 E280A*, sAD and PCA-AD; *PSEN1 A431E* vs. *PSEN1 F105L*, *PSEN1 E280A*, sAD and PCA-AD; *PSEN1 F105L* vs. *PSEN1 E280A*, sAD and PCA-AD; and sAD vs. PCA-AD (all probabilities at least $P < 0.05$). An exceptional sAD case, AD34 (denoted by arrows in C and E), is a previously described case with reduced high-affinity binding of the PiB radioligand (15). Error bars represent the SEM. (F) Scatter plot of all plaques analyzed using fluorescence at 588 nm vs. 502 nm per AD subgroup reveals that plaque spectral properties within the AD subgroups occupy distinct clouds, which overlap between AD subgroups.



Strikingly, when brain sections from the recipient mice were stained using the same LCO protocol as that used for the human tissue (Fig. 1), quite remarkable differences in the emission spectra of individual plaque cores were observed (Fig. 3A). The mean emission spectra of all seeded hippocampal plaque cores were computed for each injected mouse, and a Euclidean distance calculation was applied to determine differences (Fig. 3C). Similar to the LCO spectral patterns in plaques from the human donors, seeded amyloid in the *PSEN1 A431E*-injected mice was most different from that in the sAD groups, albeit with more variation (Fig. 3C and D). For statistical comparison of the experimental groups, the 502-nm/588-nm spectral ratio was calculated for each plaque core, and the mean ratios for each injected mouse were computed (Fig. 3D and E). The spectral ratios in the different groups of seeded host mice displayed relatively similar patterns to those in the donor humans (compare Figs. 1E and 3E); the group difference was statistically significant between *PSEN1 A431E*- and sAD-seeded mice, but the other group differences did not reach statistical significance. The amount of induced A β deposition did not correlate with the spectral ratio, suggesting these two factors are independent (Fig. 3F). As with the human tissue, all plaque

cores analyzed in the mice were plotted based on the fluorescence intensity at 502 nm against 588 nm (Fig. 3G). The plaques in seeded mice occupied similar clouds within an injection group, although these clouds showed more overlap in the injected mice than in the original human tissue (Fig. 1), suggestive of differential host-agent interactions (9).

Discussion

The extraordinary phenotypic variability of AD (1–3) currently defies explanation. It is likely that many factors are involved, including the age at disease onset, location of the initial abnormalities in the brain and their pattern of spread, the inflammatory response to the lesions, and the presence of comorbid conditions. The present findings support growing evidence that the heterogeneity of AD may also be influenced by the heterogeneous molecular architecture of misfolded A β in the brain.

Using synthetic A β that was aggregated in vitro, multimeric A β assemblies have been shown to assume diverse tertiary and quaternary structures (13, 34–37). These findings have greatly augmented our understanding of A β fibril structure, but their relevance to the pathobiology of A β in vivo, in the native disease

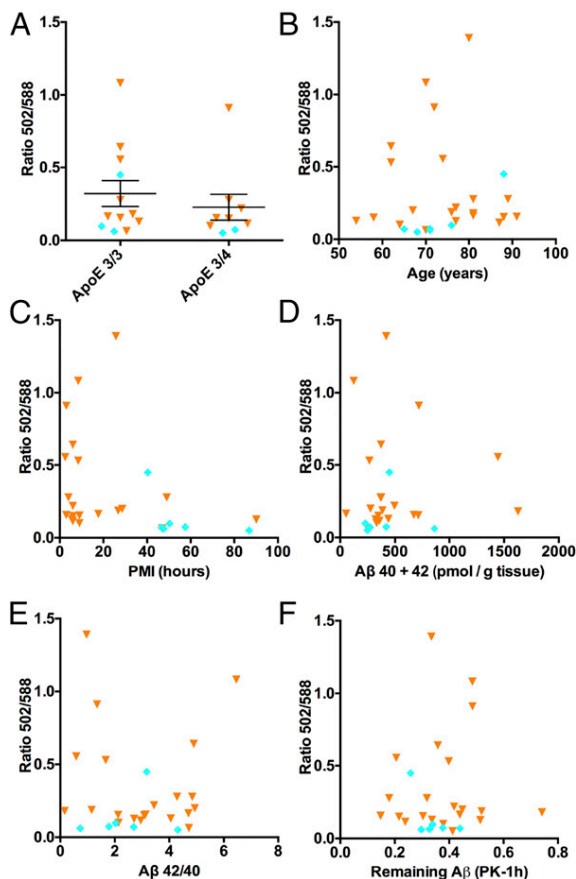


Fig. 2. Spectral properties of LCO-labeled amyloid plaques are not explained by ApoE genotype, patient age, PMI, or A β biochemistry. (A) LCO spectral ratio of fluorescence at 502 nm and 588 nm separated into ApoE genotype subgroups (mean of the three regions; Fig. 1E; only subjects with sAD and PCA-AD were used to remove the confounding effects of the familial mutations on the data; orange triangles, sAD; cyan diamonds, PCA-AD). The Mann-Whitney test was used to determine significance between ApoE 3/3 vs. 3/4 cases ($P = 0.4221$). Error bars represent the SEM. (B) LCO spectral ratio vs. patient age. Nonparametric Spearman correlation: $P = 0.38$. (C) LCO spectral ratio vs. PMI. Nonparametric Spearman correlation: $P = 0.29$ for PCA-AD and $P = 0.32$ for sAD. (D and E) LCO spectral ratios vs. ELISA measurements (mean of all brain regions) of A β 40 + 42 and the A β 42/40 ratio (A β measurements are shown in Fig. S2). Nonparametric Spearman correlation analysis yielded $P = 0.26$ and $P = 0.81$, respectively. (F) LCO spectral ratio vs. A β remaining after 1 h of digestion with PK (mean of all brain regions). Nonparametric Spearman correlation: $P = 0.78$. Detailed results for PK digestion are shown in Fig. S3.

state, remains uncertain (38). For instance, in most cases, these experiments involved the analysis of a single isoform of A β , either 40 aa or 42 aa long, whereas there are multiple isoforms, fragments, and posttranslational modifications of A β in the living brain (39, 40).

Tycko and coworkers (12, 13) have demonstrated that A β derived from different cases of AD is able to induce synthetic A β to assemble into corresponding structural “strains,” and the authors suggest that a single A β structure predominates in a particular AD brain. Our observations generally support the concept of a predominant, case-specific A β strain in that the mean LCO spectral emission of plaque cores (where the A β adopts an amyloid conformation) was similar in different cortical regions of each patient, regardless of the AD subtype. However, direct microscopic analysis of individual plaque cores with LCOs allowed us to determine that minor populations of A β aggregates

with different molecular architectures also are present within a given AD brain. We therefore speculate that the presence of these structural variants in other investigations (12, 13) may have been masked by the conformational selection and in vitro propagation of a dominant strain in preparation for the NMR analysis. In support of this possibility, and in agreement with our findings, X-ray microdiffraction analysis has revealed structural polymorphism among amyloid plaques within the same tissue section (16).

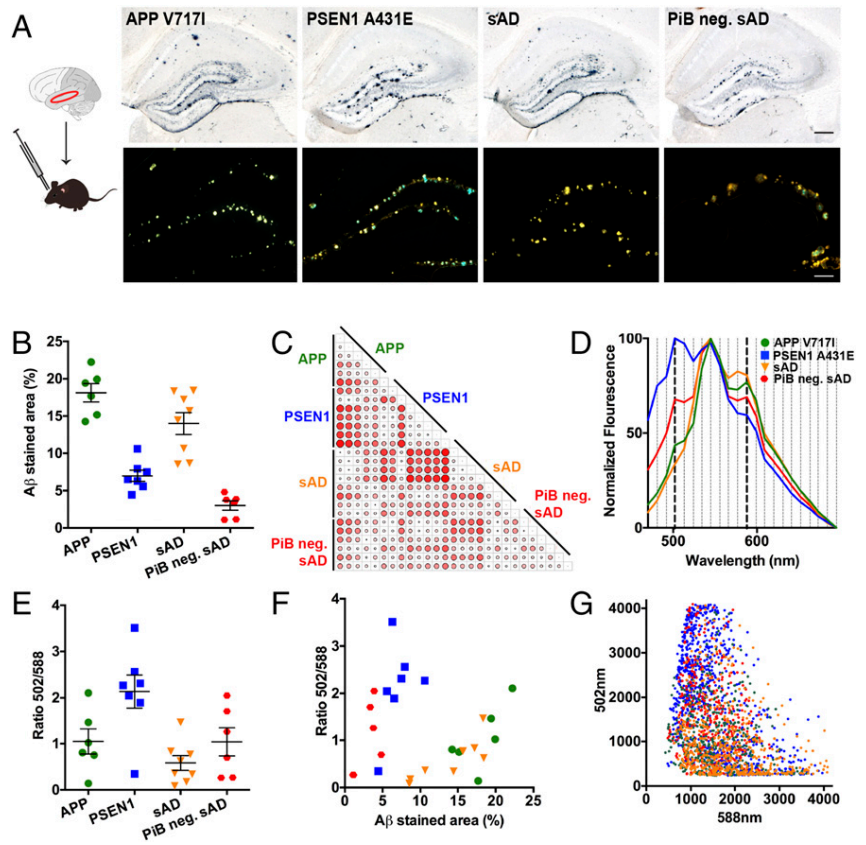
In light of the intra- and interindividual variability in the LCO spectral characteristics of plaque amyloid, it is remarkable that we still found differences among patient subgroups, particularly between some of the familial AD and sAD cases (note that the familial AD mutations in the present study do not change the A β sequence). Neuropathological analyses also have revealed differences in plaque morphotypes between some familial AD mutations and sAD (18, 20, 23). However, while these observations were made on A β -immunostained plaques, our LCO-based spectral analysis was confined to the core of the plaque, and thus to A β in the amyloid conformation.

We were somewhat surprised to observe differences in the amyloid spectral characteristics between typical patients with sAD and patients with the PCA variant of AD. Both the regional distribution of amyloid and the clinical phenotype are different in PCA-AD and sAD (41). A previous NMR analysis did not indicate molecular structural differences between PCA-AD and sAD (13), but, as noted above, the analysis could have been confounded by conformational selection of A β species best suited for the seeded in vitro growth of fibrils. The clinicopathological distinctiveness of PCA-AD appears to result, in part, from a disease-specific site of origin and/or pattern of A β dissemination (41), but our findings indicate that the molecular architecture of misfolded A β may also play a role. Similarly, in a rapidly progressive subtype of AD, there is biochemical evidence for increased conformational heterogeneity of A β 42 (14), and a recent NMR study using seeded growth of synthetic A β fibrils from brain-derived material supports this finding (13).

In the present study, the LCO spectral characteristics of amyloid in plaques did not correspond in a consistent way to the PK resistance or the abundance of the two major A β species (A β 40 and A β 42) in tissue homogenates. One possible explanation for this is that the spectral analysis and biochemical tests do not probe identical populations of A β [i.e., the amyloid core (LCOs) vs. the total pool of aggregated A β (biochemistry)]. Another possibility is that variation in amyloid structure revealed by the LCO spectral analysis is more sensitive at identifying subtle differences that biochemical analyses currently are unable to detect. Elucidation of the mechanisms underlying the architectural variability of A β in plaques could reveal pathogenetically important targets for the development of personalized treatments for AD.

LCO binding and spectra are dependent on the orientation, side-chain interactions, and packing of amyloid fibrils, and the ability of LCOs to recognize amyloid features in protein pathologies has been well characterized (25). These ligands thus are exquisitely sensitive indicators of molecular architectural differences in proteopathic fibrils, for example, the strain-like diversity of prion protein aggregates (42). In recent studies, it has been shown that the arrangement and packing of A β -amyloid fibrils influence the spectral output of the LCOs, especially when the ligands are used in combination (29, 30, 43). Since LCO spectra indicate the presence of different structural conformations of A β , we predicted from previous experiments that these properties should be transmissible to susceptible hosts (44). Our studies in APP-transgenic mice confirm that A β -rich brain extracts from different subtypes of AD seed A β deposits that are correspondingly differentiable using LCOs. The LCO spectral traits of amyloid in the seeded transgenic mice did not perfectly mirror those of the human donor tissue; however, this is expected because both

Fig. 3. Variant conformations of aggregated A β can be induced by exogenous seeding in APP-transgenic mice. (A) Seeding extracts were prepared from the middle temporal gyrus of pooled ($n = 3$) brain samples from human APP V717I, PSEN1 A431E, sAD [AD15, AD16, and AD24; patients collected in the same year at the same site (Emory University)] and a single PiB-refractory sAD case (AD34) (Fig. 1 and Table S1). A β concentrations of the seeding extracts were adjusted to 7.5 $\mu\text{g}/\mu\text{L}$ (Methods). Extracts were injected into young (4-mo-old) female APP23 mice [APP V717I ($n = 6$), PSEN1 A431E ($n = 7$), sAD ($n = 8$), and PiB-negative (neg.) sAD ($n = 6$)]. Brains of recipient mice were analyzed 6 mo after injection. Induced A β deposition in the hippocampus was stained with a polyclonal A β antibody (Top) or the LCO double-staining protocol (Bottom). (Scale bars: Top, 200 μm ; Bottom, 50 μm .) (B) Stereological quantification of A β -immunostained area in the hippocampus. The Kruskal–Wallis test followed by Dunn’s multiple comparison test revealed significant differences in the degree of induction between APP V717I vs. PSEN1 A431E ($P < 0.05$) donors, PiB-neg. sAD vs. APP V717I donors ($P < 0.001$), and PiB-neg. sAD vs. sAD donors ($P < 0.01$). Error bars represent SEM. (C) Heat map of the Euclidean distance between LCO spectra calculated for each mouse (details are provided in Fig. 1). Larger and more darkly colored circles represent more dissimilar spectra. (D) Mean LCO fluorescence spectra of induced plaque cores for mice injected with different human extracts (20–30 plaques were analyzed per mouse; details are provided in Fig. 1). (E) For statistical analysis, the mean ratio of the fluorescence intensity at 502 nm and 588 nm was calculated for each mouse. The Kruskal–Wallis test followed by Dunn’s multiple comparison test revealed significantly different spectral signatures in plaques seeded by PSEN1 A431E vs. sAD brain extracts ($P < 0.05$). Error bars represent the SEM. (F) Amount of A β induction did not correlate with the LCO spectral ratio of the induced amyloid (nonparametric Spearman correlation, $P = 0.9687$). (G) Scatter plot of LCO fluorescence spectra emitted by all plaques analyzed in seeded mice demonstrates an overall preservation of clustering among the groups, although the group differences were less distinct compared with plaque spectra in the original human donor samples (Fig. 1).



the agent and host influence the propagation of A β and the characteristics of the resulting deposits (9). In addition, the mice were seeded with extracts of brain tissue, which may have a seed composition that differs from that in the plaque cores. The existence of LCO spectral clouds that only partially recapitulate those of the AD donors thus may reflect the composition of seeds in the donor extract as well as the Darwinian selection of different A β strains in the host mice (45).

The spectral properties of LCOs bound to plaques change as APP-transgenic mice grow older, suggestive of age-related conformational rearrangement of the A β (30). Thus, it is possible that the spectral variation of plaques in individual patients with AD at least partially reflects the presence of plaques of different ages. The AD brains analyzed in the present study were all from patients with end-stage disease, at which point amyloid, per se, may no longer be the primary driver of the disease (46). Nevertheless, the deposited amyloid shows remarkable LCO spectral variability among patients with sporadic end-stage AD. Furthermore, the LCO spectral signals detected within an individual brain, although generally similar in the three cortical regions, constitute a cloud of variable emission spectra. It is possible that the composition of the amyloid may be more complex late in the pathogenic process than at earlier time points. If so, the LCO spectra might reveal more clearly differentiable disease patterns in the earlier stages. Analysis of incipient amyloid plaques in persons who died of other causes before the onset of AD symptoms will be informative in this regard. Finally, it will be important to establish the relationship between the variant molecular structure of plaque cores and the pathobiologically potent oligomeric forms of A β (31, 47).

The present findings have several implications for diagnostics and treatment. Variations in amyloid structure are likely a complicating factor when determining the distribution and severity of A β deposition by PET imaging in patients with AD, as demonstrated by an unusual case of AD with very high A β levels in the brain but negligible high-affinity binding of PiB (15). We found that the plaque cores in this case displayed an LCO spectral pattern that differed from that of most other sAD cases. If antibody binding to A β is similarly influenced by the molecular architecture of the misfolded protein, it is conceivable that a particular monoclonal antibody might fail to recognize the full range of A β aggregates that can arise within a brain and among different patients. Thus, it may be advantageous to use multiple antibodies to create a “polyclonal” mixture for treatment of A β pathology. Finally, future work should investigate the therapeutic potential of LCOs for AD and other proteopathies, as has been shown for prion disease (27), and, additionally, determine the feasibility of using LCOs to examine A β aggregates in bodily fluids such as cerebrospinal fluid and blood to augment the personalized diagnosis of AD.

Methods

Patient Samples. Fresh tissue samples were obtained from the midtemporal gyrus (temporal), pericalcarine gyri (occipital), and midfrontal gyrus (frontal) of 40 clinically and pathologically diagnosed AD cases (Table S1). The tissues were acquired under the proper Institutional Review Board protocols from the Tübingen Review Board for the work in the Queen Square Brain Bank at University College London samples (202/2016B02), the Emory University Alzheimer’s Disease Research Center to do the work on these samples (IRB 00045782), and the University of Antioquia, Medellin, Colombia (09-10-232). Informed consent was given by families (see SI Methods for details).

LCO Staining Spectral Analysis. Two LCO variants, qFTAA and hFTAA, were used to stain fresh-frozen tissue (30). Amyloid plaques were randomly chosen, and continuous emission spectra were acquired (Figs. S1 and S2). Only the dense cores of plaques were analyzed. Details are provided in *SI Methods*.

A β Quantification, Mass Spectrometry, and PK Digestion. For A β quantification, human tissue was extracted with 70% formic acid. Extracts were also analyzed by targeted mass spectrometry for A β (48). PK digestion was carried out on fresh tissue at 37 °C for 0, 1, 2, and 4 h and analyzed with A β immunoblots. Details are provided in *SI Methods*.

In Vivo Inoculations of the Mice. Seeding extracts were generated from the middle temporal gyrus (33). Pooled extracts [APP V717I (AD1–3), PSEN1 A431E (AD4–6), and typical sAD (AD15, AD16, and AD24)] and the distinct PiB-negative sAD case (AD34) (Table S1) were adjusted to the same A β concentration. Intrahippocampal injections were done in 4-mo-old APP23 mice (49). After 6 mo of incubation, brain sections were A β -immunostained and quantified (50, 51).

Sections were also stained with the LCOs. All mouse experiments were approved by the local animal care and use committee in Baden-Württemberg, Germany (Regierungspräsidium Tübingen). Details are provided in *SI Methods*.

Statistical Analysis. GraphPad Prism (v.5) was used for statistical analyses. R (v. 3.3.2) was used for Euclidean distances. Details are provided in *SI Methods*.

ACKNOWLEDGMENTS. We thank Juliane Schelle and all other laboratory members for experimental help. We are grateful to I. Zerr and M. Schmitz (Goettingen, Germany), C. Glabe (Irvine, CA), Markus Fändrich (Ulm, Germany), and J. Morris and N. Cairns (St. Louis, MO) for help. This work was supported by grants from the EC Joint Programme on Neurodegenerative Diseases (JPNDR-REfrAME), the NIH (Grants P50-AG025688, RR00165, OD11132, and P30-AG010133), Public Health Service Grant P30-AG010133, the Alexander von Humboldt Foundation, the Göran Gustafsson Foundation, the Swedish Research Council, and the University College London Hospitals–National Institute for Health Research Biomedical Research Centre. T.L. is supported by a Senior Fellowship from Alzheimer's Research UK.

- Morris JC (1999) Clinical presentation and course of Alzheimer disease. *Alzheimer Disease*, eds Terry RD, Katzman R, Bick KL, Sisodia SS (Lippincott Williams & Wilkins, Philadelphia), pp 11–24.
- Nelson PT, et al. (2012) Correlation of Alzheimer disease neuropathologic changes with cognitive status: A review of the literature. *J Neuropathol Exp Neurol* 71: 362–381.
- Lam B, Masellis M, Freedman M, Stuss DT, Black SE (2013) Clinical, imaging, and pathological heterogeneity of the Alzheimer's disease syndrome. *Alzheimers Res Ther* 5:1.
- Ryan NS, et al. (2016) Clinical phenotype and genetic associations in autosomal dominant familial Alzheimer's disease: A case series. *Lancet Neurol* 15:1326–1335.
- Hardy J, Selkoe DJ (2002) The amyloid hypothesis of Alzheimer's disease: Progress and problems on the road to therapeutics. *Science* 297:353–356.
- Holtzman DM, Goate A, Kelly J, Sperling R (2011) Mapping the road forward in Alzheimer's disease. *Sci Transl Med* 3:114ps48.
- Eisenberg D, Jucker M (2012) The amyloid state of proteins in human diseases. *Cell* 148:1188–1203.
- Tycko R (2015) Amyloid polymorphism: Structural basis and neurobiological relevance. *Neuron* 86:632–645.
- Meyer-Luehmann M, et al. (2006) Exogenous induction of cerebral beta-amyloidogenesis is governed by agent and host. *Science* 313:1781–1784.
- Heilbronner G, et al. (2013) Seeded strain-like transmission of β -amyloid morphotypes in APP transgenic mice. *EMBO Rep* 14:1017–1022.
- Watts JC, et al. (2014) Serial propagation of distinct strains of A β prions from Alzheimer's disease patients. *Proc Natl Acad Sci USA* 111:10323–10328.
- Lu JX, et al. (2013) Molecular structure of β -amyloid fibrils in Alzheimer's disease brain tissue. *Cell* 154:1257–1268.
- Qiang W, Yau WM, Lu JX, Collinge J, Tycko R (2017) Structural variation in amyloid- β fibrils from Alzheimer's disease clinical subtypes. *Nature* 541:217–221.
- Cohen ML, et al. (2015) Rapidly progressive Alzheimer's disease features distinct structures of amyloid- β . *Brain* 138:1009–1022.
- Rosen RF, et al. (2010) Deficient high-affinity binding of Pittsburgh compound B in a case of Alzheimer's disease. *Acta Neuropathol* 119:221–233.
- Liu J, et al. (2016) Amyloid structure exhibits polymorphism on multiple length scales in human brain tissue. *Sci Rep* 6:33079.
- Tagliavini F, Giaccone G, Frangione B, Bugiani O (1988) Pre-amyloid deposits in the cerebral cortex of patients with Alzheimer's disease and nondemented individuals. *Neurosci Lett* 93:191–196.
- Yamaguchi H, Hirai S, Morimatsu M, Shoji M, Ihara Y (1988) A variety of cerebral amyloid deposits in the brains of the Alzheimer-type dementia demonstrated by beta protein immunostaining. *Acta Neuropathol* 76:541–549.
- Ikeda S, Allsop D, Glenner GG (1989) Morphology and distribution of plaque and related deposits in the brains of Alzheimer's disease and control cases. An immunohistochemical study using amyloid beta-protein antibody. *Lab Invest* 60:113–122.
- Wisniewski HM, Bancher C, Barcikowska M, Wen GY, Currie J (1989) Spectrum of morphological appearance of amyloid deposits in Alzheimer's disease. *Acta Neuropathol* 78:337–347.
- Dickson TC, Vickers JC (2001) The morphological phenotype of beta-amyloid plaques and associated neuritic changes in Alzheimer's disease. *Neuroscience* 105:99–107.
- Thal DR, Capetillo-Zarate E, Del Tredici K, Braak H (2006) The development of amyloid beta protein deposits in the aged brain. *Sci Aging Knowledge Environ* 2006:re1.
- Maarouf CL, et al. (2008) Histopathological and molecular heterogeneity among individuals with dementia associated with Presenilin mutations. *Mol Neurodegener* 3: 20.
- Walker LC (2016) Proteopathic strains and the heterogeneity of neurodegenerative diseases. *Annu Rev Genet* 50:329–346.
- Aslund A, et al. (2009) Novel pentameric thiophene derivatives for in vitro and in vivo optical imaging of a plethora of protein aggregates in cerebral amyloidosis. *ACS Chem Biol* 4:673–684.
- Wegenast-Braun BM, et al. (2012) Spectral discrimination of cerebral amyloid lesions after peripheral application of luminescent conjugated oligothiophenes. *Am J Pathol* 181:1953–1960.
- Herrmann US, et al. (2015) Structure-based drug design identifies polythiophenes as antiprion compounds. *Sci Transl Med* 7:299ra123.
- Bäck M, Appelqvist H, LeVine H, 3rd, Nilsson KP (2016) Anionic oligothiophenes compete for binding of X-34 but not PIB to recombinant A β amyloid fibrils and Alzheimer's disease brain-derived A β . *Chemistry* 22:18335–18338.
- Psonka-Antonczyk KM, et al. (2016) Nanoscale structure and spectroscopic probing of A β 1-40 fibril bundle formation. *Front Chem* 4:44.
- Nyström S, et al. (2013) Evidence for age-dependent in vivo conformational rearrangement within A β amyloid deposits. *ACS Chem Biol* 8:1128–1133.
- Langer F, et al. (2011) Soluble A β seeds are potent inducers of cerebral β -amyloid deposition. *J Neurosci* 31:14488–14495.
- Stöhr J, et al. (2012) Purified and synthetic Alzheimer's amyloid beta (A β) prions. *Proc Natl Acad Sci USA* 109:11025–11030.
- Ye L, et al. (2017) A β seeding potency peaks in the early stages of cerebral β -amyloidosis. *EMBO Rep* 18:1536–1544.
- Schmidt M, et al. (2009) Comparison of Alzheimer Abeta(1-40) and Abeta(1-42) amyloid fibrils reveals similar protofilament structures. *Proc Natl Acad Sci USA* 106: 19813–19818.
- Schmidt M, et al. (2015) Peptide dimer structure in an A β (1-42) fibril visualized with cryo-EM. *Proc Natl Acad Sci USA* 112:11858–11863.
- Xiao Y, et al. (2015) A β (1-42) fibril structure illuminates self-recognition and replication of amyloid in Alzheimer's disease. *Nat Struct Mol Biol* 22:499–505.
- Gremer L, et al. (2017) Fibril structure of amyloid- β (1-42) by cryo-electron microscopy. *Science* 358:116–119.
- Condello C, Stöhr J (March 28, 2017) Abeta propagation and strains: Implications for the phenotypic diversity in Alzheimer's disease. *Neurobiol Dis*, 10.1016/j.nbd.2017.03.014.
- Näslund J, et al. (1994) Relative abundance of Alzheimer A beta amyloid peptide variants in Alzheimer disease and normal aging. *Proc Natl Acad Sci USA* 91: 8378–8382.
- Portelius E, et al. (2010) Mass spectrometric characterization of brain amyloid beta isoform signatures in familial and sporadic Alzheimer's disease. *Acta Neuropathol* 120:185–193.
- Crutch SJ, et al. (2017) Consensus classification of posterior cortical atrophy. *Alzheimers Dement* 13:870–884.
- Magnusson K, et al. (2014) Multimodal fluorescence microscopy of prion strain specific PrP deposits stained by thiophene-based amyloid ligands. *Prion* 8:319–329.
- Klingstedt T, et al. (2015) Distinct spacing between anionic groups: An essential chemical determinant for achieving thiophene-based ligands to distinguish β -amyloid or Tau polymorphic aggregates. *Chemistry* 21:9072–9082.
- Jucker M, Walker LC (2013) Self-propagation of pathogenic protein aggregates in neurodegenerative diseases. *Nature* 501:45–51.
- Li J, Browning S, Mahal SP, Oelschlegel AM, Weissmann C (2010) Darwinian evolution of prions in cell culture. *Science* 327:869–872.
- Karran E, Mercken M, De Strooper B (2011) The amyloid cascade hypothesis for Alzheimer's disease: An appraisal for the development of therapeutics. *Nat Rev Drug Discov* 10:698–712.
- Haass C, Selkoe DJ (2007) Soluble protein oligomers in neurodegeneration: Lessons from the Alzheimer's amyloid beta-peptide. *Nat Rev Mol Cell Biol* 8:101–112.
- Portelius E, et al. (2007) Characterization of amyloid beta peptides in cerebrospinal fluid by an automated immunoprecipitation procedure followed by mass spectrometry. *J Proteome Res* 6:4433–4439.
- Sturchler-Pierrat C, et al. (1997) Two amyloid precursor protein transgenic mouse models with Alzheimer disease-like pathology. *Proc Natl Acad Sci USA* 94: 13287–13292.
- Eisele YS, et al. (2010) Peripherally applied Abeta-containing inoculates induce cerebral beta-amyloidosis. *Science* 330:980–982.
- Bondolfi L, et al. (2002) Amyloid-associated neuron loss and gliogenesis in the neocortex of amyloid precursor protein transgenic mice. *J Neurosci* 22:515–522.

Supporting Information

Rasmussen et al. 10.1073/pnas.1713215114

SI Methods

Patient Samples. Tissue samples were obtained from the mid-temporal gyrus (temporal), pericalcarine gyri (occipital), and mid-frontal gyrus (frontal) of 40 clinically and pathologically diagnosed AD cases (Table S1). Among them, 13 familial cases (AD 1–13) had the following mutations: *V717I* in *APP*, three cases; *A431E* in *PSEN1*, three cases; *F105L* in *PSEN1*, two cases; and *E280A* in *PSEN1*, five cases. The remaining 27 cases had a typical sporadic (idiopathic) etiology (AD14–34) or a sporadic PCA variant of AD (AD35–40). The samples were obtained from four different sources, the Emory University Alzheimer's Disease Research Center; the Dementia Laboratory, Department of Pathology and Laboratory Medicine, Indiana University School of Medicine; the Queen Square Brain Bank at University College London; and the Institute of Medical Research, Faculty of Medicine, University of Antioquia, Medellín, Colombia. Human postmortem tissues were acquired under proper Institutional Review Board protocols with consent from families.

LCO Staining and Immunohistochemistry on Patient Samples. Two different LCO variants, qFTAA and hFTAA, were used for detection and analysis of amyloid pathology. Fresh-frozen human tissue was cut into 12- μ m-thick sections on a cryotome, dried at room temperature (RT) overnight, and stored at -80°C . Tissue was thawed, air-dried, and then double-stained with qFTAA and hFTAA (2.4 μM qFTAA and 0.77 μM hFTAA in PBS) similar to a previously described protocol (30). Sections were incubated for 30 min at RT in the dark.

Immunohistochemistry was performed using a polyclonal primary antibody directed against A β (CN6) as previously described (50). Staining with Congo red and Thioflavin-S for amyloid was conducted according to standard protocols.

Spectral Analysis. Spectra were acquired on a Zeiss LSM 510 META confocal microscope equipped with an argon 458-nm laser for excitation and a spectral detector (Carl Zeiss MicroImaging GmbH). A 40 \times oil-immersion objective (1.3 N.A.; Zeiss) was used for spectral imaging of A β -amyloid cores. Continuous emission spectra were acquired from 470 to 695 nm. The amyloid plaques were randomly chosen, and three regions of interest were measured in the core of each deposit (Figs. S1 and S2). Only the dense cores of plaques were analyzed. Other types of A β deposits (diffuse plaques, intracellular A β , and cerebral amyloid angiopathy) were excluded. Care was taken to avoid interference of lipofuscin-induced autofluorescence with LCO signals; the use of spectral imaging allowed us to distinguish between the distinct LCO fluorescence spectrum and unwanted autofluorescence.

A total of 15 to 25 A β plaque cores were measured in each region, totaling 45–60 plaques per patient. After the spectral measurements, all emission spectra were normalized to their respective maxima. The mean spectral signature of each plaque core was calculated before averaging the values for each brain area in each patient. The ratio of the intensity of emitted light at the blue-shifted peak (502 nm) and red-shifted peak (588 nm) was used as a parameter for spectral distinction of different A β deposits. The peaks of the spectra were selected to maximize the spectral distinction.

For the heat map of Euclidean distance calculation, the average spectrum from 470 nm to 695 nm was calculated for each brain region. Different spectra were then compared in two samples using the following Euclidean distance calculation:

$$\sqrt{\sum_{470nm}^{695nm} (ADx_{470nm} - ADy_{470nm})^2 + \dots + (ADx_{695nm} - ADy_{695nm})^2}.$$

In short, the “square-root of the sum-of-squared-differences” was calculated between two samples using the 22 wavelength measurements of fluorescence intensity. This pairwise calculation was completed for every sample pair used in the study. The output of these calculations is then displayed as a heat map, with larger and more darkly colored circles representing a large Euclidean distance (more different emission spectra). This heat map represents the comparison between samples for the entire emission curve. Further statistical comparisons between samples were undertaken using the ratio of the fluorescence intensity at two wavelengths (502 nm/588 nm) representing the peaks of fluorescence for the two dyes used in this study. The Euclidean distance calculation and the heat map were generated in R (v. 3.3.2).

ECL-Based Multiarray for A β Quantification. Human tissue was homogenized in PBS (10% wt/vol) using the Precellys system with a 2 \times 20-s cycle at 5,500 rpm (Precellys24 Homogenizer, EQ03119-200-RD000.0, Bertin Instruments). Samples were then extracted with 70% formic acid (final concentration) and centrifuged at 25,000 \times g for 60 min at 4 $^{\circ}\text{C}$. Supernatants were collected and neutralized with buffer (1 M Tris base, 0.5 M Na₂NPO₄, 0.05% NaN₃) before analysis with a V-PLEX Peptide Panel 1 (6E10) A β kit from Meso Scale Discovery following the manufacturer's specifications.

PK Digestion. Samples homogenized with the Precellys system described previously were centrifuged at 800 \times g for 5 min at 4 $^{\circ}\text{C}$, and the supernatant was collected. Protein concentrations were determined using a bicinchoninic acid total protein kit, and samples were then digested with 1 μg of PK/3 μg of protein at 37 $^{\circ}\text{C}$. Samples were collected for analysis at 0, 1, 2, and 4 h and stopped with 2 mM PMSF. Samples were heated to 70 $^{\circ}\text{C}$ for 10 min in LDS sample buffer (Invitrogen), loaded onto 4–12% Bis-Tris precast gels, and run at 125 V for 44 min. Gels were transferred onto nitrocellulose and subsequently boiled at 95 $^{\circ}\text{C}$ for 5 min in PBS. Blocking was achieved with 4% skim milk in PBS with 0.05% Tween-20 for 60 min at RT. Membranes were probed with antibody 6E10 (1:5,000) overnight at 4 $^{\circ}\text{C}$ and then incubated with a goat anti-mouse secondary antibody (1:30,000) for 60 min. Development was carried out with Dura Extended Duration Substrate (Pierce) before exposure on Hyperfilm ECL film (Amersham). Band intensities were quantified using ImageJ software (NIH).

Mass Spectrometry. Human tissue was homogenized in PBS (10% wt/vol) using the Precellys system with a 2 \times 20-s cycle at 5,500 rpm (Precellys24 Homogenizer, EQ03119-200-RD000.0, Bertin Instruments). Samples were then extracted with 70% formic acid, centrifuged at 25,000 \times g for 60 min at 4 $^{\circ}\text{C}$, and dried in a speedvac. The samples were reconstituted in 200 μL of formic acid for 30 min and then neutralized to pH 7 using 0.5 M Tris. A β s were then immunoprecipitated using A β -specific antibodies [antibodies 6E10 and 4G8 (Signet Laboratories)] coupled to magnetic Dynabeads M-280 Sheep Anti-Mouse IgG (Invitrogen) as described previously (48). Mass spectrometry was performed using a MALDI TOF/TOF instrument (UltraFlex; Bruker Daltonics). Analysis was completed as described previously (48).

In Vivo Inoculations. Given that the LCO spectral characteristics of plaque cores did not differ among the three brain regions, we prepared the donor inoculum from temporal cortical samples only. Seeding extracts were generated from a 10% (wt/vol) homogenate of the middle temporal gyrus using the Precellys system as described above. The homogenates were subsequently centrifuged at $3,000 \times g$ for 5 min at 4 °C. The supernatants were then collected and stored at -80 °C. Quantification of A β in the extracts was performed after formic acid extraction using the MesoScale platform. Seeding extracts were pooled for the *APP V717I* (AD1-3), *PSEN1 A431E* (AD4-6), and typical sAD (AD15, AD16, and AD24) groups (Table S1), while the PiB-refractory case remained distinct. All samples then were adjusted to the same total A β concentration (7.5 pg/mL) using PBS as a diluent.

Predepositing 4-mo-old female APP23 mice (49) were injected bilaterally (2.5 μ L each) with seeding extracts from the *APP V717I* ($n = 6$), *PSEN1 A431E* ($n = 7$), typical sAD ($n = 8$), and PiB-negative sAD ($n = 6$) cases following anesthesia with ketamine/xylazine (100 mg/kg to 10 mg/kg of body weight). Injections were targeted to the hippocampus (anteroposterior, -2.5 mm; left/right, ± 2.0 mm; dorsoventral, -1.8 mm) and delivered with a Hamilton syringe at a speed of 1.25 μ L/min. The syringe was kept in place for an additional 2 min and then slowly withdrawn. The surgical incision then was closed, and the mice were closely monitored until regaining consciousness. All experimental procedures with the mice were carried out in accordance with the veterinary office regulations of Baden-Württemberg (Germany) and approved by the local animal care and use committees (Regierungspräsidium Tübingen).

Histological Analysis of the Mice. After 6 mo of incubation following infusion of brain extracts, the mice were killed by deep anesthesia (250 mg/kg ketamine and 25 mg/kg xylazine) and transcardial perfusion with ice-cold PBS. The brains were immersion-fixed in 4% paraformaldehyde-PBS for 48 h and then cryoprotected in 30% sucrose-PBS. After snap-freezing in methyl butane, brains were sectioned at 25- μ m thickness on a freezing-sliding microtome (Microm; Thermo Scientific) and collected in 12-well plates (every 12th section was represented in a well) containing cryoprotectant solution (35% ethylene glycerol and 25% glycerol in PBS). Sections were immunostained for A β using either a polyclonal antibody (discussed above) and Vectastain Elite ABC kit (Vector Laboratories) (50) or the double-stain LCO protocol outlined for the human tissue (discussed above).

The hippocampus (every 12th section) of each animal was analyzed for the area occupied by A β -positive immunostaining with stereological analysis on a video-microscopy system (Zeiss Axioskop 2) equipped with a motorized x-y-z stage and Stereo Investigator software (MicroBrightField) as previously described (51). The area occupied by A β -positive staining was determined using 2D sectors in a single focal plane (magnification of 20 \times /0.45-N.A. objective) as sampling sites.

Statistical Analysis. To test normality, the D'Agostino-Pearson omnibus normality test was used. For two-way ANOVA followed by Tukey's multiple comparisons test, data were logarithmically transformed when not normally distributed. The nonparametric Spearman correlation or Kruskal-Wallis test followed by Dunn's multiple comparison test were used in all other analyses. GraphPad Prism (v.5) was used for all statistical analyses.

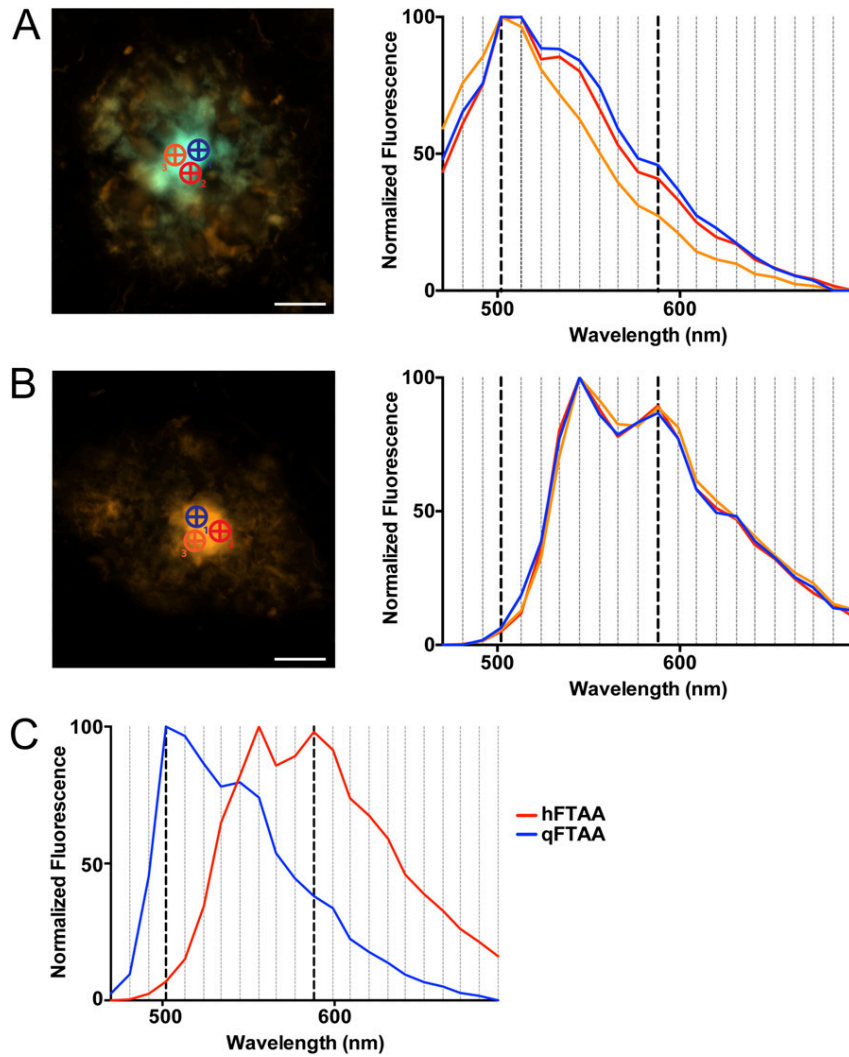


Fig. 51. Analysis of LCO-stained amyloid plaque cores. (A and B) Two representative images of the temporal cortical region of a sAD case (AD16) that was stained with hFTAA and qFTAA. For each plaque core, three regions of interest (circle/cross symbols) were set and the fluorescence intensity was measured at 22 wavelengths. A plaque core with an emission peak in the blue spectrum is shown in A, whereas B shows a plaque core with an emission peak in the red spectrum. For each plaque core, the mean was calculated from the three regions of interest. Diffuse plaques, cerebral amyloid angiopathy, and intracellular aggregates were not included in this analysis. (Scale bars: 20 μm .) (C) For comparative illustration, the spectra of the single-LCO dyes hFTAA and qFTAA are shown. Single staining with either hFTAA or qFTAA was performed on three different patients (AD17, AD20, and AD23), and the individual spectra were calculated from 60 different plaques. qFTAA shows a peak around 500 nm, whereas hFTAA shows two peaks around 550 and 590 nm.

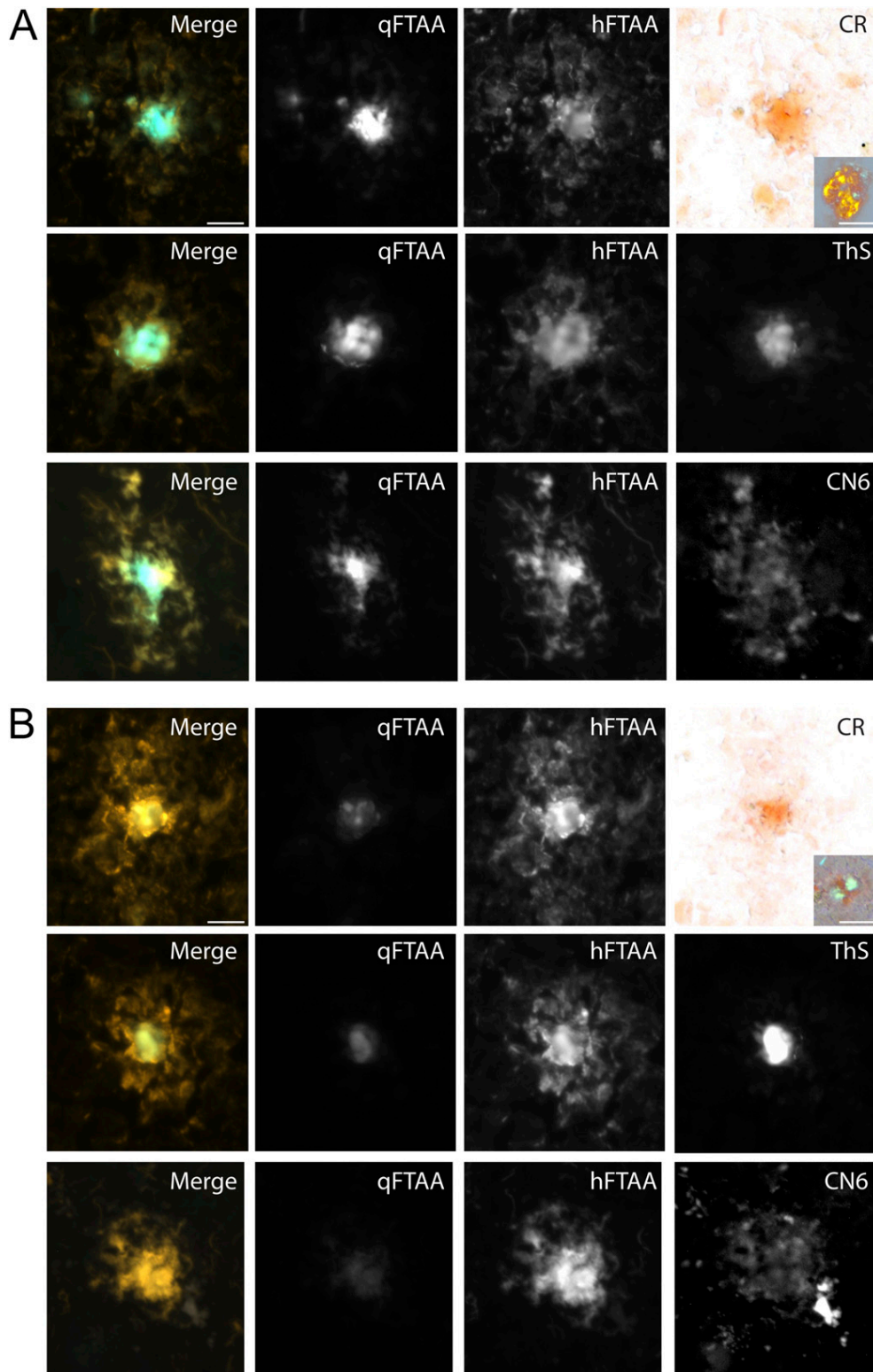


Fig. S2. Double staining of LCOs combined with other amyloid markers. Tissue from a sAD case (AD17) was stained with hFTAA and qFTAA and in adjacent sections with Congo Red (CR), Thioflavin-S (ThS), or the polyclonal A β antibody CN6. (A) Three blue-shifted plaques are shown with adjacent sections stained for CR (Inset shows birefringence), ThS, or CN6. (B) Three red-shifted plaques are shown with adjacent sections stained for CR (Inset shows birefringence), ThS, or CN6. No differences in staining between the blue- and red-shifted plaque (cores) were detected with CR, ThS, or the A β antibody. (Scale bars: 20 μ m.)

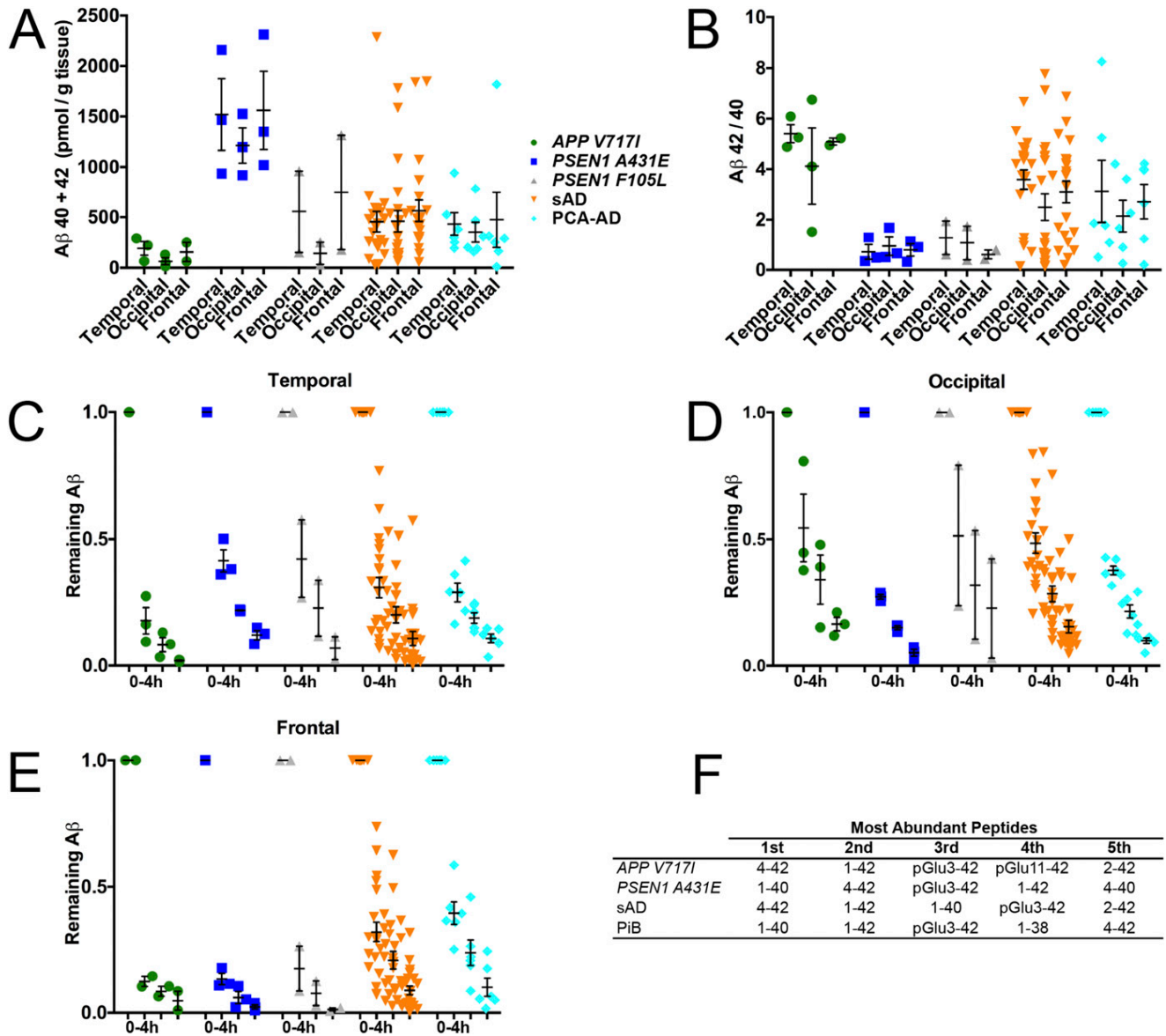


Fig. S3. Biochemical analysis of brain tissue from different AD subtypes. Levels of total Aβ₄₀ + Aβ₄₂ (A) and Aβ_{42/40} ratio (B) for each patient (formic acid extraction before 25,000 × g centrifugation) were assessed by ECL-based multiarray. Two-way ANOVA (brain region × subtype) revealed significantly different levels of Aβ among AD subtypes [$F_{(4,89)} = 8.278, P < 0.0001$], but no significant differences among brain regions [$F_{(2,89)} = 2.375, P = 0.0989$]. No subtype × region interaction was found [$F_{(8,89)} = 0.8558, P = 0.5568$]. Tukey's multiple comparisons test revealed significant differences in total Aβ between APP V717I vs. PSEN1 A431E and sAD; PSEN1 A431E vs. PSEN1 F105L, sAD, and PCA-AD (all probabilities at least $P < 0.05$). Two-way ANOVA also revealed significantly different Aβ_{42/40} ratios in the AD subtypes [$F_{(4,89)} = 4.744, P = 0.0016$], but no significant differences among brain regions [$F_{(2,89)} = 0.3785, P = 0.6860$] or in the subtype × region interaction [$F_{(8,89)} = 0.2835, P = 0.9698$]. Tukey's multiple comparisons test revealed significant differences in the Aβ_{42/40} ratio between APP V717I vs. PSEN1 A431E and PSEN1 F105L; PSEN1 A431E vs. sAD (all probabilities at least $P < 0.05$). (C–E) PK digestion of brain samples was used to determine protease resistance of Aβ over time (0, 1, 2, and 4 h), expressed as the fraction remaining after digestion compared with the undigested sample. Brain regions were analyzed individually. No significant differences were found among patient subtypes using two-way ANOVA (time × subtype) for the temporal [$F_{(4,30)} = 1.197, P = 0.3325$], occipital [$F_{(4,30)} = 2.080, P = 0.1083$], or frontal [$F_{(4,29)} = 2.184, P = 0.0957$] region. Significant differences for the time effect were seen in the temporal [$F_{(3,90)} = 106.7, P < 0.0001$], occipital [$F_{(3,90)} = 152.9, P < 0.0001$], and frontal [$F_{(3,87)} = 134.5, P < 0.0001$] regions. Interactions were not significant in the temporal [$F_{(12,90)} = 1.351, P = 0.2049$], occipital [$F_{(12,90)} = 1.211, P = 0.2877$], or frontal [$F_{(12,87)} = 1.717, P = 0.0767$] region. Note that PSEN1 E280A cases were not included for biochemical analysis because fresh-frozen tissue samples were not available when other measurements were completed. (F) Mass spectrometry analysis of the brain samples used for injections (Fig. 3) revealed that all samples contained Aβ_{1–42}, Aβ_{4–42}, and pGlu_{3–42}, with APP V717I samples containing additional Aβ_{x–42} peptide species and patients with PSEN1 A431E and sAD harboring Aβ_{1–40}. The PiB refractory case also had abundant Aβ_{1–40} as well as Aβ_{1–38} in the tissue.

Table S1. Patient information

Case	Etiology	Age, y	Sex	PMI, h	ApoE status
AD1	<i>APP V717I</i>	45	M	4.0	n.a.
AD2	<i>APP V717I</i>	49	F	2.7	E3/3
AD3	<i>APP V717I</i>	54	F	5.3	E3/3
AD4	<i>PSEN1 A431E</i>	43	F	4.0	E3/3
AD5	<i>PSEN1 A431E</i>	47	n.a.	n.a.	E3/3
AD6	<i>PSEN1 A431E</i>	44	M	n.a.	E3/3
AD7	<i>PSEN1 F105L</i>	68	F	36.0	E2/3
AD8	<i>PSEN1 F105L</i>	67	F	8.0	E2/3
AD9	<i>PSEN1 E280A</i>	52	M	4.8	E3/3
AD10	<i>PSEN1 E280A</i>	42	F	6.5	E3/3
AD11	<i>PSEN1 E280A</i>	63	F	6.5	E3/3
AD12	<i>PSEN1 E280A</i>	63	M	3.8	E3/3
AD13	<i>PSEN1 E280A</i>	58	M	3.5	E3/3
AD14	sAD	80	F	25.8	n.a.
AD15	sAD	62	M	8.5	E2/3
AD16	sAD	81	F	17.7	E3/3
AD17	sAD	70	M	8.5	E3/3
AD18	sAD	81	F	n.a.	E3/3
AD19	sAD	62	F	6.0	E3/3
AD20	sAD	74	M	2.5	E3/3
AD21	sAD	54	M	5.5	E3/3
AD22	sAD	91	F	3.0	E3/3
AD23	sAD	81	M	4.0	E3/3
AD24	sAD	89	M	49.0	E3/4
AD25	sAD	64	M	9.0	E3/4
AD26	sAD	87	F	6.0	E3/4
AD27	sAD	58	F	6.0	E3/4
AD28	sAD	77	M	6.0	E3/4
AD29	sAD	88	M	9.0	E3/4
AD30	sAD	70	F	46.9	E3/3
AD31	sAD	67	M	28.6	n.a.
AD32	sAD	77	M	90.1	E4/4
AD33	sAD	76	F	26.8	n.a.
AD34*	sAD	72	F	3.0	E3/4
AD35	PCA-AD	76	M	50.3	E3/3
AD36	PCA-AD	71	M	57.5	E3/4
AD37	PCA-AD	68	F	86.8	E3/4
AD38	PCA-AD	88	F	40.3	E3/3
AD39	PCA-AD	71	M	47.6	E3/3
AD40	PCA-AD	65	F	46.6	n.a.

F, female; M, male; n.a., information not available.

*PiB-negative sAD case: AD34.

3.3 A β seeding potency peaks in the early stages of cerebral β -amyloidosis


Ye L*, Rasmussen J*, Kaeser SA, Marzesco A, Obermueller U, Mahler J, Schelle J, Odenthal J, Krueger C, Fritschi SK, Walker LC, Staufenbiel M, Baumann F, Jucker M. EMBO Rep 2017; 18: 1536-1544.

(doi:10.15252/embr.201744067)

*equal contribution



A β seeding potency peaks in the early stages of cerebral β -amyloidosis

Lan Ye^{1,2,3,†,‡}, Jay Rasmussen^{1,2,3,†}, Stephan A Kaeser^{1,2}, Anne-Marie Marzesco^{1,2,§}, Ulrike Obermüller^{1,2}, Jasmin Mahler^{1,2,3}, Juliane Schelle^{1,2,3}, Jörg Odenthal^{1,2}, Christian Krüger^{1,2}, Sarah K Fritschl^{1,2}, Lary C Walker^{1,4}, Matthias Staufenbiel¹, Frank Baumann^{1,2} & Mathias Jucker^{1,2,*} 

Abstract

Little is known about the extent to which pathogenic factors drive the development of Alzheimer's disease (AD) at different stages of the long preclinical and clinical phases. Given that the aggregation of the β -amyloid peptide (A β) is an important factor in AD pathogenesis, we asked whether A β seeds from brain extracts of mice at different stages of amyloid deposition differ in their biological activity. Specifically, we assessed the effect of age on A β seeding activity in two mouse models of cerebral A β amyloidosis (APPPS1 and APP23) with different ages of onset and rates of progression of A β deposition. Brain extracts from these mice were serially diluted and inoculated into host mice. Strikingly, the seeding activity (seeding dose SD₅₀) in extracts from donor mice of both models reached a plateau relatively early in the amyloidogenic process. When normalized to total brain A β , the resulting specific seeding activity sharply peaked at the initial phase of A β deposition, which in turn is characterized by a temporary several-fold increase in the A β 42/A β 40 ratio. At all stages, the specific seeding activity of the APPPS1 extract was higher compared to that of APP23 brain extract, consistent with a more important contribution of A β 42 than A β 40 to seed activity. Our findings indicate that the A β seeding potency is greatest early in the pathogenic cascade and diminishes as A β increasingly accumulates in brain. The present results provide experimental support for directing anti-A β therapeutics to the earliest stage of the pathogenic cascade, preferably before the onset of amyloid deposition.

Keywords Alzheimer; amyloid; A β ; bioassay; seeding

Subject Categories Molecular Biology of Disease; Neuroscience

DOI 10.15252/embr.201744067 | Received 13 February 2017 | Revised 24 May 2017 | Accepted 26 May 2017 | Published online 12 July 2017

EMBO Reports (2017) 18: 1536–1544

Introduction

The accumulation of amyloid in the brain parenchyma and vasculature is a defining histopathological feature of Alzheimer's disease (AD) that begins at least a decade before clinical symptoms appear [1–3]. In the AD brain, amyloid consists mainly of β -sheet-rich amyloid- β peptide (A β), a cleavage product of the A β precursor protein (APP). A β is generated in various lengths, with the majority ending at amino acid 40 or 42 (A β 40 and A β 42, respectively), and the ratio of these two isoforms influences their pathobiology [4] as well as the disease phenotype [5–7].

The misfolding and aggregation of A β is thought to follow a prion-like seeding mechanism [8]. *In vitro*, A β self-assembles into small nuclei (slow nucleation phase), which in turn act as corruptive templates (seeds) to incite a chain reaction of protein misfolding and multimerization. The subsequent aggregation then yields polymeric fibrils (rapid growth phase) that are typical of amyloid [8,9]. *In vivo* studies suggest that a similar seeding mechanism drives cerebral β -amyloidosis [10]. Injection of A β -rich brain extracts or synthetic, pre-aggregated A β initiates and accelerates A β plaque deposition in APP transgenic (tg) mice [11–14].

Given the importance of A β seeds in the initiation and progression of the amyloid cascade, we asked whether A β from brain extracts of mice at different stages of the disease process differs in its seeding activity. Surprisingly, in two mouse models of cerebral β -amyloidosis, we found that the seeding potency per A β molecule (specific seeding activity) is greatest early in the pathogenic cascade and declines with the deposition of A β in brain. This observation provides experimental support for the view that treatments for AD are likely to be most effective at the very beginning of the long preclinical phase that precedes the emergence of symptoms [15].

¹ Department of Cellular Neurology, Hertie Institute for Clinical Brain Research, University of Tübingen, Tübingen, Germany

² German Center for Neurodegenerative Diseases (DZNE), Tübingen, Germany

³ Graduate School of Cellular and Molecular Neuroscience, University of Tübingen, Tübingen, Germany

⁴ Department of Neurology and Yerkes National Primate Research Center, Emory University, Atlanta, GA, USA

*Corresponding author. Tel: +49 7071 29 86863; E-mail: mathias.jucker@uni-tuebingen.de

[†]These authors contributed equally to this work

[‡]Present address: Department of Neurology, Ruijin Hospital, Shanghai, China

[§]Present address: Luxembourg Centre for Systems Biomedicine, University of Luxembourg, Esch-sur-Alzette, Luxembourg

Results and Discussion

The trajectory of cerebral A β aggregation differs in aging APP23 and APPPS1 mice

Two well-described mouse models of cerebral β -amyloidosis were used, APP23 [16] and APPPS1 [17]. To determine the approximate average lifespan of each model, 15-month-old male animals of each mouse strain were closely monitored and further aged until fulfilling the euthanasia criteria ("end stage"; see Materials and Methods). Results revealed a median lifespan of 28.6 months for male APP23 mice and 22.1 months for male APPPS1 mice (Fig 1A). Based on this observation, age groups were determined *a priori*, and brains were collected from 2-, 6-, 12-, 18-, 25-month-old and end-stage mice for the APP23 line, and from 1.2-, 3-, 6-, 12-, 18-month-old and end-stage mice for the APPPS1 line.

Immunohistochemical staining revealed a progressive increase of A β deposition for both mouse lines with advancing age. In APP23 mice, A β deposition was rarely seen at 6 months of age, but was conspicuous at 12 months, particularly in the frontal cortex (Fig 1B). At 18 months of age and beyond, parenchymal A β deposits occurred in most forebrain regions, and cerebral β -amyloid angiopathy (CAA) also was present. In APPPS1 mice, the onset of A β deposition was much earlier than in APP23 mice (Fig 1C). While 1.2-month-old APPPS1 mice did not show A β deposition, robust deposition was present in most brain regions at 3 months of age, with the frontal region again being most affected. The number of A β plaques continued to increase thereafter (Fig 1C). CAA was not a prominent feature in the APPPS1 mouse model.

Consistent with the immunohistochemical appearance of the A β lesions, human sequence A β 40 and A β 42 in brain homogenates from APP23 and APPPS1 mice increased with advancing age (Fig 1D and E). While the increases at early stages appeared to be exponential, at later stages, the increase was 1.5- to twofold in APP23 mice (from 18 to 25 months to end stage) and 1.1- to 1.4-fold in APPPS1 mice (from 12 to 18 months to end stage). At end stage, A β 42 levels were 1.8-fold higher in the APPPS1 mice compared to APP23 mice (33,000 vs. 18,000 pmol/g wet brain weight); in contrast, A β 40 levels at end stage were 10-fold higher in APP23 mice compared to APPPS1 mice (120,000 vs. 12,000 pmol/g wet brain weight).

Of note, the A β 42/A β 40 ratio in both models sharply increased around the onset of A β deposition (12 months in APP23 mice and 3 months in APPPS1 mice) and declined thereafter (Fig 1D and E). Overall, the A β 42/A β 40 ratios were higher in the APPPS1 model, consistent with the expression of L166P-mutated human PS1, which is known to favor cleavage at the A β 42 site [17].

The β -amyloid-inducing activity in brain extracts reaches a plateau with aging

We have previously found that both membrane-bound pellet and soluble fractions of β -amyloid-laden brains are seeding active [18,19]. In particular, the PBS-soluble 100,000 g fraction was highly active but represented only a small fraction of the entire seeding activity [18]. Therefore, in this study, the 3,000 g supernatant (total without large debris) has been used to compare the (total) β -amyloid-inducing activity of brain extracts among the mouse lines and age groups.

To this end, an endpoint titration bioassay was applied (see Materials and Methods). Extracts from APP23 and APPPS1 mice were serially diluted up to 10^{-4} in PBS, and each dilution was stereotactically injected into the hippocampus of 3- to 4-month-old APP23 mice. Host mice were analyzed 6 months later by A β immunohistochemistry, and the number of positively seeded mice was assessed for each dilution, age group, and mouse line (Fig 2A–C).

Brain extracts (undiluted) from 2- and 6-month-old male APP23 donor mice, which lacked immunohistochemically detectable A β deposition (see Fig 1), failed to induce A β deposition in host mice during the 6-month incubation period employed in this assay. In contrast, brain extracts prepared from APP23 mice at 12 months or older efficiently induced cerebral β -amyloidosis in the host mice (Fig 2B). Similarly, brain extracts (undiluted) from 1.2-month-old APPPS1 mice failed to induce A β deposition, while extracts from APPPS1 mice at 3 months and older were robustly seeding active (Fig 2C). Notably, the A β deposition induced with the APP23 extracts was morphologically different from the A β deposition induced with the APPPS1 extracts, and this was independent of the age of the donors (Fig 2B and C). This observation is reminiscent of the previously reported strain-like transmission of A β morphotypes [20].

To determine the seeding activity of the various brain extracts quantitatively, the number of host mice with induced A β deposition in the hippocampus was assessed for each extract and dilution (Fig 2D and E). Subsequently, the seeding dilution (SD_{50}) at which half of the inoculated animals showed seeded hippocampal A β deposition was calculated using the Reed and Muench method [21]. The SD_{50} increased from $10^{0.85}$ at 12 months to 10^3 at the end stage in the APP23 line (Fig 2F and G). For the APPPS1 line, the titers were similar, but were reached at a younger age, that is, the SD_{50} increased from $10^{1.63}$ at 3 months of age to $10^{2.57}$ at the end stage (Fig 2F and G). Surprisingly, from 18 months of age in APP23 mice and from 6 months of age in APPPS1 mice, the SD_{50} reached a plateau and did not increase further. To validate the Reed and Muench method, the Spearman–Kärber method [22,23] was alternatively applied, and this yielded similar results (Table 1). Finally, logarithmic curve-fitting using a built-in method of Prism™ (Equation Log agonist vs. response with or without Hill Slope correction) was used to calculate statistical differences (Table 1).

The specific β -amyloid-inducing activity peaks during the earliest stages of A β deposition

The β -amyloid-inducing activity of brain extracts is dependent on the presence of A β [11,24]. Thus, the specific SD_{50} was calculated (Fig 2F and G; Table 2), that is, SD_{50} normalized to the A β concentration (monomeric A β equivalent). Remarkably, in both mouse models, the highest specific SD_{50} occurred at the onset of A β plaque deposition, independent of whether it is normalized to the concentration of A β 40 or A β 42 (not shown), or total A β (i.e., A β 40 + A β 42; Fig 2F and G; Table 2). Notably, this time point also coincides with a temporary increase in the brain A β 42/A β 40 ratio in both models (Fig 1D and E). Except for the extracts from young donor mice that failed to induce seeding in our assay, the specific SD_{50} was higher in APPPS1 mouse brains than in APP23 mouse brains (Fig 2F and G). Moreover, the specific SD_{50} in APPPS1 mice

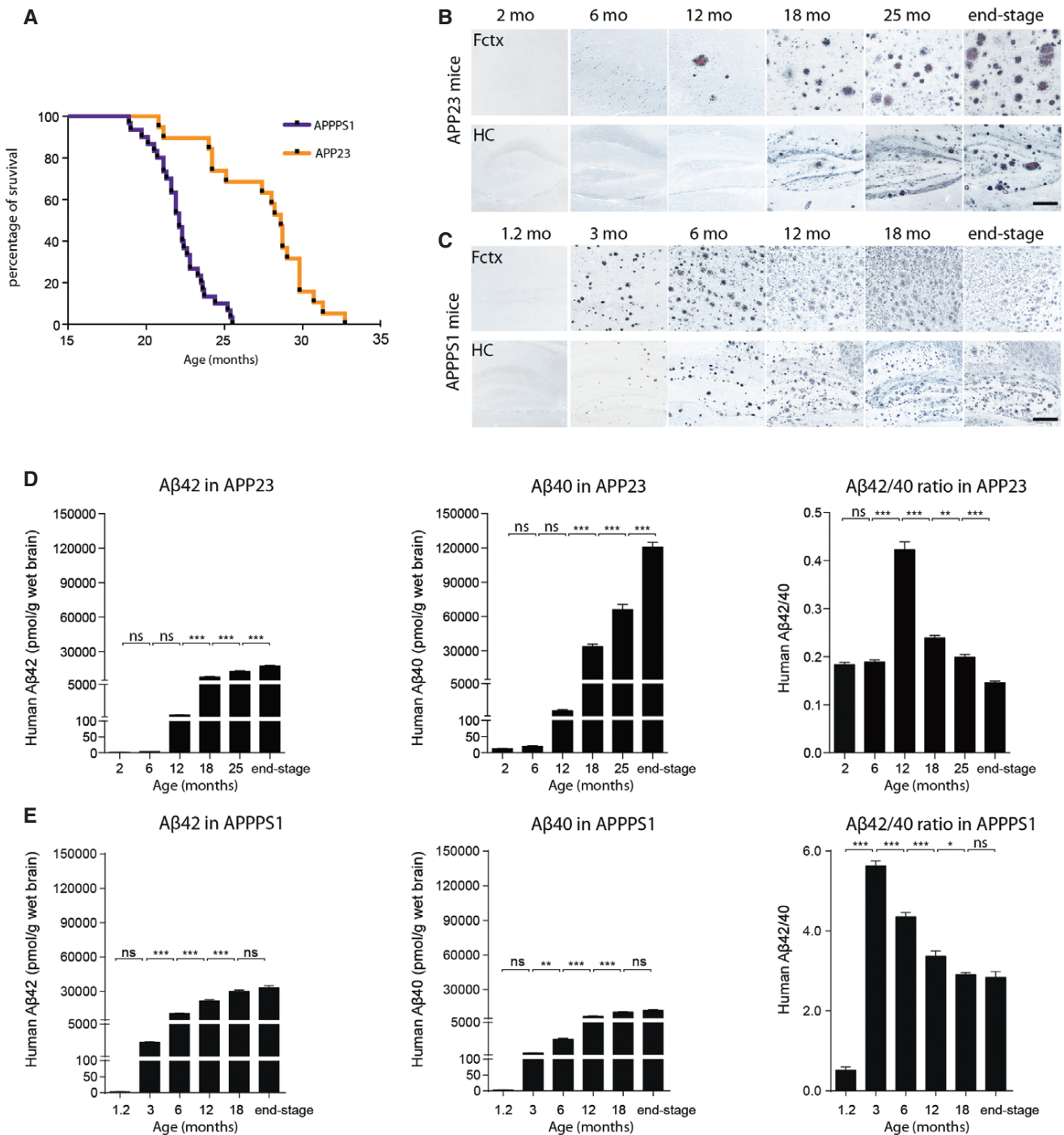


Figure 1. Age-related changes in cerebral A β load in APP23 and APPS1 tg mice.

- A** Survival curves of APP23 ($n = 19$; males) and APPS1 ($n = 29$; males) mice were generated by following cohorts of both strains from 15 months of age until the mice were sacrificed due to deteriorating health. Median survival time for APP23 mice was 28.6 months, and for APPS1 mice 22.1 months (Chi square = 29.63, $df = 1$; $P < 0.001$).
- B, C** A β immunostaining (black) combined with Congo red staining (red) shows A β deposits in the neocortex (upper row) and hippocampus (lower row) of male APP23 mice (**B**) and male APPS1 mice (**C**) at different ages. End stage was defined as the point at which mice had to be terminated due to poor health ($n = 5-9$ male mice/group; representative images from each time point are shown). Scale bars: 200 μ m.
- D, E** A β 40, A β 42, and A β 42/A β 40 ratio in total brain homogenates of separate animal cohorts ($n = 7-11$ male mice per group) for APP23 mice ($F_{5,56} = 339.7$, $F_{5,56} = 332.8$, $F_{5,56} = 145.5$, respectively) (**D**) and APPS1 mice ($F_{5,41} = 168.4$, $F_{5,41} = 257.2$, $F_{5,41} = 182.4$, respectively) (**E**) measured by immunoassays (mean \pm SEM); ANOVA followed by *post hoc* Bonferroni test: * $P < 0.05$, ** $P < 0.01$, *** $P < 0.001$, ns = not significant.

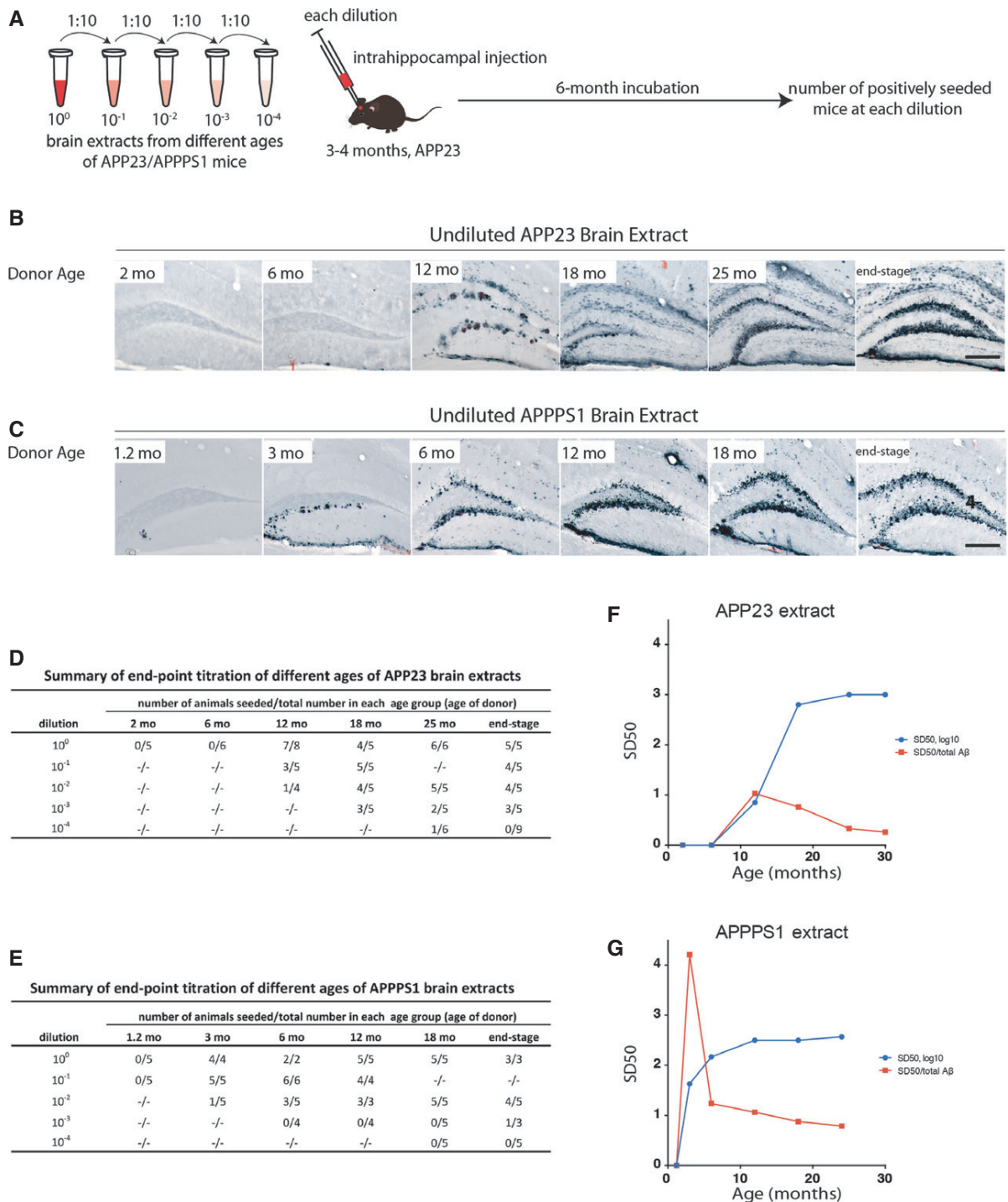


Figure 2. Seeding activity of brain extracts from APP23 and APPPS1 tg mice increases with donor age and plateaus in late stages.

A–C Brain extracts from APP23 (B) and APPPS1 (C) mice at different ages were injected into the hippocampus of young, pre-depositing 3- to 4-month-old male APP23 host mice. Brains were immunohistochemically analyzed for A β deposition 6 months later. A β immunostaining combined with Congo red staining is shown. Note the more diffuse and filamentous A β deposition induced with the APP23 extracts in contrast to the punctate and compact A β deposition induced with the APPPS1 extracts. Scale bars: 200 μ m.

D, E Number of mice with induced A β deposition at each dilution from the different age groups (n = mainly 3–6/group) of APP23 (D) and APPPS1 (E) brain extracts.

F, G SD₅₀ of APP23 (F) and APPPS1 (G) brain extracts (blue line; Reed-Muench method, see Table 1 for statistical analysis). SD₅₀ (half-maximal seeding dose) was defined as the log₁₀ of the brain extract dilution at which 50% of the host mice showed induced A β deposition (see Materials and Methods). The specific seeding activity (SD₅₀/total A β ; red line) for each extract indicates a peak at early ages in brain extracts from both mouse lines (see Table 2).

Table 1. Comparison of SD₅₀ values (log₁₀) calculated with different methods for all age groups of APP23 and APPPS1 brain extracts.

	APP23						APPPS1					
	2 months	6 months	12 months	18 months	25 months	End-stage	1.2 months	3 months	6 months	12 months	18 months	End-stage
Reed-Muench	0.00	0.00	0.85	2.80	3.00	3.00	0.00	1.63	2.17	2.50	2.50	2.57
Spearman-Kärber	0.00	0.00	1.23	2.90	3.07	2.81	0.00	1.70	2.10	2.50	2.50	2.63
Curve-fitting	0.00	0.00	1.12 ± 0.00	3.08 ± 0.06	2.99 ± 0.18	2.95 ± 0.16	0.00	1.61 ± 0.38	2.15 ± 0.14	2.55 ± 0.14	2.54 ± 0.43	2.63 ± 0.08

Curve-fitting based on the Reed-Muench method was used for statistical analysis. The SEM is indicated. Two-way ANOVA revealed a significant effect for age group ($F_{5,184} = 25.88$; $P < 0.001$) but not for genotype ($F_{1,184} = 1.35$; $P = 0.25$). There was a significant interaction of genotype x age group ($F_{5,184} = 3.537$; $P < 0.01$). N was 5–29 and results from the summed numbers of mice examined in Fig 2D and E. Subsequent *post hoc* Bonferroni tests revealed that seed titers plateaued starting at 18 months for APP23, and at 6 months for APPPS1, group comparisons $P > 0.05$.

Table 2. Specific seeding activity (SD₅₀ per total A β) contained in injected material from donor mice of different ages.

	APP23						APPPS1					
	2 months	6 months	12 months	18 months	25 months	End-stage	1.2 months	3 months	6 months	12 months	18 months	End-stage
Total A β (fmol)	1.67	1.52	6.91	824.87	3075.50	3830.74	3.78	10.11	118.53	296.76	360.38	473.08
SD ₅₀ /total A β	(0.00)	(0.00)	1.03	0.76	0.33	0.26	(0.00)	4.21	1.24	1.07	0.88	0.78

differed by roughly 3 log₁₀ between early and late time points (Fig 2G; Table 2).

Rationale for directing anti-A β therapeutics to the earliest stage of the pathogenic cascade

Despite the importance of A β aggregation as a trigger of AD pathogenesis, there is little information on whether the biological activity of the aggregated peptide changes as the disease evolves. In this series of studies, we determined the potency of A β seeds using the *in vivo* induction of A β aggregation as a readout. For this purpose, we used two distinct APP-tg mouse models with differing rates of deposition. Although the age at which A β deposits first appear in these models is quite different, the emergence of A β seeds that are able to induce detectable deposition within the time-frame of our assay coincides with the earliest ages of deposition in the donor mouse (note that the exact age of onset is 8–9 months and 1.5 months in male APP23 and APPPS1 mice, respectively, but these ages were not tested in the current study). Remarkably, at later stages of life in both models, the correlation of seeding activity with the A β load diminishes, as seeding activity reaches a plateau even though A β deposition continues to increase as the mice age. Consequently, the highest seeding activity relative to total A β (the specific seeding activity) occurs at the inception of A β deposition, and this coincides with a peak of the A β 42/A β 40 ratio.

We first followed A β deposition across the average lifespan of APP23 and APPPS1 mouse models. Consistent with previous reports [25–28], we observed a steep increase of both A β 40 and A β 42 levels beginning at the age of onset of plaque deposition in both mouse lines. At end stage, total A β levels (A β 40 + A β 42) were threefold higher in APP23 mice compared to APPPS1 mice, and this was due to a massive increase of A β 40 in aged APP23 mice. This was not only due to insoluble aggregates as *post hoc* analysis of the 100,000 g soluble fractions from a different study also showed an age-related increase in both models (not further analyzed here).

Nonetheless, longevity is shorter in APPPS1 mice than in APP23 mice, possibly indicating a minor contribution or protective effect of A β 40. The shorter lifespan of APPPS1 mice could also be a consequence of the PS1 transgene overexpression.

Although A β seeds are known to induce cerebral A β aggregation in a concentration-dependent manner [29,30], the potency of A β seeds, that is, the amount of A β -containing species needed to induce A β deposition, has been difficult to quantify. The latter, however, is important for current efforts to purify A β seeding activity. In the present study, we therefore developed an endpoint titration bioassay similar to those used to measure prion infectivity [31,32] and more recently for A β [33]. We were thus able to establish the dose of A β seeds that induces deposition in 50% of the animals (the seeding dilution or dose 50, or SD₅₀) as a reliable measure of the activity of A β seeds. Using this assay, we found that the seeding activity of PBS-soluble brain extracts initially increases exponentially with age, but then reaches a plateau in both mouse models. At the plateau stage, a single APP23 mouse brain contains approximately 1,600,000 seeding units, while an APPPS1 brain contains roughly 600,000 units (based on the assumption of a mouse brain weighing 400 mg). Interestingly, in prion disease, infectious prions in the brain first increase exponentially, followed by a plateau in prion titers that governs the onset of clinical disease, suggesting a transition to the generation of toxic assemblies of the prion protein that differ from the infectious prion seeds [32]. Whether similarly distinct species of A β exist over the course of AD pathogenesis and whether the earlier plateauing of seeding potency in the APPPS1 line is responsible for the early death of these mice is not known.

Strikingly, the seeding potency of A β (specific SD₅₀) in both mouse models peaks during the earliest stages of A β deposition. Moreover, this spike in seeding potency coincides with a transient increase in the A β 42/A β 40 ratio, which occurs shortly after the onset of A β deposition and then decreases as plaques and CAA proliferate in the brain [27,28]. Therefore, A β seed potency, the A β 42/A β 40 ratio, and deposition stage are closely linked, and this is

true in both APP23 and APPPS1 mouse models. The greater potency of A β seeds during all stages of deposition in APPPS1 mice corresponds to the higher A β 42/A β 40 ratio (Fig 1) and relatively more aggregated A β species (Fig EV1) in APPPS1 mice compared to APP23 mice. Our results thus support the hypothesis that A β 42-containing aggregates are particularly effective components of bioactive A β seeds.

The peak in specific seeding activity of A β early during deposition may be due to the predominance of relatively small aggregates at this time, which results in a large number of molecular seeding surfaces relative to the number of total A β molecules present. With increasing aggregation (and increasing total A β), an increasing fraction of molecular seeding surfaces may be buried within the aggregates and unable to template other A β molecules. However, it is also possible that the evolving potency of A β seeds results from features of the assemblies that change as the disease process advances in the brain, a possibility also in line with the coincident spikes in seeding potency and the A β 42/A β 40 ratio. Although the preparation of our injectable material (3,000 g) was relatively gentle, we cannot exclude effects on the aggregation state of the seeds or their interaction with other proteins that might modulate the seeding activity.

Implications

Our findings in transgenic mouse models indicate that A β seeds are most potent in the early stages of A β deposition and that this spike in specific seeding activity is associated with a transient increase in the A β 42/A β 40 ratio. Thereafter, both A β levels and the total seeding activity increase rapidly, followed by a leveling-off of the seeding activity even as total A β levels continue to climb. Our results demonstrate that the pathobiology of A β changes as the disease process evolves, at least with respect to the seeding capacity of aberrant A β . The particular potency of A β seeds in the initial stages underscores the importance of therapeutically targeting A β deposition in the brain before it becomes detectable by PET imaging or CSF biomarker analysis. In this light, more sensitive biomarkers are needed that will enable earlier or even predictive identification of the AD pathogenic process. Therapeutically, compounds that prevent the formation or activity of A β seeds hold particular promise for the prevention and treatment of AD.

Materials and Methods

Mice

All animal experiments were conducted in compliance with protocols approved by the local Animal Care and Use Committee. APP23 mice overexpress KM670/671NL-mutated human APP under the control of a neuronal Thy1 promoter. The mice were generated on a B6D2 background [16], but they have been backcrossed to C57BL/6J for more than 25 generations. APPPS1 mice express the same mutant form of APP together with L166P-mutated presenilin-1, again under the control of the neuron-specific Thy1 promoter element, and were generated and maintained on a C57BL/6J genetic background [17]. Male and female APP23 mice differ in the age at which endogenous amyloid deposition begins [27]. Therefore, to

reduce variation in age-related deposition, male APP23 and, consistently, male APPPS1 mice were used. All donor mice were group-housed under specific pathogen-free conditions (APP23 in Basel, Novartis; APPPS1 in Tübingen, Hertie Institute for Clinical Brain Research). Mice were inspected regularly for health issues. Mice were euthanized when they reached a pre-specified age or in the event that they were deemed to be in intractable distress based on an independent assessment by the animal caretaker according to AVMA Guidelines (<https://www.avma.org/KB/Policies/Documents/euthanasia.pdf>). The latter criterion was used to determine the end-stage time point that defined the median lifespan of each of the mouse lines. Mice were sacrificed by cervical dislocation under isoflurane anesthesia. Brains were removed from sacrificed mice, immediately frozen using dry ice, and stored at -80°C until use for either histological staining or brain tissue homogenate preparation. All experimental procedures with the mice were carried out in accordance with the veterinary office regulations of Baden-Wuerttemberg (Germany) and approved by the local Animal Care and Use Committees.

A β immunohistochemical analysis of APP23 and APPPS1 mice

Brains (hemispheres) were cut sagittally (15 μm thickness) with a cryostat, and a representative set of sections (every 20th section) was stained immunohistochemically with an in-house polyclonal antibody directed against A β and the Vectastain Elite ABC kit (Vector Laboratories, Burlingame, CA) as previously described [12]. Sections were then co-stained with Congo red according to standard protocols. Representative images are shown in Fig 1 for each time point and genotype ($n = 5\text{--}9$ male mice were used per age group).

Preparation of brain tissue homogenates

Brains from a separate cohort of male mice ($n = 7\text{--}11$ per age group) were homogenized in sterile PBS (10%, w/v) at 4°C (2×10 s at 5,500 rpm, each round separated by a 10 s pause) using a Precellys 24 Dual homogenizer (Bertin, Montigny-le-Bretonneux, France; 7 ml lysing tubes with 2.8 mm ceramic beads). Samples were stored at -80°C . Brain homogenates were either kept for further quantitative A β analysis or used for intracerebral injections.

Quantification of A β by electrochemiluminescence-linked immunoassay

A β peptides (A β 40 and A β 42) in brain homogenates were quantified with an electrochemiluminescence-linked immunoassay using the MSD[®] 96-well Human (6E10) A β Triplex Assay (MesoScale Discovery); 96-well plates that had been pre-spotted with capture antibodies against A β 40 and A β 42 were blocked for 1 h with 1% bovine serum albumin in Tris buffer and washed three times with $1 \times$ Tris buffer. Samples were treated with formic acid (final concentration: 70%) (Sigma), sonicated for 30 s on ice, and centrifuged at $25,000 \times g$ for 1 h at 4°C . Supernatants were equilibrated in neutralization buffer (1 M Tris base, 0.5 M Na₂HPO₄, 0.05% NaN₃) and diluted up to 1:1,000 (depending on A β load, to stay within the linear range of the assay) in 1% BSA. Samples were then co-incubated with the SULFO-TAG 6E10 detection antibody solution on the plate for 2 h. After washing, MSD Read Buffer T was added and

the plate was read immediately on a Sector Imager 6000. Data analysis used MSD DISCOVERY WORKBENCH software 2.0.

Intracerebral injections and serial dilution of brain extracts

For intracerebral injections, brain homogenates were centrifuged at $3,000 \times g$ for 5 min at 4°C and the supernatant collected (hereafter referred as “brain extract”). In order to reduce individual mouse variability, for each age group, brain extracts from all the mice within an age group were pooled ($n = 8\text{--}10$ per group; see above) and then serially diluted up to 10^{-4} fold in sterile PBS. Host mice were 3- to 4-month-old male APP23 mice ($n =$ mainly 3–6 per group). The mice were anaesthetized with a mixture of ketamine (110 mg/kg body weight) and xylazine (20 mg/kg body weight) in saline; 2.5 μ l of each brain extract or dilution thereof were bilaterally delivered to the hippocampus (AP: -2.5 mm, L: ± 2.0 mm, DV: -1.8 mm) with a Hamilton syringe. Injections were performed at 1.25 μ l/min, and the needle was kept in place for an additional 2.5 min before being slowly withdrawn. The surgical area was cleaned with sterile saline, the incision was sutured, and the mice were monitored until recovery from anesthesia.

Endpoint titration assay to estimate SD₅₀

After 6 months of incubation, mice inoculated with brain extracts were deeply anaesthetized with ketamine (250 mg/kg)/xylazine (25 mg/kg) and sacrificed by transcardial perfusion with ice-cold PBS. Brains were immersion-fixed for 48 h in 4% paraformaldehyde in PBS and then cryoprotected in 30% sucrose in PBS for an additional 48 h. Fixed brains were serially cut into 25- μ m-thick coronal sections on a freezing-sliding microtome (Microm, Thermo Scientific) and collected in a 12-well plate containing cryoprotectant (35% ethylene glycol, 25% glycerol in PBS) for storage at -20°C . Sections from a single well (containing every 12th section) were then stained immunohistochemically with a polyclonal antibody directed against A β and co-stained with Congo red according to standard protocols (see A β immunohistochemical analysis above).

To quantify the seeding activity of extracts from donors at different ages, we calculated the half-maximal A β seeding titers (SD₅₀) using titration assays similar to those used in prion infectivity titer measurements. The classic methods for measuring scrapie prion infectivity *in vivo* are the endpoint titration bioassay and the incubation time interval assay [34–36]. Although the latter is less costly and time-consuming [36], the absence of reliable and obvious clinical symptoms in APP transgenic mouse models limited its feasibility for these models. Therefore, we chose the endpoint titration bioassay and killed animals after a fixed incubation time.

Positive or negative induction of A β deposition was rated on the A β -immunostained sections throughout the hippocampus for each animal. Note that endogenous A β plaques in the hippocampus of male 9- to 10-month-old APP23 mice are absent [11] or limited to no more than one plaque per section. Moreover, rare endogenous A β plaques can be distinguished from induced A β deposition, which reveals the typical induction pattern along the layers in the dentate gyrus (see Fig 2B and C). Two independent raters performed the quantification blinded, and their assessments were 100% congruent.

The number of animals that showed induced A β deposition at each dilution was determined in order to calculate the A β seeding titer. Titers (SD₅₀) were calculated by counting positively seeded animals vs total animals according to Reed and Muench [21] or the Spearman–Kärber method [22,23]. Calculation with logarithmic curve-fitting was based on the numbers of positive vs total animals as determined with the Reed and Muench method [21] using Equation Log agonist vs. response with or without Hill Slope correction, as provided by GraphPad Prism™ version 5.

Dot blot assay

For further characterization, “brain extracts” of a given age group were pooled, IgG-depleted using Sheep Anti-Mouse Dynabeads (Life Technologies, 11201D) and total protein determined by BCA assay (Thermo). Samples were serially diluted in PBS containing protease- and phosphatase-inhibitors (Thermo) at the following dilutions: 10^{-1} , 10^{-2} and 10^{-3} . Samples were spotted on nitrocellulose membranes so that 3 μ g total protein was contained in the undiluted (10^0) area. An aged non-transgenic mouse (29 months old; wild type) seeding extract was included in addition to synthetic A β samples. Synthetic A β 1–40 and A β 1–42 (Bachem, H-1194 and H-8146, respectively) were fibrillized at 37°C (100 μ M A β , 10 mM HCl, 150 mM NaCl) for 5 days without shaking and 5 ng of each was spotted on membranes, in addition to a monomeric A β 1–40 control (5 ng). Blotting and probing with OC (Millipore, AB2286) were performed as previously described [37]. Briefly, membranes were rehydrated in Tris–glycine (25–192 mM) buffer containing 20% MeOH, then incubated in hydrogen peroxide (0.3% in PBS) for 15 min. After washing, membranes were blocked in skim milk (10% in PBS-0.05% Tween \rightarrow PBS-T) for 60 min and probed with OC overnight at 4°C (1:10,000, PBS-T with 5% BSA). Membranes were washed with PBS-T and incubated in donkey anti-rabbit-HRP secondary (1:30,000; Jackson ImmunoResearch Laboratories, 711-035-152) for 60 min, then washed (PBS-T) prior to developing with SuperSignal™ West Dura Extended Duration Substrate (Thermo) and exposed on Hyperfilm (Amersham). Staining with 6E10 (BioLegend, 803017) and N25 (gift of M. Mercken) [38] was done in parallel, with membranes being heated in PBS after rehydration (95°C for 5 min) and blocked in skim milk (5% in PBS-T) for 60 min. Membranes were incubated in 6E10 (1:5,000 in PBS-T) or N25 (1:5,000 in PBS-T) overnight at 4°C before being washed (PBS-T) and incubated in goat anti-mouse (1:30,000; Jackson ImmunoResearch Laboratories, 115-035-068) for 60 min. Membranes were developed in the same way as for OC. Control blots without addition of primary antibodies were also done in parallel with both anti-rabbit and anti-mouse secondaries.

Statistical analysis

GraphPad Prism™ version 5 was used for all statistical analyses.

Expanded View for this article is available online.

Acknowledgements

We would like to thank our laboratory members for experimental help and Peter Nilsson and Per Hammarstrom (Linköping) for advice. We are grateful to M. Mercken (Johnson & Johnson Pharmaceutical Research & Development) for

providing the N25 A β antibody. This work was supported by a grant from the Competence Network on Degenerative Dementias (BMBF-01GI0705). LY. was financially supported by the Chinese Scholarship Council, and L.C.W. was supported by an award from the Alexander von Humboldt Foundation.

Author contributions

LY, JR, SAK, A-MM, UO, JM, JS, JO, CK, and SKF performed the experimental work. LY, JR, A-MM, and FB carried out the statistical analysis. FB and MJ designed the study, and LCW and MS helped with the interpretation of the data. LY, JR, LCW, MS, and MJ prepared the manuscript with the help of all other authors.

Conflict of interest

The authors declare that they have no conflict of interest.

References

- Bateman RJ, Xiong C, Benzinger TL, Fagan AM, Goate A, Fox NC, Marcus DS, Cairns NJ, Xie X, Blazey TM *et al* (2012) Clinical and biomarker changes in dominantly inherited Alzheimer's disease. *N Engl J Med* 367: 795–804
- Jack CR Jr, Holtzman DM (2013) Biomarker modeling of Alzheimer's disease. *Neuron* 80: 1347–1358
- Dubois B, Hampel H, Feldman HH, Scheltens P, Aisen P, Andrieu S, Bakardjian H, Benali H, Bertram L, Blennow K *et al* (2016) Preclinical Alzheimer's disease: definition, natural history, and diagnostic criteria. *Alzheimers Dement* 12: 292–323
- De Strooper B (2010) Proteases and proteolysis in Alzheimer disease: a multifactorial view on the disease process. *Physiol Rev* 90: 465–494
- Duering M, Grimm MO, Grimm HS, Schröder J, Hartmann T (2005) Mean age of onset in familial Alzheimer's disease is determined by amyloid beta 42. *Neurobiol Aging* 26: 785–788
- Kumar-Singh S, Theuns J, Van Broeck B, Pirici D, Vennekens K, Corsmit E, Cruts M, Dermaut B, Wang R, Van Broeckhoven C (2006) Mean age-of-onset of familial Alzheimer disease caused by presenilin mutations correlates with both increased Abeta42 and decreased Abeta40. *Hum Mutat* 27: 686–695
- Szaruga M, Veugelen S, Benurwar M, Lismont S, Sepulveda-Falla D, Lleo A, Ryan NS, Lashley T, Fox NC, Murayama S *et al* (2015) Qualitative changes in human gamma-secretase underlie familial Alzheimer's disease. *J Exp Med* 212: 2003–2013
- Jucker M, Walker LC (2013) Self-propagation of pathogenic protein aggregates in neurodegenerative diseases. *Nature* 501: 45–51
- Harper JD, Lansbury PT Jr (1997) Models of amyloid seeding in Alzheimer's disease and scrapie: mechanistic truths and physiological consequences of the time-dependent solubility of amyloid proteins. *Annu Rev Biochem* 66: 385–407
- Walker LC, Jucker M (2015) Neurodegenerative diseases: expanding the prion concept. *Annu Rev Neurosci* 38: 87–103
- Meyer-Luehmann M, Coomaraswamy J, Bolmont T, Kaeser S, Schaefer C, Kilger E, Neuenschwander A, Abramowski D, Frey P, Jaton AL *et al* (2006) Exogenous induction of cerebral beta-amyloidogenesis is governed by agent and host. *Science* 313: 1781–1784
- Eisele YS, Obermüller U, Heilbronner G, Baumann F, Kaeser SA, Wolburg H, Walker LC, Staufenberg M, Heikenwalder M, Jucker M (2010) Peripherally applied Abeta-containing inoculates induce cerebral beta-amyloidosis. *Science* 330: 980–982
- Stöhr J, Condello C, Watts JC, Bloch L, Oehler A, Nick M, DeArmond SJ, Giles K, DeGrado WF, Prusiner SB (2014) Distinct synthetic Abeta prion strains producing different amyloid deposits in bigenic mice. *Proc Natl Acad Sci USA* 111: 10329–10334
- Morales R, Duran-Aniotz C, Castilla J, Estrada LD, Soto C (2012) De novo induction of amyloid-beta deposition *in vivo*. *Mol Psychiatry* 17: 1347–1353
- Sperling R, Mormino E, Johnson K (2014) The evolution of preclinical Alzheimer's disease: implications for prevention trials. *Neuron* 84: 608–622
- Stürchler-Pierrat C, Abramowski D, Duke M, Wiederhold KH, Mistl C, Rothacher S, Ledermann B, Burki K, Frey P, Paganetti PA *et al* (1997) Two amyloid precursor protein transgenic mouse models with Alzheimer disease-like pathology. *Proc Natl Acad Sci USA* 94: 13287–13292
- Radde R, Bolmont T, Kaeser SA, Coomaraswamy J, Lindau D, Stoltze L, Calhoun ME, Jäggi F, Wolburg H, Gengler S *et al* (2006) Abeta42-driven cerebral amyloidosis in transgenic mice reveals early and robust pathology. *EMBO Rep* 7: 940–946
- Langer F, Eisele YS, Fritschi SK, Staufenberg M, Walker LC, Jucker M (2011) Soluble Abeta seeds are potent inducers of cerebral beta-amyloid deposition. *J Neurosci* 31: 14488–14495
- Marzesco AM, Flotenmeyer M, Buhler A, Obermüller U, Staufenberg M, Jucker M, Baumann F (2016) Highly potent intracellular membrane-associated Abeta seeds. *Sci Rep* 6: 28125
- Heilbronner G, Eisele YS, Langer F, Kaeser SA, Novotny R, Nagarathinam A, Aslund A, Hammarstrom P, Nilsson KP, Jucker M (2013) Seeded strain-like transmission of beta-amyloid morphotypes in APP transgenic mice. *EMBO Rep* 14: 1017–1022
- Reed LJ, Muench H (1938) A simple method of estimating fifty per cent endpoints. *Am J Epidemiol* 27: 493–497
- Armitage P, Allen I (1950) Methods of estimating the LD 50 in quantal response data. *J Hyg (Lond)* 48: 298–322
- Kärber G (1931) Beitrag zur kollektiven Behandlung pharmakologischer Reihenversuche. *Arch Exp Pathol Pharmacol* 162: 480–483
- Duran-Aniotz C, Morales R, Moreno-Gonzalez I, Hu PP, Fedynshyn J, Soto C (2014) Aggregate-depleted brain fails to induce Abeta deposition in a mouse model of Alzheimer's disease. *PLoS One* 9: e89014
- Kawarabayashi T, Younkin LH, Saido TC, Shoji M, Ashe KH, Younkin SG (2001) Age-dependent changes in brain, CSF, and plasma amyloid-beta protein in the Tg2576 transgenic mouse model of Alzheimer's disease. *J Neurosci* 21: 372–381
- Lesne S, Kotilinek L, Ashe KH (2008) Plaque-bearing mice with reduced levels of oligomeric amyloid-beta assemblies have intact memory function. *Neuroscience* 151: 745–749
- Maia LF, Kaeser SA, Reichwald J, Hruscha M, Martus P, Staufenberg M, Jucker M (2013) Changes in amyloid-beta and Tau in the cerebrospinal fluid of transgenic mice overexpressing amyloid precursor protein. *Sci Transl Med* 5: 194re192
- Maia LF, Kaeser SA, Reichwald J, Lambert M, Obermüller U, Schelle J, Odenthal J, Martus P, Staufenberg M, Jucker M (2015) Increased CSF Abeta during the very early phase of cerebral Abeta deposition in mouse models. *EMBO Mol Med* 7: 895–903
- Eisele YS, Fritschi SK, Hamaguchi T, Obermüller U, Fuger P, Skodras A, Schaefer C, Odenthal J, Heikenwalder M, Staufenberg M *et al* (2014) Multiple factors contribute to the peripheral induction of cerebral beta-amyloidosis. *J Neurosci* 34: 10264–10273
- Fritschi SK, Langer F, Kaeser SA, Maia LF, Portelius E, Pinotsi D, Kaminski CF, Winkler DT, Maetzler W, Keyvani K *et al* (2014) Highly potent soluble amyloid-beta seeds in human Alzheimer brain but not cerebrospinal fluid. *Brain* 137: 2909–2915

31. Flechsig E, Shmerling D, Hegyi I, Raeber AJ, Fischer M, Cozzio A, von Mering C, Aguzzi A, Weissmann C (2000) Prion protein devoid of the octapeptide repeat region restores susceptibility to scrapie in PrP knock-out mice. *Neuron* 27: 399–408
32. Sandberg MK, Al-Doujaily H, Sharps B, Clarke AR, Collinge J (2011) Prion propagation and toxicity *in vivo* occur in two distinct mechanistic phases. *Nature* 470: 540–542
33. Morales R, Bravo-Alegria J, Duran-Aniotz C, Soto C (2015) Titration of biologically active amyloid-beta seeds in a transgenic mouse model of Alzheimer's disease. *Sci Rep* 5: 9349
34. Makarava N, Savtchenko R, Alexeeva I, Rohwer RG, Baskakov IV (2012) Fast and ultrasensitive method for quantitating prion infectivity titre. *Nat Commun* 3: 741
35. Maramorosch K, McKelvey JJJ (1985) *Subviral pathogens of plants and animals: Viroids and Prions*. Orlando, FL: Academic Press
36. Prusiner SB, Cochran SP, Groth DF, Downey DE, Bowman KA, Martinez HM (1982) Measurement of the scrapie agent using an incubation time interval assay. *Ann Neurol* 11: 353–358
37. Liu P, Reed MN, Kotilinek LA, Grant MK, Forster CL, Qiang W, Shapiro SL, Reichl JH, Chiang AC, Jankowsky JL et al (2015) Quaternary structure defines a large class of Amyloid-beta oligomers neutralized by sequestration. *Cell Rep* 11: 1760–1771
38. Vandermeeren M, Geraerts M, Pype S, Dillen L, Van Hove C, Mercken M (2001) The functional gamma-secretase inhibitor prevents production of amyloid beta 1-34 in human and murine cell lines. *Neurosci Lett* 315: 145–148

Expanded View Figures

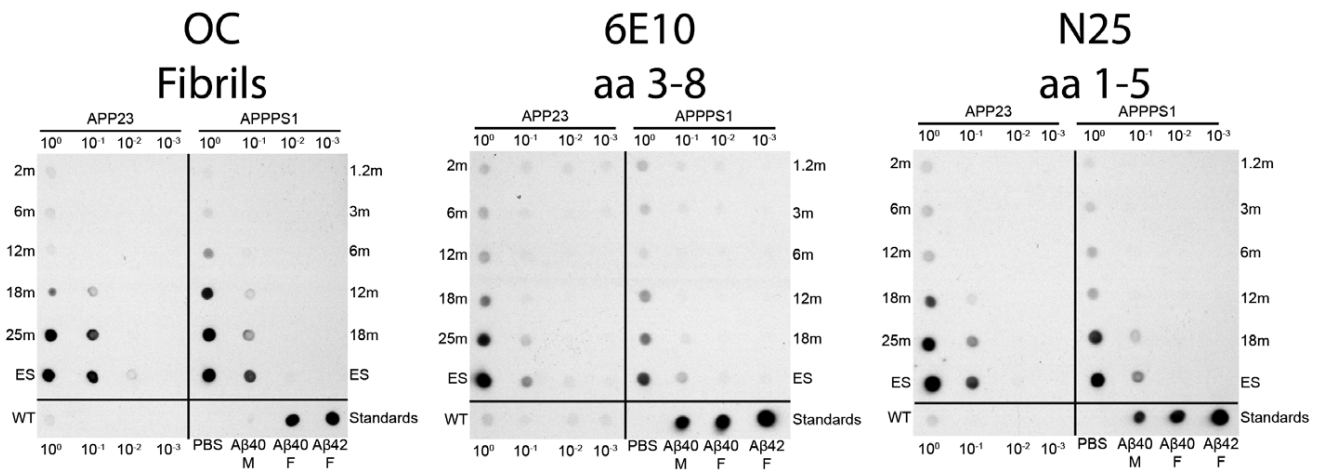


Figure EV1. Age-dependent increase of fibrillar A β species in seeding extracts for both transgenic mouse models.

Pooled seeding extracts used for *in vivo* inoculations were spotted on nitrocellulose membranes and probed with antibodies against fibrillar A β epitopes (OC) or monomeric A β epitopes at amino acids (aa) 3–8 (6E10) or aa 1–5 (N25). An aged wild-type (WT) control brain extract was used at the same total protein concentration as the transgenic samples (i.e., 3 μ g total protein in 10⁰) in addition to 5 ng of each monomeric A β 1–40, fibrillar A β 1–40, and fibrillar A β 1–42. Presented is a representative blot performed in duplicate. M = monomer, F = fibril, ES = end stage.

3.4 An agarose gel fractionation method for enriching brain-derived proteopathic seeds

Rasmussen J, Bühler A, Baumann F, Jucker M.

in preparation

An agarose gel fractionation method for enriching brain-derived proteopathic seeds

Jay Rasmussen^{a,b,c}, Anika Bühler^a, Frank Baumann^a and Mathias Jucker^{§,a,b}

^aDepartment of Cellular Neurology, Hertie Institute for Clinical Brain Research, University of Tübingen, D-72076 Tübingen, Germany; ^bGerman Center for Neurodegenerative Diseases (DZNE), Tübingen, D-72076 Tübingen, Germany; ^cGraduate Training Center of Neuroscience, University of Tübingen, D-72074 Tübingen, Germany;

§ To whom correspondence may be addressed. Email: mathias.jucker@uni-tuebingen.de

Keywords: amyloid, Alzheimer, seeding, aggregation

Abstract

The seminal event in Alzheimer's disease pathogenesis is the aggregation and deposition of the β -amyloid (A β) peptide. A β aggregation produces a diverse population of different A β assemblies in the brain, ranging from monomers to large fibrillar aggregates. A detailed analysis of the biochemical or biological properties of aggregated A β species is lacking because of the inherent difficulties to isolate these species in their native form. Here, an agarose fractionation method is presented that separates brain-derived A β assemblies based on size. The agarose fractions are then enzymatically digested to liberate the native A β assemblies that can then be tested for their biological activities. Indeed using this novel approach we could show that brain-derived A β assemblies displayed migration patterns that were different from synthetic A β aggregates. Additionally, we could show that the quaternary structure and biological in vivo seeding activity of brain-derived A β aggregates was preserved after fractionation and liberation of the A β assemblies. Finally, immunoprecipitation of the fractionated native A β assemblies allowed for the screening of A β antibodies for their recognition of various assemblies. This method for enriching seeding active subpopulations of A β has enormous potential for investigating the correlation between structure and pathobiology but also for the screening and development of novel therapeutics. Moreover, the same method can be exploited for other proteopathic protein assemblies such as tau and α -synuclein.

Introduction

The progression of Alzheimer's disease (AD) is currently an unstoppable neurodegenerative process that devastates many elderly people. The β -amyloid ($A\beta$) peptide is the principle component of senile plaques and additionally is hypothesized as the initiating factor for disease (Masters *et al.* 1985; Wong *et al.* 1985; Selkoe and Hardy 2016). Given its central role in disease, many attempts at slowing neurodegeneration therapeutically have targeted the $A\beta$ peptide (Karran *et al.* 2011).

It is well known that along the aggregation pathway of $A\beta$ there exists many different species, from small monomers and oligomers to larger protofibrils and fibrils (Haass and Selkoe 2007; Jucker and Walker 2013). A central debate within the AD field is what role each distinct $A\beta$ species has on the disease process. A number of studies have shown the soluble dimers and oligomers can modulate synapses (Walsh *et al.* 2002; Lesne *et al.* 2006; Klyubin *et al.* 2008; Shankar *et al.* 2008; Amar *et al.* 2017). It has been proposed that there are even on-pathway and off-pathway oligomers generated in the fibrillization cascade (Liu *et al.* 2015). These diverse multimeric species clearly modulate the brain environment, however, it is important to consider the source of $A\beta$ being used for *in vivo* characterization. It has been shown that *in vitro* $A\beta$ does not replicate certain aspects of *in vivo* samples, such as the ability to seed $A\beta$ deposition in APP transgenic hosts (Meyer-Luehmann *et al.* 2006; Novotny *et al.* 2016). Additionally, there is evidence that the potency of $A\beta$ changes over the course of amyloidosis and this further emphasizes the need to carefully select *in vivo* $A\beta$ species for further characterization (Ye *et al.* 2017). Thus a method for investigating different structures of *in vivo* $A\beta$ is of need to enhance the understanding of disease.

This study aimed at developing a method for the enrichment of $A\beta$ species of different sizes with an agarose gel fractionation system. We demonstrate that $A\beta$ species can be separated by size while retaining quaternary structural features and biological seeding properties. The application of this to an array of downstream applications such as therapeutic screening and novel immunotherapy generation is highly promising.

Methods

Mouse brain extracts

Transgenic mice overexpressing the human APP protein with the Swedish mutation (KM670/671NL) under control of the Thy1 promoter on a C57/Bl6 background were used throughout the study (Sturchler-Pierrat *et al.* 1997). Mice were deeply anesthetized with ketamine/xylazine (250/25 mg/kg) and sacrificed by cervical dislocation. After removal of the brain stem and cerebellum, mouse brains were homogenized (10%) with the Precellys system in PBS (2x20 sec, 5500 rpm; Precellys24 Homogenizer, Bertin Instruments). Homogenates were centrifuged for 5 min at 3000 g and the supernatants were collected and stored at -80°C until further analysis. Pooled brain extracts from Ye *et al.* (2017) were used for the characterization of different ages (Fig 1C-E). Extracts used in later analysis were prepared from 28 mo old mice (Fig 2).

In vitro A β samples

Monomeric A β was prepared using synthetic A β 1-40 (Bachem) and was dissolved in DMSO and stored at -80°C prior to analysis. For preparation of oligomers, a protocol for A β derived diffusible ligands (ADDLs) was followed using A β 1-42 (Ryan *et al.* 2010). Briefly, A β 1-42 (Bachem) was dissolved in HFIP and, after evaporation, resuspended in DMSO to a concentration of 5 mM then further diluted in PBS-SDS (0.05%) to 100 μ M and incubated at 4°C for 24 h. Samples were then diluted to 11 μ M and incubated for 2 weeks at 4°C. Fibrils were prepared from A β 1-42 by incubating at 37°C for 24 h at a concentration of 100 μ M (10 mM HCl, 150 mM NaCl).

Semi-denaturing agarose fractionation

The methodology for resolving larger aggregates of A β was adapted from a previous study (Bagriantsev *et al.* 2006). Samples were mixed with loading buffer (50 mM Tris pH 6.8, 2% SDS, 5% glycerol) at RT for 7 min then electrophoresed on a 2% low melting point (LMP) agarose gel (20 mM Tris, 200 mM Glycine, 0.1% SDS) at 25 V for 45 min in Tris-Glycine buffer (20 mM-200 mM) and subsequently cut into 1-centimeter fractions.

For direct analysis of A β , gel pieces were then melted in denaturing sample buffer (62.5 mM Tris pH 6.8, 8.3% glycerol, 2% SDS, 100 mM DTT) and loaded on a NuPAGE 4-12% Bis-Tris gel, electrophoresed in NuPAGE MES buffer (Thermo Scientific) then transferred to a nitrocellulose membrane. Membranes were probed with 6E10 (1:5000, Covance) and Goat Anti-Mouse HRP (1:30000, Jackson Laboratories), developed with Super Signal West Dura Extended Duration substrate (Thermo Scientific) and the monomeric A β signal was quantified by densitometry (ImageJ, NIH) from autoradiography films (Amersham Hyperfilm ECL). Results are representative of two technical replicates.

Gel Fraction Digestion and Immunoprecipitation

Agarose gel fractions were equilibrated in buffer (50 mM Bis-Tris pH 6.5, 1 mM EDTA), diluted to a 1% agarose concentration and then melted at 65°C for 10 min, cooled to 42°C and digested for 60 min with agarase (Sigma-Aldrich, A6306). Liquid samples were then aliquoted and stored at -80°C prior to sample analysis. Samples were thawed on ice and incubated on a rotator overnight at 4°C with Protein G Dynabeads (Thermo Scientific) coupled to different antibodies (4.8 μ g IgG / 20 μ l beads). A β antibodies with a linear epitope including N25 (gift from Janssen Pharmaceuticals) and 4G8 (Covance) were used in addition to the conformation-specific amyloid antibody mOC31 (Hatami *et al.* 2014) and control anti-wheat germ antibody (gift from Biogen). Beads were washed with PBS-Tween20 (0.05%) prior to the eluted antigen being recovered with heating at 70°C for 10min in LDS Sample Buffer (Thermo Scientific). Denatured eluate was then electrophoresed on NuPAGE 4-12% Bis-Tris gels in NuPAGE MES buffer (Thermo Scientific), transferred to nitrocellulose and probed with 6E10 (1:5000, Covance) and Goat Anti-Mouse HRP (1:30000, Jackson Laboratories). Signals were captured with autoradiography film (Amersham Hyperfilm ECL). Results are representative of three technical replicates.

Mouse Injections

Pre-depositing male APP23 mice (4 mo) were anesthetized with ketamine/xylazine (100/10 mg/kg) and 2.5 μ L of fraction 2 from an APP23 end-stage (ES, n=7) or aged WT (n=3) was infused at a rate of 1.25 μ L/min into both hippocampi (bregma: -2.5 mm anterior/posterior; +/- 2.0 mm lateral; -1.8 mm dorsal/ventral). Mice were monitored closely until regaining consciousness and weighed weekly until the completion of the experiment. After six months, mice were deeply anaesthetized with ketamine/xylazine (250/25 mg/kg) and perfused with

ice-cold PBS. Brains were immersion fixed in paraformaldehyde (4%) for 48 h, incubated in 30% sucrose for another 48 h, then snap frozen in methyl butane. Brains were sectioned on a freeze-sliding microtome (25 μ m, Microme Leica) and stained with a polyclonal A β antibody using the Vectastain ABC system (Rasmussen *et al.* 2017).

Results

The resolution of larger aggregates was achieved using Invitrogen cassettes (1.5 mm) and a low-melting point (LMP; 2%) semi-denaturing agarose gel. The running behavior was controlled using a stained protein ladder (SeeBlue Plus 2, Invitrogen) as a reference for migration distance (Fig. 1A). Gels were then cut into seven 1 cm fractions with the first fraction containing only the bottom of wells (0.5 cm) to analyze A β species too large to enter the agarose gel (Fig. 1A). To confirm the running behavior of different *in vitro* A β preparations, monomers, oligomers and fibrils were run on the semi-denaturing gel and fractions were collected and analyzed by complete denaturing PAGE (Fig. 1B). A β was found only in the smaller fractions for monomers, while oligomers harboured A β in moderately sized fractions and fibril samples had A β populating all fractions (Fig. 1B). Next, the migration behavior of *in vivo* A β from APP23 mouse brain extracts was investigated (Fig 1C-E). In all ages of mouse extract investigated, there was A β present in every fraction, but predominantly in the first and last fraction (Fig 1D-E). The pattern of A β distribution between ages was largely similar (Fig. 1E).

The agarose fractionation methodology was then expanded to produce a liquid suspension from LMP agar fractions using enzymatic agarase digestion. Aged brain extracts were first separated by agarose electrophoresis and cut into fractions as above but then digested with agarase. After digestion, immunoprecipitation was performed on different liquid fractions with different A β antibodies coupled to magnetic beads (Fig 2A). Similar to the distribution of A β after direct analysis with melting (Fig 1D), antibodies with a linear epitope (N25 and 4G8) recognized A β in almost all fractions with a similar pattern (Fig. 2A). However, the aggregate-specific mOC31 antibody (Hatami *et al.* 2014) only recognized A β in the high molecular weight fractions (Fig 2A). A mock-labeled control revealed a weak signal in the high molecular weight fractions (Fig 2A).

To further test the nature of the liberated high molecular weight structures of A β , the second agarose fraction was injected into the hippocampus of pre-depositing APP23 mice (Fig 2B). After six months of incubation, mice were sacrificed and analyzed for A β deposition histologically. Only mice injected with fraction two from the APP23 ES sample had detectable seeded A β deposition, while aged WT injected animals lacked this typical seeding pattern (Fig 2B).

Discussion

The investigation of subpopulations of A β is crucial to better understand its overall role in the progression of AD. The data presented outlines a novel method for separating native A β assemblies based on size, especially the high molecular weight complexes. Crucially, the size fractions displayed evidence of a preserved quaternary structure, enabling biochemical studies of A β composition and biological seeding activity to determine how these fractions are different on multiple levels (Fig 2).

The comparison of *in vitro* fibrillized A β to *in vivo* material revealed an interesting finding in terms of the distribution of A β (Fig 1). All *in vivo* samples had a peak in A β abundance in the highest and lowest molecular weight fractions to suggest a predominance of very large order aggregates and monomers (Fig 1D). The excess of monomers can be explained by physiological production of A β in the APP23 transgenic mouse brain and the higher order structures are likely the result of the advanced aggregation state achieved with age and the scaffolding supplied by the brain (Sturchler-Pierrat *et al.* 1997). The *in vitro* fibrils failed to achieve an excess of these large structures (Fig 1B). It is tempting to suggest that the failure of *in vitro* fibrils to act as potent seeds may be due to this discrepancy (Meyer-Luehmann *et al.* 2006; Novotny *et al.* 2016).

The liberation of A β from agarose fractions was crucial for determining whether the peptide features were preserved during separation. The relative distribution of A β through fractions was confirmed with linear-epitope antibodies while the general lack of A β signal after control pull-down confirmed the specificity of antibodies. The reactivity of the aggregate-specific mOC31 antibody only in high molecular weight fractions is strong evidence that A β retains an aggregated form throughout the fractionation procedure (Hatami *et al.* 2014). It is worth

noting that the mOC31 antibody preferentially stains vascular deposits of A β (cerebral amyloid angiopathy, CAA) in histological stains as opposed to parenchymal plaques (Hatami *et al.* 2014). It is unclear whether the high molecular weight fractions in this procedure contain A β derived from CAA exclusively but analysis of another cerebral β -amyloidosis model without CAA could clarify this.

The confirmation that A β contained in higher molecular weight fractions is capable of inducing deposition *in vivo* confirms that further characterization of samples produced by this method is valid. It has shown that highly potent seeds exist in soluble brain extracts (Langer *et al.* 2011; Fritschi *et al.* 2014). Further analysis of these soluble A β species with agarose fractionation could determine whether a certain A β size is responsible for this increased potency. It will be important for such future studies to use a seeding activity bioassay to accurately determine the potency of different fractions (Ye *et al.* 2017). Additionally, it will be interesting to investigate a diverse set of biological samples using agarose fractionation, from different transgenic mouse lines with various ages to human AD samples. Delineating the size of the most potent seeds from transgenic mouse models and humans samples would be invaluable to understanding the onset of A β pathology.

Previous research has suggested that different subtypes of AD contain A β with varying biochemical and biological characteristics (Lu *et al.* 2013; Watts *et al.* 2014; Cohen *et al.* 2015; Qiang *et al.* 2017; Rasmussen *et al.* 2017). By applying agarose fractionation, it would be possible to determine whether these differences in A β are present throughout the entire population of aggregates or within a single size class. This information could then be used to develop therapeutics directed against subspecies of A β with the most potent seeding activity. Generating a novel therapeutic based on *in vivo* derived A β with a defined biological activity would be invaluable. Detailed structural analysis of A β contained within different fractions can also be used to gain insight into the relation between structure and biological properties of *in vivo* species. The pairing of structural information and amyloid binding dyes with some therapeutic potential, like polythiophenes, has been employed for prion diseases and such a guide could be applied for A β (Herrmann *et al.* 2015; Schütz *et al.* 2017)

The composition of the total A β population within different biological samples has not been well studied. Further investigation of *in vivo* A β subpopulations using agarose fractionation

will lead to a more detailed understanding of the link between biochemistry and structure to biological properties such as seeding. Additionally, the simplicity of this system could easily be adapted to other amyloid proteins associated with disease to gain insight into the relationship of size and seeding for various aggregates. Finally, this method can also be used for any other brain-derived protein assemblies, in particular proteopathic assemblies associated with neurodegenerative disease such as α -synuclein and tau.

References

- Amar F, Sherman MA, Rush T, Larson M, Boyle G, Chang L, *et al.* The amyloid-beta oligomer A β *56 induces specific alterations in neuronal signaling that lead to tau phosphorylation and aggregation. *Sci Signal* 2017; 10: eaal2021.
- Bagriantsev SN, Kushnirov VV, Liebman SW. Analysis of amyloid aggregates using agarose gel electrophoresis. *Methods Enzymol* 2006; 412: 33-48.
- Cohen ML, Kim C, Haldiman T, El Hag M, Mehndiratta P, Pichet T, *et al.* Rapidly progressive Alzheimer's disease features distinct structures of amyloid-beta. *Brain* 2015; 138: 1009-1022.
- Fritschy SK, Langer F, Kaeser SA, Maia LF, Portelius E, Pinotsi D, *et al.* Highly potent soluble amyloid-beta seeds in human Alzheimer brain but not cerebrospinal fluid. *Brain* 2014; 137: 2909-2915.
- Haass C, Selkoe DJ. Soluble protein oligomers in neurodegeneration: lessons from the Alzheimer's amyloid beta-peptide. *Nat Rev Mol Cell Biol* 2007; 8: 101-112.
- Hatami A, Albay R, Monjazeb S, Milton S, Glabe C. Monoclonal Antibodies against A β 42 Fibrils Distinguish Multiple Aggregation State Polymorphisms in Vitro and in Alzheimer Disease Brain. *J Biol Chem* 2014; 289: 32131-32143.
- Herrmann US, Schütz AK, Shirani H, Huang D, Saban D, Nuvolone M, *et al.* Structure-based drug design identifies polythiophenes as antiprion compounds. *Sci Transl Med* 2015; 7: 299ra123.
- Jucker M, Walker LC. Self-propagation of pathogenic protein aggregates in neurodegenerative diseases. *Nature* 2013; 501: 45-51.
- Karran E, Mercken M, De Strooper B. The amyloid cascade hypothesis for Alzheimer's disease: an appraisal for the development of therapeutics. *Nat Rev Drug Discov* 2011; 10: 698-712.
- Klyubin I, Betts V, Welzel AT, Blennow K, Zetterberg H, Wallin A, *et al.* Amyloid beta protein dimer-containing human CSF disrupts synaptic plasticity: prevention by systemic passive immunization. *J Neurosci* 2008; 28: 4231-4237.
- Langer F, Eisele YS, Fritschy SK, Staufenbiel M, Walker LC, Jucker M. Soluble A β seeds are potent inducers of cerebral beta-amyloid deposition. *J Neurosci* 2011; 31: 14488-14495.
- Lesne S, Koh MT, Kotilinek L, Kaye R, Glabe CG, Yang A, *et al.* A specific amyloid-beta protein assembly in the brain impairs memory. *Nature* 2006; 440: 352-357.
- Liu P, Reed MN, Kotilinek LA, Grant MK, Forster CL, Qiang W, *et al.* Quaternary structure defines a large class of amyloid-beta oligomers neutralized by sequestration. *Cell Rep* 2015; 11: 1760-1771.
- Lu JX, Qiang W, Yau WM, Schwieters CD, Meredith SC, Tycko R. Molecular structure of beta-amyloid fibrils in Alzheimer's disease brain tissue. *Cell* 2013; 154: 1257-1268.
- Masters CL, Simms G, Weinman NA, Multhaup G, McDonald BL, Beyreuther K. Amyloid plaque core protein in Alzheimer disease and Down syndrome. *Proc Natl Acad Sci U S A* 1985; 82: 4245-4249.
- Meyer-Luehmann M, Coomaraswamy J, Bolmont T, Kaeser S, Schaefer C, Kilger E, *et al.* Exogenous induction of cerebral beta-amyloidogenesis is governed by agent and host. *Science* 2006; 313: 1781-1784.
- Novotny R, Langer F, Mahler J, Skodras A, Vlachos A, Wegenast-Braun BM, *et al.* Conversion of synthetic A β to in vivo active seeds and amyloid plaque formation in a hippocampal slice culture model. *J Neurosci* 2016; 36: 5084-5093.
- Qiang W, Yau WM, Lu JX, Collinge J, Tycko R. Structural variation in amyloid-beta fibrils from Alzheimer's disease clinical subtypes. *Nature* 2017; 541: 217-221.

- Rasmussen J, Mahler J, Beschorner N, Kaeser SA, Hasler LM, Baumann F, *et al.* Amyloid polymorphisms constitute distinct clouds of conformational variants in different etiological subtypes of Alzheimer's disease. *Proc Natl Acad Sci U S A* 2017; 114: 13018-13023.
- Ryan DA, Narrow WC, Federoff HJ, Bowers WJ. An improved method for generating consistent soluble amyloid-beta oligomer preparations for in vitro neurotoxicity studies. *J Neurosci Methods* 2010; 190: 171-179.
- Schütz AK, Hornemann S, Walti MA, Greuter L, Tiberi C, Cadalbert R, *et al.* Binding of polythiophenes to amyloids: Structural mapping of the pharmacophore. *ACS Chem Neurosci* 2017
- Selkoe DJ, Hardy J. The amyloid hypothesis of Alzheimer's disease at 25 years. *EMBO Mol Med* 2016; 8: 595-608.
- Shankar GM, Li S, Mehta TH, Garcia-Munoz A, Shepardson NE, Smith I, *et al.* Amyloid-beta protein dimers isolated directly from Alzheimer's brains impair synaptic plasticity and memory. *Nat Med* 2008; 14: 837-842.
- Sturchler-Pierrat C, Abramowski D, Duke M, Wiederhold KH, Mistl C, Rothacher S, *et al.* Two amyloid precursor protein transgenic mouse models with Alzheimer disease-like pathology. *Proc Natl Acad Sci U S A* 1997; 94: 13287-13292.
- Walsh DM, Klyubin I, Fadeeva JV, Cullen WK, Anwyl R, Wolfe MS, *et al.* Naturally secreted oligomers of amyloid beta protein potently inhibit hippocampal long-term potentiation in vivo. *Nature* 2002; 416: 535-539.
- Watts JC, Condello C, Stöhr J, Oehler A, Lee J, DeArmond SJ, *et al.* Serial propagation of distinct strains of Abeta prions from Alzheimer's disease patients. *Proc Natl Acad Sci U S A* 2014; 111: 10323-10328.
- Wong CW, Quaranta V, Glenner GG. Neuritic plaques and cerebrovascular amyloid in Alzheimer disease are antigenically related. *Proc Natl Acad Sci U S A* 1985; 82: 8729-8732.
- Ye L, Rasmussen J, Kaeser SA, Marzesco AM, Obermuller U, Mahler J, *et al.* Abeta seeding potency peaks in the early stages of cerebral beta-amyloidosis. *EMBO Rep* 2017; 18: 1536-1544.

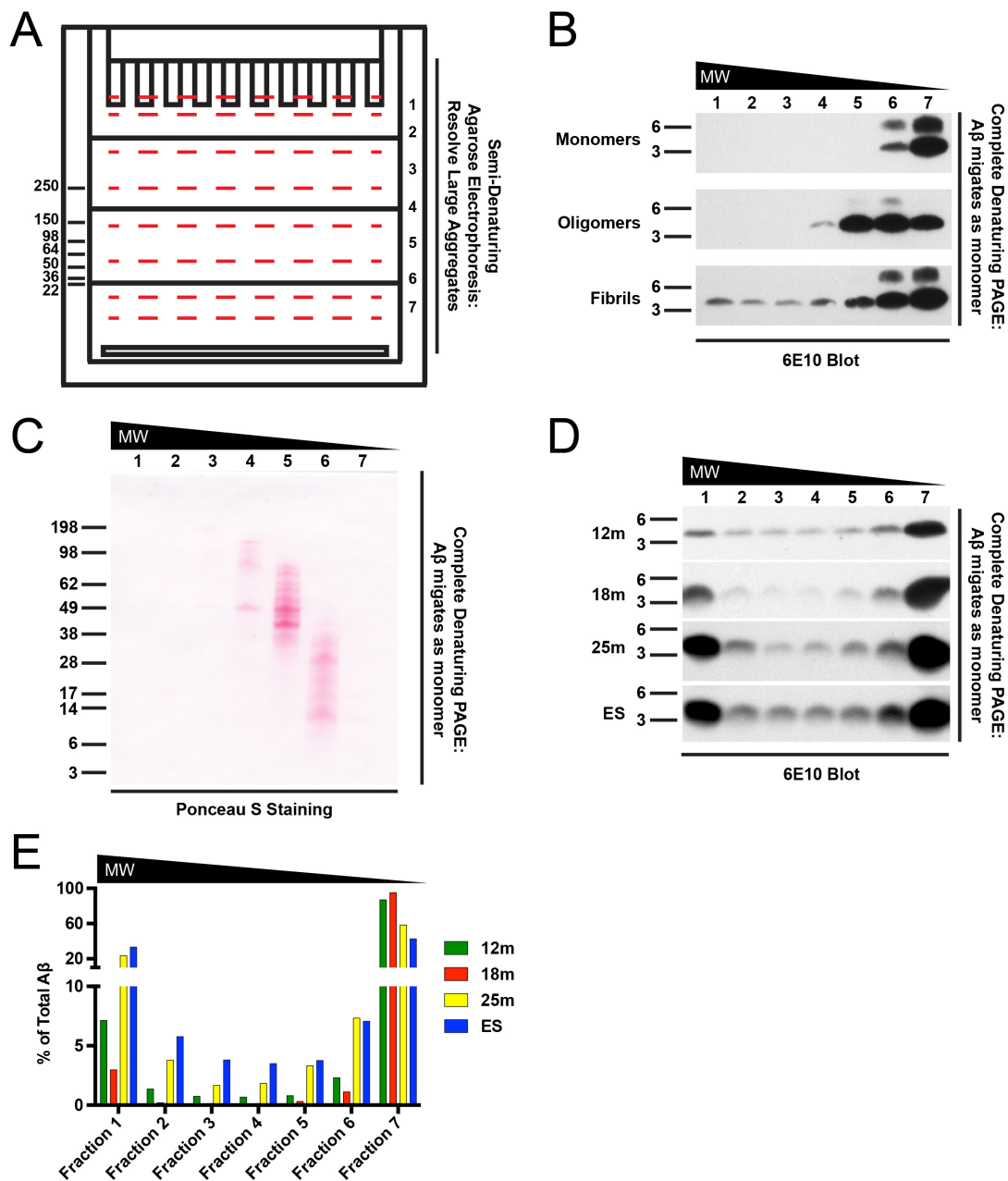


Figure 1. Agarose gel fractionation is able to separate different subpopulations of A β . (A) Depiction of a cassette used for semi-denaturing agarose gel electrophoresis with the different fractions represented by red dashed lines (Fraction 1-7; decreasing in molecular weight) and the running behavior of protein standards shown on the side. (B-E) Gel fractions were melted in complete denaturing sample buffer and ran on complete denaturing NuPAGE 4-12% Bis-Tris gels (PAGE) to resolve proteins contained within the fractions. (B) *In vitro* A β preparations of monomers, oligomers and fibrils display expected size distributions when analyzed with a 6E10 blot. (C) Ponceau S staining of a mouse extract (APP23 End-stage) shows the distribution of protein species contained within fractions. (D-E) Pooled seeding extracts from different ages of APP23 mice (Ye *et al.* 2017) were fractionated and ran on complete denaturing gels (D) and the monomeric A β signal (6E10 blot) was analyzed for the different size fractions (E). The majority of A β is contained within the first (1) and last (7) fractions for all extracts. ES=End-stage; MW=molecular weight.

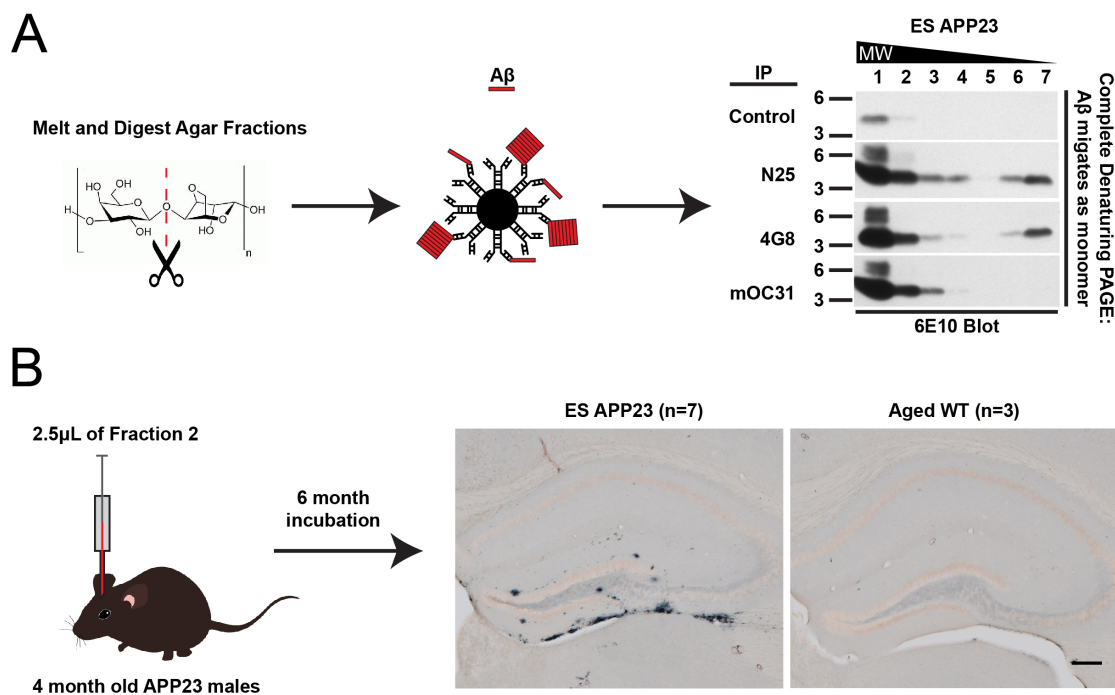


Figure 2. Agarose gel fractions can be digested and used for subsequent analysis showing a preservation of quaternary structure and biological activity. (A) Gel fractions were melted and enzymatically digested with agarase then A β was immuno-precipitated with different antibodies (Protein G Dynabeads). A control antibody (anti-wheat germ) showed slight reactivity with the first fraction (high molecular weight), while N25 (amino acids 1-8) and 4G8 (amino acids 18-22) pull down A β from both large and small molecular weight fractions. The fibril-specific antibody mOC31 (Hatami *et al.* 2014) only showed reactivity with larger A β species (Fractions 1-3) to suggest a preservation of quaternary structure. (B) As a proof-of-concept, fraction 2 from both APP23 ES and an age matched WT extract were stereotactically injected (bilateral intra-hippocampus) into pre-depositing male APP23 mice and left to incubate for 6 months. Mice injected with fraction 2 from APP23 mice showed A β deposition within the hippocampus (blue=polyclonal A β antibody) but the corresponding WT controls did not, demonstrating retention of biological seeding activity. Scale bar=200 μ m. ES=End-stage; MW=molecular weight.

4. Appendix

4.1 Abbreviations

A β ; A β 40; A β 42	β -amyloid; 40 aa variant; 42 aa variant
A η	η -amyloid
aa	amino acid
AD; fAD; sAD	Alzheimer's disease; familial variant; sporadic variant
ADAM10	a disintegrin and metalloproteinase domain containing protein 10
ADDL	amyloid derived diffusible ligands
AICD	APP intracellular domain
ApoE; ApoE4	apolipoprotein E; ApoE variant 4
APP; sAPP	amyloid precursor protein; soluble fragment of APP
ASA	amyloid seeding assay
BACE1/2	β -site APP cleaving enzyme 1/2
BSE	bovine spongiform encephalopathy
C83; C99	C-terminal fragment 83; C-terminal fragment 99
CAA	cerebral amyloid angiopathy
CJD; iCJD; sCJD; vCJD	Creutzfeldt-Jakob disease; iatrogenic; sporadic; variant
Cryo-EM	electron cryomicroscopy
CSF	cerebrospinal fluid
GWAS	genome wide association study
h-FTAA	heptamer-formylthiophene acetic acid
LCO	luminescent conjugated oligothiophenes
LD50	lethal dose 50
LDL; vLDL	low-density lipoprotein; very-low-density lipoprotein
LTP	long-term potentiation
MT5-MMP	membrane-type 5 matrix metalloproteinase
NFT	neurofibrillary tangles
PET	positron emission tomography
PCA	posterior cortical atrophy variant of AD
PiB	Pittsburgh compound B
PMCA	protein misfolding cyclic amplification
PrP ^C	cellular prion protein
PrP ^{TSE}	misfolded, disease-associated prion protein
PSEN1/2	presenilin 1/2
q-FTAA	quadro-formylthiophene acetic acid
RT-QuIC	real-time quaking induced conversion

SEM	scanning electron microscopy
SD ₅₀	seeding dose 50
ssNMR	solid-state nuclear magnetic resonance
ThT	thioflavin T
TME	transmissible mink encephalopathy
TREM2	triggering receptor expressed on myeloid cells 2
TSE	transmissible spongiform encephalopathy
USD	American dollars (currency of the United States of America)

4.2 Curriculum vitae

Jay Rasmussen

Date of birth: 12.07.1989

Place of birth: Medicine Hat, Alberta, Canada

Nationality: Canadian

Business Address:

German Center for Neurodegenerative Diseases

Hertie Institute for Clinical Brain Research

Department of Cellular Neurology

Otfried-Müller-Str. 27

72076 Tübingen, Germany

Personal Address: Depotstr. 7, 72072 Tübingen, Germany

E-mail: jdrasmus@ualberta.ca

Phone: +49 176 26883540

Education

- 07/2014 - present **PhD candidate** at the Hertie-Institute for Clinical Brain Research, University Tübingen; German Center for Neurodegenerative Diseases (DZNE), Germany
Field of study: Cellular Neuroscience
Thesis title: “ β -amyloid in Alzheimer’s disease initiation and phenotypic diversity”
- 09/2011 - 11/2013 **Master of Science (4.0/4.0)** at the University of Alberta, Department of Agricultural, Food and Nutritional Science, Canada
Field of study: Animal Science
Thesis title: “Investigation on the uptake of functional proteins and infectious prions into wheat plants through the root system”
- 09/2007 - 06/2011 **Bachelor of Science (3.8/4.0)** at the University of Alberta, Department of Biological Sciences, Canada
Field of study: Physiology and Developmental Biology
-

Review:

- (1) **Rasmussen J**, Jucker M, Walker LC. A β seeds and prions: How close the fit? *Prion* 2017; 11: 215-225. (doi:10.1080/19336896.2017.1334029)

Primary literature:

- (1) **Rasmussen J**, Bühler A, Baumann F, Jucker M. An agarose gel fractionation method for enriching brain-derived proteopathic seeds. *in preparation*.
- (2) **Rasmussen J**, Krasemann S, Altmeyen H, Schwarz P, Schelle J, Aguzzi A, Glatzel M, Jucker M. Infectious prions are not capable of inducing A β deposition in an *in vivo* seeding paradigm. *in preparation*.
- (3) **Rasmussen J***, Mahler J*, Beschorner N*, Kaeser SA, Häsler LM, Baumann F, Nyström S, Portelius E, Blennow K, Lashley T, Fox NC, Sepulveda-Falla D, Glatzel M, Oblak AL, Ghetti B, Nilsson KPR, Hammarström P, Staufenbiel M, Walker LC, Jucker M. Amyloid polymorphisms constitute distinct clouds of conformational variants in different etiological subtypes of Alzheimer's disease. *Proc Natl Acad Sci U S A* 2017; 114: 13018-13023. (doi:10.1073/pnas.1713215114) *equal contribution
- (4) Ye L*, **Rasmussen J***, Kaeser SA, Marzesco A, Obermueller U, Mahler J, Schelle J, Odenthal J, Krueger C, Fritschi SK, Walker LC, Staufenbiel M, Baumann F, Jucker M. A β seeding potency peaks in the early stages of cerebral β -amyloidosis. *EMBO Rep* 2017; 18: 1536-1544. (doi:10.15252/embr.201744067) *equal contribution
- (5) Klima CL, Zaheer R, Cook SR, **Rasmussen J**, Alexander T, Potter A, Hendrick S, McAllister TA. *In silico* identification and high throughput screening of antigenic proteins as candidates for a *Mannheimia haemolytica* vaccine. *Vet Immunol Immunopathol* 2017; 195: 19-24. (doi:10.1016/j.vetimm.2017.11.004)
- (6) Klima CL, Cook SR, Zaheer R, Laing C, Gannon VP, Xu Y, **Rasmussen J**, Potter A, Hendrick S, Alexander TW, McAllister TA. Comparative Genomic Analysis of *Mannheimia haemolytica* from Bovine Sources. *PLoS One* 2016; 11: e0149520. (doi:10.1371/journal.pone.0149520)
- (7) **Rasmussen J**, Gilroyed BH, Reuter T, Badea A, Eudes F, Graf R, Laroche A, Kav NNV, McAllister TA. Protein can be taken up by damaged wheat roots and transported to the stem. *J Plant Biol* 2015; 58: 1-7. (doi: 10.1007/s12374-014-0258-z)
- (8) Xu S, **Rasmussen J**, Ding N, Neumann NF, Belosevic M, McAllister TA. Approaches to inactivate infectious prions in the environment: A mini-review. *J Environ Eng Sci* 2014; 9: 125-136. (doi: 10.1680/jees.13.00014)

- (9) **Rasmussen J**, Gilroyed BH, Reuter T, Dudas S, Neumann NF, Balachandran A, Kav NNV, Graham C, Czub S, McAllister TA. Can plants serve as a vector for prions causing Chronic Wasting Disease? *Prion* 2014; 8: 138-144. (doi:10.4161/pri.27963)
- (10) **Rasmussen J**, Gilroyed BH, Reuter T, Badea A, Eudes F, Graf R, Laroche A, Kav NNV, McAllister TA. Efficiency of protein as a nitrogen source for wheat and morphological changes in roots exposed to high protein concentrations. *Can J Plant Sci* 2014; 94: 1-11. (doi:10.4141/CJPS2013-187)
- (11) Campeau JL, Wu G, Bell JR, **Rasmussen J**, Sim VL. Early Increase and Late Decrease of Purkinje Cell Dendritic Spine Density in Prion-Infected Organotypic Mouse Cerebellar Cultures. *PLoS One* 2013; 8: e81776. (doi: 10.1371/journal.pone.0081776)
- (12) Kooistra MK, Leduc RYM, Dawe CE, Fairbridge NA, **Rasmussen J**, Man JHY, Bujold M, Juriloff D, King-Jones K, McDermid HE. Strain-specific modifier genes of *Cecr2*-associated exencephaly in mice: genetic analysis and identification of differentially expressed candidate genes. *Physiol Genom* 2012; 44: 35-46. (doi:10.1152/physiolgenomics.00124.2011)

Conference proceedings:

- (1) **Rasmussen J**, Mahler J, Diamond MI, Nilsson KPR, Walker LC, Oblak AL, Ghetti B, Baumann F, Jucker M. Conformationally distinct amyloid- β variants in human Alzheimer's disease brains. GRC 2016; Girona, Spain (*Poster Presentation*).
- (2) Mahler J, **Rasmussen J**, Diamond MI, Nilsson KPR, Walker LC, Baumann F, Jucker M. Structurally distinct amyloid- β species among Alzheimer's disease patients – revisiting a Pittsburgh compound B-refractory case. SfN 2015; Chicago, USA (*Poster Presentation*).
- (3) **Rasmussen J**, Gilroyed BH, Reuter T, Dudas S, Graham C, Neumann NF, Balachandran A, Czub S, Kav NNV, McAllister TA. 2013. Are plants a potential transmission route for infectious prions? PRION 2013. Banff, Canada. (*Poster Presentation*)
- (4) **Rasmussen J**, Gilroyed BH, Reuter T, Badea A, Eudes F, Graf R, Laroche A, Kav NNV, McAllister TA. 2012. The uptake of functional proteins and infectious prions into major crop plants. PrP Canada 2012 & Protein Folding and Disease Conference. Toronto, Canada. (*Poster Presentation*)
-

Scholarships and Honors

2012 - 2013	NSERC Alexander Graham Bell CGS
2012 - 2013	Alberta Innovates GSS
2012 - 2013	Walter H. Johns Fellowship
2012	Best Graduate Student Poster PrP Canada 2012 <i>-Honorable Mention</i>
2011	Outstanding Research in Genetics Award
2007 - 2011	University of Alberta Dean's List
